Metsähovi Radio Observatory

Narrow-line Seyfert 1 galaxies

Observational and statistical analysis

Emilia Järvelä

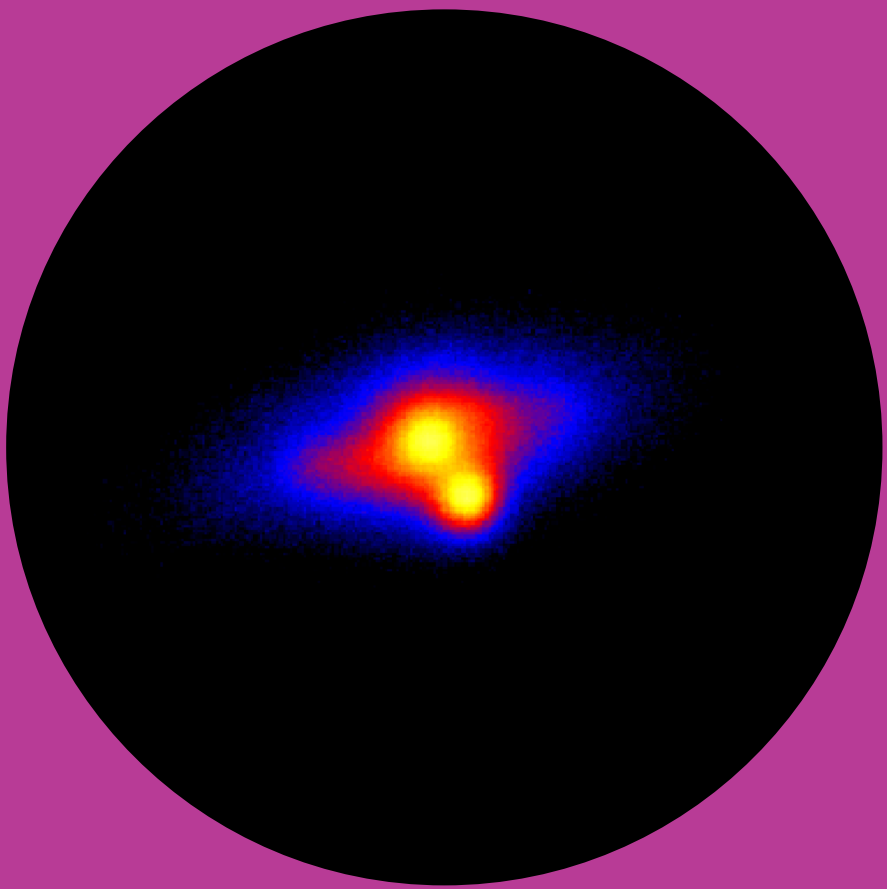

Aalto University

DOCTORAL DISSERTATIONS

Aalto University publication series
DOCTORAL DISSERTATIONS 163/2018

Narrow-line Seyfert 1 galaxies

Observational and statistical analysis

Emilia Järvelä

A doctoral dissertation completed for the degree of Doctor of Science (Technology) to be defended, with the permission of the Aalto University School of Electrical Engineering, at a public examination held at the lecture hall AS1 of the TUAS building on 12 October 2018 at 12.

Aalto University
School of Electrical Engineering
Metsähovi Radio Observatory

Supervising professor
Professor Anne Lähteenmäki, Aalto University Metsähovi Radio Observatory, Finland

Thesis advisor
Professor Anne Lähteenmäki, Aalto University Metsähovi Radio Observatory, Finland

Preliminary examiners
Professor Gabriele Giovannini, INAF, Istituto di Radioastronomia, Italy
Doctor Phil Edwards, CSIRO Astronomy & Space Science, ATNF, Australia

Opponent
Professor Chris Done, Centre for Extragalactic Astronomy, Department of Physics, University of Durham, United Kingdom

Aalto University publication series
DOCTORAL DISSERTATIONS 163/2018

ISBN 978-952-60-8153-3 (printed)
ISBN 978-952-60-8154-0 (pdf)
ISSN 1799-4934 (printed)
ISSN 1799-4942 (pdf)
http://urn.fi/URN:ISBN:978-952-60-8154-0

Unigrafia Oy
Helsinki 2018

Finland

441 697
Printed matter

Aalto University

Abstract

Aalto University, P.O. Box 11000, FI-00076 Aalto www.aalto.fi

Author
Emilia Järvelä

Name of the doctoral dissertation
Narrow-line Seyfert 1 galaxies: Observational and statistical analysis

Publisher School of Electrical Engineering

Unit Metsähovi Radio Observatory

Series Aalto University publication series DOCTORAL DISSERTATIONS 163/2018

Field of research Space technology

Manuscript submitted 7 May 2018 **Date of the defence** 12 October 2018

Permission to publish granted (date) 13 August 2018 **Language** English

☐ **Monograph** ☒ **Article dissertation** ☐ **Essay dissertation**

Abstract

Narrow-line Seyfert 1 (NLS1) galaxies are young active galactic nuclei (AGN). They harbour low-mass black holes accreting close to the Eddington limit and are preferentially hosted by spiral galaxies. So far ~20 NLS1 galaxies have been detected at gamma-rays, confirming the presence of powerful relativistic jets in them. This contradicts the conventional view that only supermassive black holes residing in massive ellipticals are able to launch relatistic jets, and therefore a revision of the evolution and unification schemes of AGN is required.

In this thesis large samples of NLS1 galaxies are examined, complemented by targeted studies of smaller samples. Novel radio, near-infrared, and large-scale environment data were obtained and, together with archival multifrequency data, used for extensive statistical studies such as correlation analyses. Principal component analysis (PCA) emerged as an excellent tool for studying the diverse NLS1 samples.

We monitored large samples of NLS1 galaxies at 37 GHz in Metsähovi Radio Observatory. This is the largest observing programme of NLS1 galaxies at radio frequencies. 19% of sources selected based on their radio properties and 12% of sources selected based on other criteria were detected, including sources previously (mis)classified as radio-silent. As detections at 37~GHz are indicators of radio emission from a jet, this implies that powerful jets in NLS1 galaxies are more frequent than previously assumed. We also found that the jets of flat-spectrum NLS1 galaxies are less powerful than those of blazars, but when scaled by the black hole mass the jet powers become comparable. Additionally, we discovered a new gamma-ray emitting source in the radio-silent NLS1 sample.

We show that the large-scale environment density affects the radio properties of NLS1 galaxies and that jetted NLS1 sources are more frequently found in denser surroundings. However, on average jetted NLS1 galaxies reside in significantly less dense large-scale environments than other jetted AGN, proving that powerful jets can be triggered in diverse environments. In addition a parameter describing the large-scale environment was included in the PCA of AGN for the first time.

Our near-infrared imaging of sources detected at 37 GHz almost tripled the number of jetted NLS1 galaxies with known host morphologies. All observed NLS1 nuclei reside in spiral galaxies. The fraction of mergers in this sample is significantly higher than among non-jetted NLS1 galaxies, suggesting that interaction may play a role in triggering the jet. The heterogeneity of the NLS1 population could be explained by disparate evolutionary stages induced by interaction.

Keywords narrow-line Seyfert 1 galaxies, active galactic nuclei, relativistic jets, large-scale structure, radio astronomy, principal component analysis

ISBN (printed) 978-952-60-8153-3 **ISBN (pdf)** 978-952-60-8154-0

ISSN (printed) 1799-4934 **ISSN (pdf)** 1799-4942

Location of publisher Helsinki **Location of printing** Helsinki **Year** 2018

Pages 280 **urn** http://urn.fi/URN:ISBN:978-952-60-8154-0

Aalto-yliopisto

Tiivistelmä

Aalto-yliopisto, PL 11000, 00076 Aalto www.aalto.fi

Tekijä
Emilia Järvelä

Väitöskirjan nimi
Narrow-line Seyfert 1 -galaksien havainnot ja tilastollinen analyysi

Julkaisija Sähkötekniikan korkeakoulu

Yksikkö Metsähovin radiotutkimusasema

Sarja Aalto University publication series DOCTORAL DISSERTATIONS 163/2018

Tutkimusala Avaruustekniikka

Käsikirjoituksen pvm 07.05.2018 **Väitöspäivä** 12.10.2018

Julkaisuluvan myöntämispäivä 13.08.2018 **Kieli** Englanti

☐ **Monografia** ☒ **Artikkeliväitöskirja** ☐ **Esseeväitöskirja**

Tiivistelmä

Narrow-line Seyfert 1 -galaksit (NLS1, nylsyt) ovat nuoria aktiivisia galakseja, joiden spektrin sallitut emissioviivat ovat epätavallisen kapeita. Nylsyjen emogalaksi on yleensä spiraaligalaksi, ja sen ytimen mustan aukon massa on tavallista pienempi, mutta ydin säteilee lähellä Eddingtonin rajaa. Noin 20 nylsystä on detektoitu gammasäteilyä, mikä tarkoittaa että niissä on voimakas relativistinen plasmasuihku. Aiemmin oletettiin että vain supermassiiviset mustat aukot elliptisten galaksien ytimissä pystyvät synnyttämään relativistisia plasmasuihkuja. Löydös on selvästi ristiriidassa tämän kanssa, joten ymmärrystämme aktiivisista galaksiytimistä ja niiden evoluutiosta tulee arvioida uudelleen ja päivittää.

Tässä väitöskirjassa tutkitaan isoja nylsyotoksia, joita täydennetään pienempien otosten tutkimuksilla. Teimme uusia radio- ja lähi-infrapunahavaintoja, sekä keräsimme uutta tietoa nylsyjen suuren mittakaavan ympäristön ominaisuuksista. Myös jo olemassa olevaa dataa käytettiin yhdessä uuden datan kanssa laajojen tilastollisten tutkimusten, kuten korrelaatio- ja pääkomponenttianalyysien, tekoon.

Metsähovin radiotutkimusasemalla monitoroitiin tähän mennessä suurinta otosta nylsyjä korkeilla radiotaajuuksilla. Radio-ominaisuuksien perusteella valituista lähteistä 19% detektoitiin, ja vastaavasti kohteista, jotka oli valittu muiden ominaisuuksien perusteella, detektoitiin 12%. Jäljempi otos sisältää kohteita, jotka oli aiemmin virheellisesti luokiteltu radiohiljaiseksi, ja yksi niistä osoittautui uudeksi gammataajuuksilla detektoiduksi nylsyksi. Detektio 37 GHz taajuudella tarkoittaa kohteen radiosäteilyn tulevan plasmasuihkusta, osoittaen että voimakkaat suihkut nylsyissä ovat yleisempiä kuin aiemmin on luultu. Nylsyjen plasmasuihkut ovat heikompia kuin blasaarien, mutta skaalattaessa suihkun voima mustan aukon massalla tulee niistä samanveroisia.

Osoittautui että suuren mittakaavan ympäristön tiheys vaikuttaa nylsyjen radio-ominaisuuksiin, ja että plasmasuihkulliset nylsyt sijaitsevat tiheämmillä alueilla kuin suihkuttomat. Keskimäärin nylsyjen suuren mittakaavan ympäristö on kuitenkin huomattavasti harvempi kuin muiden suihkullisten aktiivisten galaksiydinten. Tämä osoittaa että voimakas plasmasuihku voi syntyä millaisessa vain ympäristössä.

Lähi-infrapunahavaintomme Metsähovissa detektoiduista kohteista melkein kolminkertaistivat sellaisten suihkullisten nylsyjen määrän joiden emogalaksin morfologia tunnetaan. Kaikkien havaitsemiemme nylsyjen emogalaksit ovat spiraaligalakseja, mutta toisen galaksin kanssa vuorovaikuttavien galaksien määrä on huomattavasti suurempi kuin ei-suihkullisilla nylsyillä. Tämä viittaa siihen että galaksien välisellä vuorovaikutuksella saattaa olla merkittävä rooli plasmasuihkujen synnyssä. Nylsypopulaation heterogeenisyys olisi selitettävissä sillä että osa niistä on kehittyneempiä kuin toiset, todennäköisesti juuri galaksien välisen vuorovaikutuksen takia.

Avainsanat nylsyt, aktiiviset galaksiytimet, relativistiset plasmasuihkut, suuren mittakaavan rakenne, radioastronomia, pääkomponenttianalyysi

ISBN (painettu) 978-952-60-8153-3 **ISBN (pdf)** 978-952-60-8154-0

ISSN (painettu) 1799-4934 **ISSN (pdf)** 1799-4942

Julkaisupaikka Helsinki **Painopaikka** Helsinki **Vuosi** 2018

Sivumäärä 280 **urn** http://urn.fi/URN:ISBN:978-952-60-8154-0

Preface

First, I want to thank my supervisor, Professor Anne Lähteenmäki, for taking me under her wing and for giving me the opportunity to grow as a scientist, and hopefully also as a person. This thesis would not exist without her and I am grateful for her support through these not always so easy times, and have truly enjoyed our adventures and conversations, scientific and otherwise.

This thesis work was carried out at Aalto University Metsähovi Radio Observatory, Finland. I want to express my gratitude to the whole Metsähovi staff. Any working environment is only as good as its people and Metsähovi is the best. It is a privilege to have been part of the Metsähovi family these last more than eight years. All my other collaborators deserve a thank you as well. Especially Luigi Foschini in Italy and Maret Einasto and Antti Tamm in Estonia who hosted my research visits in their observatories. Part of this work was supported by the Finnish Cultural Foundation.

Great people make the journey easier, and there are too many friends that have supported me during the last four years to list here so consider yourself included. A huge thank you to all of my friends and my family. Kiitos äiti ja isi siitä talvi-illasta 90-luvun alussa ku lähitte lenkille ja jätitte mut siks aikaa kattomaan tähtiä styroksipalan päälle lumihankeen. Special thanks to Pipa and Toffee for their unconditional love.

Elisa, thank you for the unforgettable late night lankakeräkaraoke (Elisa, matkaan!), a few too many "only two" glasses of wine, and for being there when things did not go so smoothly. Thank you my sister-in-arms Aro for hours and hours of laughter (Nuu-Nuu!) and heart-to-hearts when needed. Liisa, I am grateful for our friendship that has already lasted for more than half of my life, and delighted to know that you will always be there for me.

Last, thank you Olli for countless tortilla & wine therapy evenings and brunchners, and for your unconditional support during the last 16 years. Whatever the future holds I know we will get through it – given enough wine.

Espoo, August 23, 2018,

Emilia Järvelä

Contents

List of Publications

This thesis consists of an overview and of the following publications which are referred to in the text by their Roman numerals.

I **E. Järvelä**, A. Lähteenmäki, and J. León-Tavares. Statistical multifrequency study of narrow-line Seyfert 1 galaxies. *Astronomy & Astrophysics*, 573, A76, 24 pages, January 2015.

II L. Foschini, M. Berton, A. Caccianiga, S. Ciroi, V. Cracco, B. M. Peterson, E. Angelakis, V. Braito, L. Fuhrmann, L. Gallo, D. Grupe, **E. Järvelä**, S. Kaufmann, S. Komossa, Y. Y. Kovalev, A. Lähteenmäki, M. M. Lisakov, M. L. Lister, S. Mathur, J. L. Richards, P. Romano, A. Sievers, G. Tagliaferri, J. Tammi, O. Tibolla, M. Tornikoski, S. Vercellone, G. La Mura, L. Maraschi, and P. Rafanelli. Properties of flat-spectrum radio-loud narrow-line Seyfert 1 galaxies. *Astronomy & Astrophysics*, 575, A13, 33 pages, March 2015.

III A. Lähteenmäki, **E. Järvelä**, T. Hovatta, M. Tornikoski, D. L. Harrison, M. López-Caniego, W. Max-Moerbeck, M. Mingaliev, T. J. Pearson, V. Ramakrishnan, A. C. S. Readhead, R. A. Reeves, J. L. Richards, Y. Sotnikova, and J. Tammi. 37 GHz observations of narrow-line Seyfert 1 galaxies. *Astronomy & Astrophysics*, 603, A100, 26 pages, July 2017.

IV **E. Järvelä**, A. Lähteenmäki, H. Lietzen, A. Poudel, P. Heinämäki, and M. Einasto. Large-scale environments of narrow-line Seyfert 1 galaxies. *Astronomy & Astrophysics*, 606, A9, 16 pages, September 2017.

V M. Berton, E. Congiu, **E. Järvelä**, R. Antonucci, P. Kharb, M. L. Lister, A. Tarchi, A. Caccianiga, S. Chen, L. Foschini, A. Lähteenmäki, J. L. Richards, S. Ciroi, V. Cracco, M. Frezzato, G. La Mura, and P. Rafanelli. Radio-emitting narrow-line Seyfert 1 galaxies in the JVLA perspective. *Astronomy & Astrophysics*, 614, A87, 36 pages, June 2018.

VI E. Järvelä, A. Lähteenmäki, and M. Berton. Near-infrared morphologies of the host galaxies of narrow-line Seyfert 1 galaxies. Accepted for publication in *Astronomy & Astrophysics*, February 2018.

VII A. Lähteenmäki, **E. Järvelä**, V. Ramakrishnan, M. Tornikoski, J. Tammi, R. J. C. Vera, and W. Chamani. Radio jets and gamma-ray emission in radio-silent narrow-line Seyfert 1 galaxies. *Astronomy & Astrophysics*, 614, L1, 6 pages, June 2018.

Author's Contribution

Publication I: "Statistical multifrequency study of narrow-line Seyfert 1 galaxies"

The author collected all data, and performed the statistical correlation analyses and the principal component analysis. The author was responsible for writing the paper.

Publication II: "Properties of flat-spectrum radio-loud narrow-line Seyfert 1 galaxies"

The author performed 37 GHz observations and participated in discussion of the results.

Publication III: "37 GHz observations of narrow-line Seyfert 1 galaxies"

The author was responsible for the statistical analyses, spectral energy distribution fitting, and spectral index calculations. The author was also involved in the 37 GHz observations and participated in writing the paper.

Publication IV: "Large-scale environments of narrow-line Seyfert 1 galaxies"

The author collected the multifrequency data, and performed the correlation and statistical analyses including principal component analysis. The author was responsible for writing the paper.

Publication V: "Radio-emitting narrow-line Seyfert 1 galaxies in the JVLA perspective"

The author reduced and partly analysed the JVLA data of approximately one fourth of the sources presented in this paper, and participated in discussion of the results.

Publication VI: "Near-infrared morphologies of the host galaxies of narrow-line Seyfert 1 galaxies"

The author performed the near-infrared observations, reduced the data, and modelled the host galaxies. The author was responsible for writing the paper.

Publication VII: "Radio jets and gamma-ray emission in radio-silent narrow-line Seyfert 1 galaxies"

The author performed the initial gamma-ray data reduction and analysis. The author was also involved in the 37 GHz observations and writing the paper.

List of Figures

List of Tables

Abbreviations

4DE1 4D Eigenvector 1

6dFGS Six-degree Field Galaxy Survey

ADAF Advection Dominated Accretion Flow

AGN Active Galactic Nuclei

BLO BL Lac Object

BLR Broad-Line Region

BLRG Broad-Line Radio Galaxy

BLS1 Broad-Line Seyfert 1

BOSS Baryon Oscillation Spectroscopic Survey

CFS Compact Flat-Spectrum Source

CMASS Constant MASS

CSS Compact Steep-Spectrum

EC External inverse-Compton

ENLR Extended Narrow-Line Region

EV Eigenvector

EW Equivalent Width

F-GAMMA Fermi-GST AGN Multi-frequency Monitoring Alliance

F-NLS1 Flat-Spectrum Radio-Loud Narrow-Line Seyfert 1

Fermi-GST Fermi Gamma-ray Space Telescope

FIRST Faint Images of the Radio Sky at Twenty-Centimeters

FR-I Fanaroff-Riley Class I Radio Galaxy

FR-II Fanaroff-Riley Class II Radio Galaxy

FSRQ Flat-Spectrum Radio Quasar

FWHM Full Width at Half Maximum

GPS Giga-hertz Peaked Source

HBLR Hidden Broad-Line Region

HERG High-Excitation Radio Galaxy

IC Inverse-Compton

ILR Intermediate-Line Region

JVLA Karl G. Jansky Very Large Array

LDF Luminosity-Density Field

LERG Low-Excitation Radio Galaxy

LRG Luminous Red Galaxy

NLR Narrow-Line Region

NLRG Narrow-Line Radio Galaxy

NLS1 Narrow-Line Seyfert 1

NOT Nordic Optical Telescope

NRAO National Radio Astronomy Observatory

NVSS NRAO VLA Sky Survey

OVRO Owens Valley Radio Observatory

PCA Principal Component Analysis

PSF Point Spread Function

Q-NLS1 Radio-Quiet Narrow-Line Seyfert 1

QSO Quasi-Stellar Object

S-NLS1 Steep-Spectrum Radio-Loud Narrow-Line Seyfert 1

SDSS Sloan Digital Sky Survey

SED Spectral Energy Distribution

SKA Square Kilometer Array

SSC Synchrotron self-Compton

Sy1 Seyfert 1

Sy2 Seyfert 2

TS Test Statistic value

ULIRG Ultraluminous Infrared Galaxy

UV Ultraviolet

VBLR Very Broad-Line Region

VLA Very Large Array

VLBI Very Long Baseline Interferometry

List of Latin Symbols

G Gravitational constant

H_0 Hubble parameter

L_R, L_{IR}, L_O, L_X Radio, infrared, optical, and X-ray luminosity

$L_{R,\,\mathbf{jet}}$ Radio luminosity of the jet

$L_\odot$ Luminosity of the Sun

$L_{\mathbf{Bol}}$ Bolometric luminosity luminosity

$L_{\mathbf{Edd}}$ Eddington luminosity

$L_{\mathbf{bulge}}$ Luminosity of the bulge

M_B Optical absolute magnitude

$M_\odot$ Mass of the Sun

$M_{\mathbf{BH}}$ Black hole mass

$P_{\mathbf{1.4GHz}}$ Power at 1.4 GHz

$P_{\mathbf{jet}}$ Jet power

R_S Schwarzschild radius

R Radio loudness

S_R, S_{IR}, S_O, S_X, S_γ Radio, infrared, optical, X-ray, and gamma-ray flux density

$S_{\mathbf{0}}$, $S_{\mathbf{obs}}$ Intrinsic and observed flux density

$S_{\mathbf{j}}$, $S_{\mathbf{cj}}$ Flux density of the approaching and the receding jet

T_B Brightness temperature

$\mathscr{R}$ Ratio between the peak and the total flux density

c Speed of light

h_0 Dimensionless Hubble parameter

v Speed

z Redshift

eV Electronvolt

Jy Jansky

K Kelvin

pc Parsec

px Pixel

R4570 Flux density ratio of Fe II and the broad component of Hβ

List of Greek Symbols

Γ Photon index, $\alpha + 1$

α Spectral index

$\beta_{\mathbf{app}}$ Apparent speed

β Speed compared to the speed of light, v/c

δ Relativistic Doppler factor

ϵ Radiative efficiency

γ Lorentz factor

λ Wavelength

$\nu_{\mathbf{crit}}$ Critical frequency

ν Frequency

σ Stellar velocity dispersion of a bulge

$\theta_{\mathbf{max}}$ Major axis in milliarcseconds

$\theta_{\mathbf{min}}$ Minor axis in milliarcseconds

θ Viewing angle of the jet

1. Active galactic nuclei

1.1 Introduction

According to our current knowledge in the centre of almost every galaxy lies a massive black hole. Most of these black holes are in a dormant state, but about 10% are actively accreting matter, and as a consequence generate radiation over the whole electromagnetic spectrum from radio to TeV energies. These active black holes and the nuclear region around them are called active galactic nuclei (AGN), and they are the most energetic non-transient phenomena in our Universe.

The first optical spectrum of an AGN, NGC 1068, showing strong emission lines was obtained already in 1908 by Edward Fath (Fath 1909). At the time NGC 1068 was thought to be a galactic nebula since the existence of other galaxies was still under debate. More sources of similar nature were discovered almost 20 years later in 1926 when Edwin Hubble identified NGC 4051 and NGC 4151, which were showing the 'nebula type' emission-line spectra (Hubble 1926b). Another 20 years passed until Carl Seyfert in 1943 published his pioneering work of these sources; he obtained spectra of six galaxies with high, stellar-like central surface brightness, and all of them exhibited strong high-ionisation emission lines (Seyfert 1943). He was the first astronomer to realize that these objects form a distinct class, and they were eventually named 'Seyfert galaxies' after him, although the original definition has changed afterwards.

The first radio detection of an AGN at radio frequencies was made in 1944 by Grote Reber when he detected Cygnus A at 160 MHz (Reber 1944). The nature of the source was unclear at the time. More objects of similar nature were found in radio surveys performed in the late 1950s and early 1960s. The objects of this type were named Quasi-Stellar Radio Sources due to their stellar-like optical appearance. A breakthrough was made in 1963 when Maarten Schmidt realised that the peculiar, unidentified emission lines in the spectrum of 3C 273 were the hydrogen Balmer-series emission lines at redshift $z = 0.158$ (Schmidt 1963), placing it well beyond our Galaxy. Taking into account the vast distance, 3C 273 was estimated to be one hundred times more luminous than a normal bright spiral galaxy (Schmidt 1963). Even though the nature of these sources was still unclear it was understood that the

enormous luminosity originated in previously unknown processes. Soon after the discovery it was suggested that massive black holes might be involved in generating the unprecedented amounts of energy (Zel'dovich & Novikov 1964).

In addition to the radio surveys, the first systematic optical and ultraviolet (UV) surveys to find more AGN were performed in the 1960s by Fritz Zwicky and Benjamin Markarian (e.g., Zwicky et al. 1961, 1963; Markarian 1967; Markaryan 1969). In 1969 it was proposed that the non-thermal emission seen in Seyfert galaxies was powered by accretion to a supermassive black hole, as in quasi-stellar radio sources, later known as quasars. It was suggested that also the nearby inactive galaxies harbour supermassive black holes in their centres, understood as 'dead' quasars (Lynden-Bell 1969). Since then a variety of AGN classes with different intrinsic and observational properties has been found and classified. However, the AGN phenomenon is broad and complicated, and we still do not have a final, comprehensive picture of its diversity.

1.2 Structure of AGN

Despite the diverse observational properties of the AGN classes, the basic structure is believed to be rather similar, shown in Figure 1.1. In the centre resides a black hole, with a mass in the range of $10^5 M_\odot$ to $10^{10} M_\odot$. Its effective size, or event horizon, is determined by its mass and is called Schwarzschild radius, R_S [1]. Just outside the black hole, from few R_S to some hundreds of R_S, lies the accretion disk consisting of matter orbiting the black hole. The matter in the accretion disk loses energy due to viscous processes and eventually falls into the black hole. There are several models for the physics of the accretion disk, the most relevant three being the radiatively efficient, geometrically thin but optically thick disk model (Shakura & Sunyaev 1973, 1976), the radiatively inefficient advection dominated accretion flow (ADAF) model (Ichimaru 1977; Narayan & Yi 1994), and the slim disk model with a disk-like geometry but a significant amount of advection (Abramowicz et al. 1988; Szuszkiewicz et al. 1996; Mineshige et al. 2000a). Most accretion disks are assumed to be stardard thin disks, which radiate from optical to soft X-ray band and have a quasi-blackbody spectrum, with effective temperature around 10^5–10^7 K. Further out, around 0.01–0.5 pc, is the broad-line region (BLR) consisting of virialised gas clouds orbiting the black hole at relatively high speeds (1000-10000 km/s). The broad permitted emission lines in the optical and near-infrared spectra arise from this region. The exact geometry, whether it is spherical or flattened, of the BLR is still unknown. There is growing evidence that the BLR might consist of two kinematically separate regions: a very broad-line region (VBLR) and an intermediate-line region (ILR, e.g., Hu et al. 2008; Zhu et al. 2009; Adhikari et al. 2018), which might reach up to the narrow-line region (NLR, see also Sulentic & Marziani 1999). At distances 10 to 100 pc lies a toroidal region of optically thick molecular clouds. These clouds absorb radiation from the central engine and re-emit it in infrared. In a region beyond 100 pc lies the NLR. It consists of very low density gas, moving at low velocities. This gas is responsible for

[1] $R_S = 2M_{\rm BH}G/c^2$, where G is the gravitational constant and c is the speed of light.

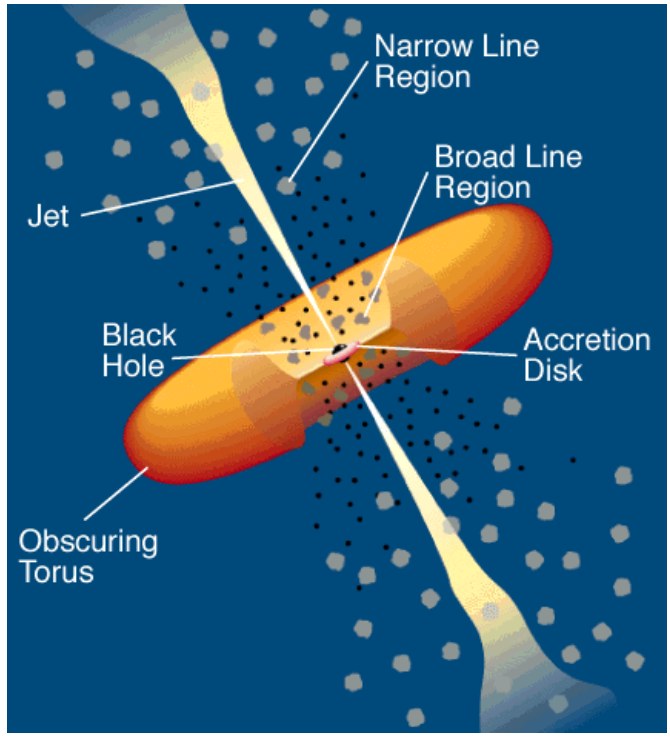

Figure 1.1. Schematic structure of an AGN (Urry & Padovani 1995).

the (semi-)forbidden narrow emission lines seen in the spectra. In some sources the region of ionised low-density gas can reach up to 15 – 20 kpc. Since the gas is being ionised by the central continuum, its distribution shows a (bi-)conical shape (Cracco et al. 2011), with an opening angle similar to that of the obscuring, molecular torus. This region is called the extended narrow-line region (ENLR). In addition to these components some AGN possess jets launched perpendicularly to the accretion disk and torus plane on both sides. There exists a variety of jets with different properties, the most powerful ones being the highly collimated relativistic jets, explained in more detail in the next Section.

1.2.1 Jets in AGN

Jets are formed when a fraction of the ionised matter falling towards the black hole interacts with the magnetic field near the black hole. Instead of falling into the black hole the matter is launched away from it along perpendicular magnetic field lines (Blandford & Znajek 1977). Depending on the initial parameters of the system, for example, the black hole spin, the strength of the magnetic field, and the density of the surrounding matter, the jets differ in power and consequently in appearance. Some

jets terminate at rather small distances (a few pc), but the most powerful ones (~10% of them) accelerate to a speed close to the speed of light (c). They can stay collimated for several kpc and reach well outside the host galaxy (Mpc-scale jets).

The charged particles spiraling along the magnetic field lines feel constant acceleration and emit non-thermal synchrotron radiation towards the direction they are moving to. The lighter electrons, and possibly also positrons, are accelerated more efficiently than heavier protons and ions, and thus emit practically all the observed radiation. The energy distribution of these particles often has a power-law shape, resulting in a power-law shaped observed spectrum with $S \propto \nu^{\alpha}$, where S is the emitted flux density, ν the frequency, and α the power-law index. Optically thin synchrotron radiation would lead to continuously rising spectrum towards the lower frequencies, but in practise this is prevented by synchrotron self-absorption. Below a critical frequency, ν_{crit}, the emitted synchrotron photons can be re-absorbed by the charged particles that emitted them. The lower the energy of the photon, the higher are the chances for it to be absorbed; this mechanism essentially leads to a decreasing spectrum towards the lower frequencies below ν_{crit}. Synchrotron radiation is generally observable from radio to optical/UV bands, depending on the source type. It corresponds to the first bump seen in the spectral energy distribution (SED) of a source whose emission is dominated by a relativistic jet. An example SED of such a source, blazar Mrk421, is shown in Figure 1.2.

The higher frequency bump, reaching up to gamma-rays and even TeV energies in some sources, is believed to be produced by inverse-Compton (IC) mechanism in a leptonic jet. In IC scattering photons gain energy from relativistic electrons. The seed photons can originate either from the ambient photon field around the jet (external inverse-Compton, EC) or they can be synchrotron photons produced by the jet itself (synchrotron self-Compton, SSC). Alternative explanations include lepto-hadronic and hadronic jet models in which also protons are accelerated to relativistic energies (Boettcher 2010).

The jet is rarely a smooth flow of relativistic electrons, but has substructure, for example, components consisting of blobs of matter propagating along the jet, and moving and standing shocks (Marscher & Gear 1985; Türler 2011). These changing and evolving features cause the variability, for example, flares, seen in AGN with jets. The variability of AGN is explained in more detail in Section 1.4.

In cases where the relativistic jet points very close to our line-of-sight, relativistic effects take place. Due to the relativistic speed of the particles travelling in the jet apparently superluminal motion of the components can be observed. The apparent speed of the photon emitting source is given by

$$\beta_{app} = \frac{\beta \sin\theta}{1 - \beta \cos\theta} \tag{1.1}$$

where β is the actual speed in units of the speed of the light, v/c, and θ the angle between the jet and the line of sight of the observer. This time dilation effect also boosts radiation arriving from a relativistic source, because in the rest frame of the observer the delay between the arriving photons is shorter than in the rest frame of the

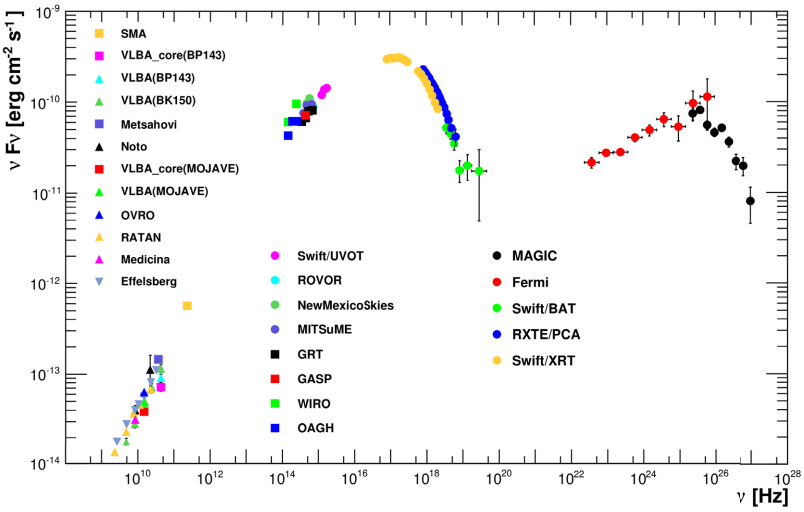

Figure 1.2. Simultaneous SED of Mrk421 (Lorenz & Wagner 2012).

emitter.

Another relevant effect is the relativistic Doppler boosting. The strength of this effect is given by the relativistic Doppler factor

$$\delta = \frac{\sqrt{1-\beta^2}}{1-\beta\cos\theta} = \frac{1}{\gamma(1-\beta\cos\theta)} \tag{1.2}$$

where γ is the Lorentz factor

$$\gamma = \frac{1}{\sqrt{1-\beta^2}}. \tag{1.3}$$

At a given redshift the observed Doppler factor is $\delta/(1+z)$. This effect boosts radiation traveling towards the observer and dims radiation traveling away from the observer. Due to relativistic Doppler boosting also the changes in the brightness of the jet are considerably boosted. Furthermore, relativistic Doppler effect can explain why radio galaxies often show a jet and a counter-jet, whereas only the approaching jet is seen in quasars and blazars. Flux ratio between the approaching and receding jet is expressed as

$$\frac{S_{\rm j}}{S_{\rm cj}} = \left(\frac{1+\beta\cos\theta}{1-\beta\cos\theta}\right)^{2-\alpha}. \tag{1.4}$$

where $S_{\rm j}$ is the flux density of the approaching jet, $S_{\rm cj}$ the flux density of the receding jet, and α the spectral index of the jet.

A third effect increasing the observed flux density is the relativistic aberration, or beaming. Radiation from a source emitting isotropically (or in a doughnut-shape as in the case of synchrotron electrons) in its co-moving rest frame concentrates into a narrow cone, pointing towards the direction the emitter is moving to. The cone

becomes narrower with increasing speed; for $\gamma \gg 1$, the half-width of the cone is $\sim 1/\gamma$.

Taking into account all these relativistic effects – time dilation, Doppler boosting, and beaming – the observed radiation is in practice enhanced by

$$S_{\rm obs} = S_0 \delta^{3-\alpha} \tag{1.5}$$

where $S_{\rm obs}$ is the observed, or beamed flux density, S_O the flux density in the frame co-moving with the jet, that is, the unbeamed flux density, and α is the intrinsic spectral index of the jet power-law.

1.2.2 The jet paradigm

Conventionally extreme radio loudness[2] (R) and consequently the most powerful relativistic jets have almost exclusively been associated with the most massive black holes ($M_{\rm BH} > 10^8 M_\odot$) residing in highly evolved, massive elliptical galaxies (e.g., McLure et al. 1999; Laor 2000), whereas the AGN found in spiral galaxies seem to consistently belong to the radio-weak population (Bahcall et al. 1997). However, among the radio-loud AGN the black hole mass does not seem to correlate with other observed properties, for example, the radio luminosity, radio loudness or Eddington ratio, nor with any host galaxy properties – except that they consistently are ellipticals (Urry 2003). It has been proposed that the period of enhanced black hole accretion activity – and the formation of jets – is a phase most galaxies undergo, and it coincides with the formation of a classical bulge, probably via merger-induced, dissipative collapse (Kormendy & Gebhardt 2001; Urry 2003). Depending on the properties of this event, the black hole and its nearby environment, the forming jet could exhibit a variety of properties accounting for both radio-quiet and radio-loud AGN. This scenario could explain the absence of powerful relativistic jets in spirals whose bulge-growth and black hole activity is dominated by secular processes.

Kaviraj et al. (2015) studied a sample of AGN hosted by late-type[3] galaxies and with radio luminosities comparable to 'normal' radio AGN hosted by ellipticals. They found the stellar masses in radio AGN hosted by late-type galaxies are higher than in late-type galaxies in general, and the merger fraction among them is ~4 times higher than in the general population of late-type galaxies. This result supports the essential role of mergers in triggering the nuclear activity. Furthermore, about a dozen spiral galaxies have been found to host kpc-scale or even Mpc-scale relativistic jets, or relic radio lobes indicating earlier activity (Hota et al. 2011; Bagchi et al. 2014; Singh et al. 2015). Their stellar ($M_{\rm stellar} > 10^{11} M_\odot$) and black hole ($M_{\rm BH} > 10^8 M_\odot$) masses are comparable to massive ellipticals that usually host radio-loud AGN (Bagchi et al. 2014; Tadhunter 2016). Also a few of them are mergers, which could explain

[2]Radio loudness, R, is defined as the ratio between radio flux density, S_R, and optical flux density, S_O, originally at 5 GHz and in B-band, respectively (Kellermann et al. 1989). Sources with $R > 10$ are considered radio-loud, and sources with $R < 10$ radio-quiet.

[3]Late-type galaxies include all varieties of spiral galaxies, and early-type galaxies all elliptical galaxies, according to the galaxy morphology diagram first described in Hubble (1926a).

the triggering of a jet according to the aforementioned scenario. However, they are generally rather low-power sources (Tadhunter 2016). Bagchi et al. (2014) further argues that the black holes residing in galaxies with the most extended Mpc-scale jets are spinning rapidly and accrete via ADAF at low Eddington ratios (see Section 1.3). These sources, however, are extremely rare (Tadhunter 2016).

Indeed, the black hole spin has been proposed as an alternative explanation to the differences between radio-loud and radio-quiet sources, as well as the general absence of relativistic jets in spiral galaxies (Wilson & Colbert 1995; Sikora et al. 2007; Tchekhovskoy et al. 2010; Dotti et al. 2013). According to the spin paradigm a powerful jet cannot be formed by a non-rotating or slowly rotating black hole, but an almost maximally rotating black hole is needed. Rapidly spinning black holes can be created in mergers under ideal conditions when the central black holes coalesce, or via normal, prolonged gas accretion as long as the accretion is not isotropic (Volonteri et al. 2005; Dotti et al. 2013).

A less massive black hole ($M_{\mathrm{BH}} < 10^7 M_{\odot}$) in a spiral galaxy can also reach a high spin, but due to its small mass the spin axis of the black hole exhibits erratic behaviour, aligning with the angular momentum of the disk in each accretion episode. This is manifasted as jets showing random orientations relative to the host galaxy axis (Kinney et al. 2000; Schmitt et al. 2001). A smaller mass black hole can also experience short-lived accretion events (Capetti et al. 1999; Kharb et al. 2006) during which the disk stays counter-rotating and decreases the black hole spin. On the other hand, more massive black holes ($M_{\mathrm{BH}} > 10^7 M_{\odot}$), mostly residing in ellipticals, are massive enough, when compared to the mass of the accretion events, so that their spin axes remains stable. A more massive black hole is also able to force the accretion flow to co-rotate, and thus all accretion events increase the spin. This can explain why relativistic jets seem to exclusively be a property of elliptical galaxies. In this scenario the jet energy is drained from the spin energy of the black hole via the Blandford-Znajek mechanism (Blandford & Znajek 1977). Spin-based theories usually invoke ADAF as the accretion mechanism since a standard accretion disk cannot account for the wide range of observed jet powers (Tchekhovskoy et al. 2010).

1.3 Taxonomy and unification

Taxonomy and unification of AGN is complicated at best; our current knowledge is not sufficient enough to piece together a complete picture of the diverse AGN phenomenon. Here the main classes and their differences, and the simple orientation-based unification model of AGN will be covered. A schematic view of our current understanding of the orientation-based unification model of the most essential AGN classes is shown in Figure 1.3 – a more detailed description is available, for example, in Beckmann & Shrader (2012).

Traditionally AGN have been divided into two main types based on their radio-to-optical flux density ratio; radio-quiet and radio-loud AGN, which, based on their properties, would form two clearly distinct populations. The main assumption was

that the differences stem from the presence of a powerful relativistic jet in radio-loud AGN, and the lack of it in radio-quiet sources (e.g., Hutchings et al. 1989; Wilson & Colbert 1995). The ability of AGN to launch a relativistic jet seemed to be connected to the properties of its black hole, favouring the most massive ones, and its host galaxy, usually an old, massive elliptical, leading to the composition of the traditional jet paradigm (e.g., Laor 2000; Chiaberge & Marconi 2011).

The ambiguity of the radio loudness parameter was realised early on (Wadadekar & Kembhavi 1999), and has since lost its status as the ultimate dividing factor between AGN types. Moreover, the radio loudness parameter does not successfully predict the presence of a powerful jet in an AGN, except for the radio-loudest objects. There is growing evidence that the AGN population is not straightforwardly bimodal (Cirasuolo et al. 2003; Zamfir et al. 2008) , but exhibits continuous distributions in wide range of observable properties. Alternative ways to describe the AGN population have been proposed, for example, the 4D Eigenvector 1 (4DE1) AGN parameter space (see Section 2.4.2). Lately it has been suggested that the radio loudness parameter is obsolete and should not be used; instead sources should be grouped based on their actual physical properties, that is, whether the source has a powerful relativistic jet or not (e.g., Padovani 2016, 2017, Publication IV, Publication VII).

Approximately ∼90% of AGN do not host relativistic jets, although it is possible that they are able to launch less powerful, non-relativistic jets, and/or exhibit non-collimated outflows. However, jet activity in them is not as distinct and dominant as in the jetted sources. A large fraction of non-jetted AGN are Seyfert galaxies and quasars. These two classes were originally defined by their optical absolute magnitude: Seyfert galaxies are less luminous with $M_B >$ -21.5 + 5 log h_0 [4] (Schmidt & Green 1983) and quasars brighter with $M_B <$ -21.5 + 5 log h_0. Most Seyfert galaxies are at low redshifts and their preferably, but not exclusively, disk-like host galaxies are usually observable, whereas quasars reside at higher redshifts and often appear stellar-like point sources. Later studies have revealed that these two classes are quite similar, and non-jetted quasars might represent scaled-up and thus more luminous versions of Seyfert galaxies (Leipski et al. 2006).

Observationally most of the diversity among the non-jetted AGN arises from the obscuration of the central engine. Since the most prominent obscurer is the non-isotropic molecular torus, the most distinct observational differences are caused by the orientation of the AGN relative to the observer. When seen face-on at small inclination angles the central region of the AGN is visible to the observer and the optical spectrum exhibits both broad emission lines arising from the BLR and narrow emission lines originating in the NLR. These are called Type 1 AGN and include, for example, Seyfert 1 (Sy1) galaxies and most quasars. When the inclination increases the torus begins to gradually obscure the view to the inner region and the intensity of the broad emission lines starts to decrease. Finally the torus completely hides the nuclear region and only narrow lines from the NLR are visible in the optical spectrum; these are Type 2 AGN. However, the opening angle and the geometry of the torus are not constant,

[4] h_0 is the dimensionless Hubble parameter with a value between 0 and 1. It relates to the Hubble parameter as $H_0 = 100\,h$ km s^{-1} Mpc^{-1}.

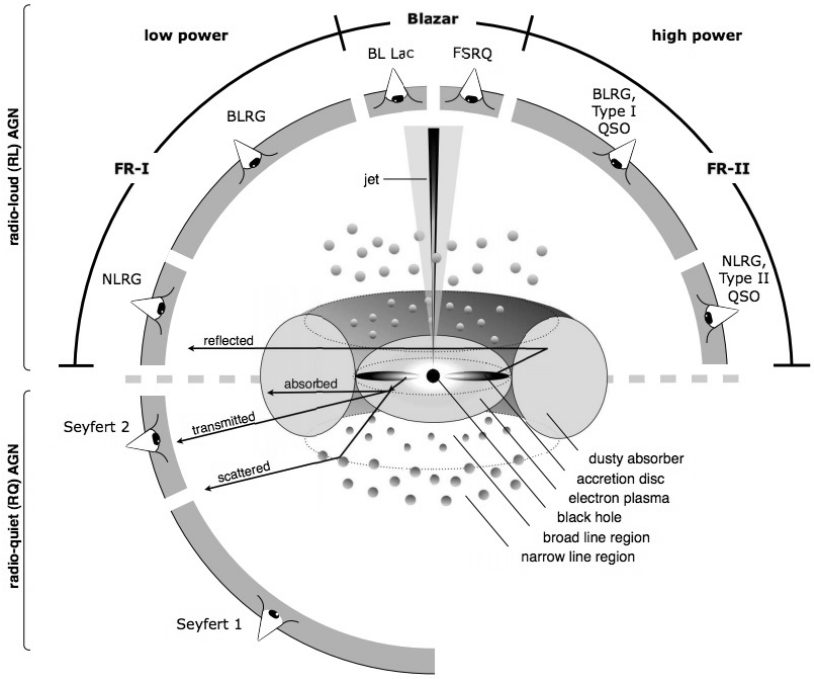

Figure 1.3. Orientation-based unification scheme of the largest AGN classes (Beckmann & Shrader 2012).

and neither are the properties of the BLR and the accretion disk. For example, some Seyfert 2 (Sy2) galaxies are 'pure' Type 2 AGN in a sense that they totally lack the BLR (Heisler et al. 1997; Tran 2001, 2003). Additionally variability can cause an AGN to seemingly change type over time (Penston & Perez 1984; LaMassa et al. 2015; Yang et al. 2017).

Orientation is a significant factor also among the jetted AGN. Jetted AGN viewed at high inclinations are called radio galaxies. Optically they can be divided into broad-line radio galaxies (BLRG) and narrow-line radio galaxies (NLRG), equivalent to Sy1 and Sy2 galaxies, respectively. The most distinct feature of radio galaxies is the massive radio jets and lobes that might reach up to several Mpc, well outside the host galaxy. Based on the properties of the jets radio galaxies are classified as Fanaroff-Riley I (FR-I) and II (FR-II): FR-I sources are less luminous and most of the radio emission comes from near the nucleus, whereas FR-II types are more luminous and the radio emission is dominated by the radio lobes far away from the nucleus (Fanaroff & Riley 1974). Compact types of jetted AGN seen almost edge-on are compact steep-spectrum sources (CSS), giga-hertz peaked sources (GPS), and compact flat-spectrum sources (CFS). They exhibit smaller jets still contained inside the host galaxy ($\sim$10 pc to 20 kpc), and are believed to be very young radio galaxies.

When moving towards smaller inclinations radio galaxies appear as radio-bright quasars, and when seen almost pole-on as blazars. The prominent difference between

the observational characteristics of quasars and blazars is due to the relativistic beaming effects at very small inclination angles (see Section 1.2.1). The main classes of blazars are BL Lac Objects (BLO) and flat-spectrum radio quasars (FSRQ), which are likely to represent the beamed versions of FR-I and FR-II radio galaxies, respectively (Kharb & Shastri 2004). It has been further proposed that there are two intrinsically disparate types of sources with powerful relativistic jets with the main observational difference being the optical spectrum; high-excitation radio galaxies (HERG) exhibit strong narrow-line emission and sometimes also broad lines, whereas low-excitation radio galaxies (LERG) show only weak or no emission lines at all. FR-I/BLO sources tend to be LERGs and FR-II/FSRQ sources HERGs, but there is substantial overlap (Landt et al. 2004). LERGs and HERGs seem to correspond to two different modes of nuclear activity in AGN (e.g., Hardcastle et al. 2006).

LERGs are proposed to be accreting slowly cooling hot gas which is unable to form traditional accretion disk and molecular torus. Instead the accretion flow is believed to be radiatively inefficient and almost spherical, or to form a puffed accretion disk; indeed the jet power has been found to be proportional to the accretion inside the Bondi radius (Allen et al. 2006). Accretion efficiency in LERGs in also very low, $L/L_{\rm Edd} \leq 1\%$. The environment near the nucleus is photon-poor and thus the electron cooling time is long which causes the characteristic bumps in the SED to move to higher energies. The IC process in LERGs is probably SSC. LERGs are mostly hosted by red ellipticals, which supports their accretion scenario (Janssen et al. 2012; Butler et al. 2018). On the other hand, HERGs have conventional accretion disks and tori, and accrete cold gas through radiatively efficient accretion flow. They accrete more efficiently with $L/L_{\rm Edd} \approx$ 1-10%. Due to a photon-rich environment electrons cool efficiently, and peaks in the SED are at lower frequencies. In contrast to LERGs, the IC process is believed to be EC. Their host galaxies are mostly blue or green star-forming galaxies, indicating that they are younger, or possible rejuvenated, sources (Janssen et al. 2012; Butler et al. 2018). There does not exist a clear divisible luminosity limit between LERGs and HERGs, but on average HERGs are more luminous than LERGs (Best & Heckman 2012; Butler et al. 2018).

1.4 Variability

AGN are variable over the whole electromagnetic spectrum, and at various amplitudes and timescales from minutes to hundreds of thousands of years and longer. While the longest timescales are associated with the evolution of the AGN and persistent changes in its intrinsic properties, for example, the black hole mass, the shorter timescale variations depict the current physical properties of the AGN and the diverse processes taking place in them. The characteristic timescales of the variability give an estimate of the size of the emitting region: the variability timescale is approximately the photon-crossing time of the region and changes at much shorter timescales will be evened out. The observed variability of non-jetted and jetted sources are vastly different.

The total emission of a non-jetted AGN is a sum of many intricately connected components of which the most relevant ones are shown in Figure 1.4. The variations in the optical and UV bands are to some extent believed to arise from instabilities in the accretion disk. This is supported by the observed effect that variability is faster at higher frequencies, arising from the hotter accretion disk closer to the black hole, and slower at lower frequencies, originating in a cooler disk farther away from the centre. Also near-infrared variability can be accounted to the changes in the accretion disk, since it is mostly accretion disk emission reprocessed by the molecular torus.

The X-ray emission of non-jetted AGN consists of multiple components. Underlying is a broad power-law component originating in a corona of hot plasma above the accretion disk. The corona reprocesses the accretion disk photons to X-ray energies via IC. The additional component seen in hard X-rays is believed to originate in the reflection of the coronal X-ray photons by the accretion disk. The most distinct feature, however, is the soft X-ray (< 1 keV) excess seen in most Type 1 AGN, especially in sources with high Eddington ratios (Boissay et al. 2016). This feature exhibits large amplitude variability at very short timescales; in the most extreme cases a flux density increase by a factor of ~50 can be seen in a few days (Boller et al. 1997), indicating that the emission is produced by a very compact region. The exact generation mechanism of this excess is still unknown, but the most plausible explanations include blurred reflection by the accretion disk (Nardini et al. 2011) or an additional Comptonisation component (Lohfink et al. 2013; Boissay et al. 2016).

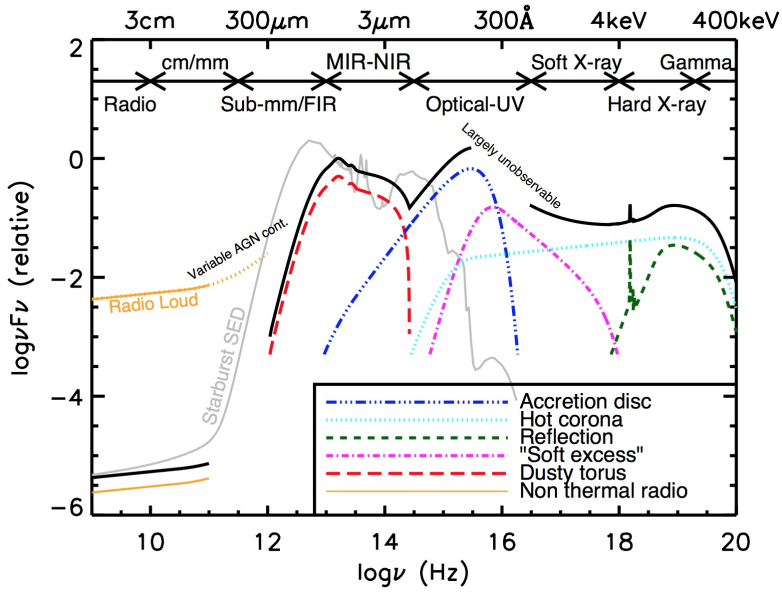

Figure 1.4. Schematic SED of a non-jetted AGN (Harrison 2014).

In jetted AGN the emission is dominated by the relativistic jet that causes most of the variability. In the SED of a jetted AGN two prominent bumps can be seen, as shown

in Figure 1.5. The origins of these bumps were elaborated in Section 1.2.1: the lower frequency bump is due to the synchrotron radiation in the jet, and the higher frequency bump originates in IC scattering via EC or SCC. The variability mechanisms seen in non-jetted AGN are also in effect, but in the most powerful jetted sources they are overpowered by the jet emission and are therefore rarely observable.

Jetted AGN often show a low and a high emission state. In the low-state emission from the accretion disk, the molecular torus and the corona can sometimes be distinguishable. High states are often associated with the ejection of a new component into the jet, also leading to considerable changes in the polarisation properties of the source. An increase in the flux density can usually first be seen in gamma-rays – or TeV energies in the most extreme cases – which is often accompanied, with a short lag, with an increase in the optical/UV emission. Sometimes the increase is simultaneous or the optical leads gamma-rays, depending on the jet characteristics. The flare then propagates to lower frequencies and radio usually lags gamma-rays by some months, but this lag is highly variable from flare to flare and source to source (e.g., Berton et al. 2017; Lisakov et al. 2017). During the high state, in addition to the increased luminosity, the peaks of the synchroton and IC emission often shift to higher frequencies – in contrast to BLOs among which the lower luminosity sources peak at higher frequencies. The synchronised changes in the SED components indicate that they originate in the same electron population. However, the amplitude of the variations compared to each other is not constant, and also orphan gamma-ray and optical/radio flares are common, showing that the situation is exceedingly complicated and the physics behind them are not yet fully understood. Moreover, variability can be due to other mechanisms as well, for example, changes in the size or position of the emitting region, or changes in the energy distribution or density of the electron population (e.g., Collmar et al. 2010; Ghisellini et al. 2013).

As a consequence of the intrinsic variability also the spectral properties of AGN vary. Multiple characteristics of the broad optical/UV emission lines vary at rather short timescales, for example, the flux density, line profiles, and shifts (Ilić et al. 2015). Since the origin of these lines is the BLR, photoionised by the central continuum source, also their variations (mainly the flux density) follow any changes in the ionising continuum with a time lag of a few days to a few weeks, comparable to the photon-crossing time from the continuum source to the BLR. Also intrinsic changes in the size and geometry of the BLR induce spectral variability. Over longer time periods dramatic changes, such as emission lines disappearing and reappearing, can occur. At times these changes are strong enough to seemingly cause the AGN to change type (Penston & Perez 1984; LaMassa et al. 2015; Yang et al. 2017).

In jetted AGN variability in the broad-band radio spectra can be seen. However, the radio spectrum does not vary in a similar fashion in all sources but various patterns have been recognised. Most observational characteristics of variability can be explained by only two different physical processes (Angelakis et al. 2012). The first kind of variability is due to an underlying steep spectrum and a superimposed flare moving from higher to lower frequencies. When multiple components are moving along the jet at the same time it also produces the flat spectrum usually seen in jetted AGN

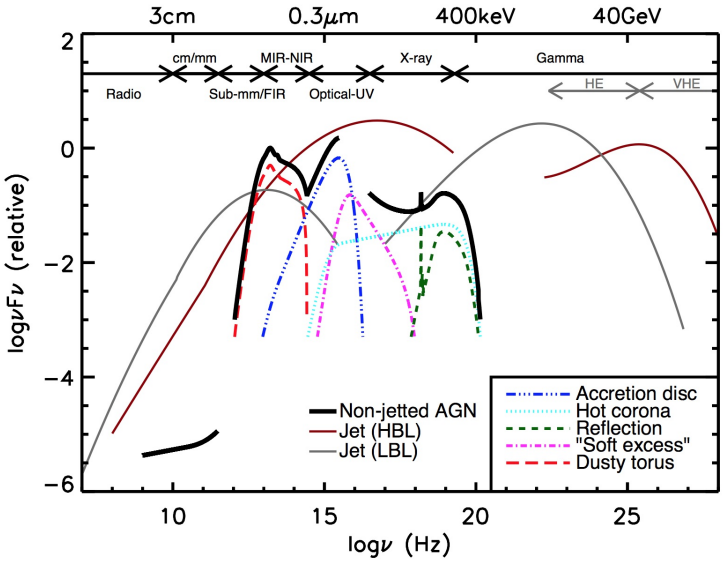

Figure 1.5. Schematic SED of a jetted AGN (Padovani 2016).

(Marscher & Gear 1985; Türler 2011; Planck Collaboration et al. 2016). Another type is achromatic variability in which the emission level of the whole radio spectrum changes at the same time without considerable frequency dependence. Angelakis et al. (2012) hypothesise that the origin of this kind of variability could be, for example, changes in the magnetic field, or the synergy of changing Doppler factors and geometrical effects.

2. Multiproperty studies of narrow-line Seyfert 1 galaxies

Narrow-line Seyfert 1 (NLS1) galaxies are a subclass of AGN, first described in 1985 (Osterbrock & Pogge 1985). Their characterising feature is the narrowness of the permitted emission lines generated in the BLR. By definition FWHM(Hβ) in NLS1 galaxies is < 2000 km s^{-1} (Goodrich 1989). Their [O III] emission, compared to the broad component of Hβ, is relatively weak, S([O III])/S([Hβ]) < 3, and Fe II compared to the total Hβ emission is relatively strong (Osterbrock & Pogge 1985). The optical spectrum is discussed in more detail in Section 2.1. NLS1 galaxies harbour low- or intermediate-mass black holes ($M_{\rm BH}$<10^8 $M_\odot$, Peterson et al. 2000) accreting at extraordinarily high rates, from 0.1 Eddington ratio to even super-Eddington accretion (Boroson & Green 1992). This indicates that the accretion disks in NLS1 nuclei are slim disks that allow high Eddington ratio accretion (Mineshige et al. 2000b; Wang & Netzer 2003). The majority of NLS1 galaxies show a strong soft X-ray excess (Boller et al. 1996), and many of them exhibit high-amplitude X-ray variability in very short timescales (e.g., Boller 2000; Fabian et al. 2013). NLS1 nuclei, at least the more studied radio-quiet ones, are preferentially, but not exclusively, hosted by late-type galaxies (Ohta et al. 2007). Only ∼10% of NLS1 galaxies are radio-loud (Komossa et al. 2006). The radio properties are discussed in Section 2.3. All of these characteristics point to the young, unevolved nature of the NLS1 class (Mathur 2000).

In 2009 an NLS1 galaxy, PMN J0948+0022, was detected at gamma-rays by the Large Area Telescope (LAT) onboard *Fermi Gamma-ray Space Telescope* (*Fermi-GST*, hereafter *Fermi*) (Abdo et al. 2009a; Foschini 2011). This discovery made NLS1 galaxies the third class of AGN detected at gamma-rays, and, more importantly, confirmed the presence of a relativistic jet in an NLS1 source. After the discovery of the first gamma-ray emitting NLS1 galaxy by *Fermi* (Abdo et al. 2009a; Foschini 2011), searches for more of these peculiar sources ensued. Since then almost 20 NLS1 sources have been detected at gamma-rays (e.g., Foschini 2011; Paliya et al. 2018, Publication VII), establishing them as a class of sources able to launch fully-developed relativistic jets. Unsurprisingly most of the NLS1 sources detected at gamma-rays so far are also some of the most radio-loud NLS1 sources, and, with a few exceptions (Schulz et al. 2016), exhibit flat radio spectra (Abdo et al. 2009b, Publication II). NLS1 galaxies are considerably variable at gamma-rays and often detectable only when flaring (Foschini 2011). This indicates that with continuous monitoring more

gamma-ray bright NLS1 galaxies can be expected to be discovered.

On average NLS1 galaxies show steep gamma-ray spectra ($\Gamma_\gamma \sim 2.6$, Publication II, Paliya et al. 2018) comparable to FSRQs ($\Gamma_\gamma \sim 2.4$) and significantly softer than the gamma-ray spectra of BLOs (Ackermann et al. 2011). The gamma-ray luminosities of NLS1 galaxies are generally between 10^{44} and 10^{46} erg s^{-1}, with only a few sources reaching 10^{47} erg s^{-1} (Paliya et al. 2018; Yang et al. 2018). This is a few orders of magnitude lower than what is seen in FSRQs but comparable to the gamma-ray luminosities of BLOs (Publication II). However, NLS1 galaxies and BLOs are otherwise clearly separate classes, as discussed in Section 3.1.2. NLS1 galaxies are more alike to FSRQs and it has been suggested that they form the low-mass tail of FSRQs. Based on their observed properties, for example, flares seen at radio and gamma-rays, and variability of their radio spectra, the jets in NLS1 galaxies behave similarly as the jets in more powerful blazars. The intrinsic properties of NLS1 galaxies are in disagreement with the traditional jet paradigm; they seem to differ from blazars in black hole masses, Eddington ratios, host galaxies (see Section 2.5.1), and radio morphologies (see Section 2.3). It has been suggested that the black hole masses calculated based on the emission line widths are underestimated due to the orientation effects caused by a disk-like broad line region seen face-on (Decarli et al. 2008). This effect would have an impact especially on the black hole mass estimates of gamma-ray-detected sources, known to be observed at small inclinations. This could in principle explain the black hole mass deficit in NLS1 galaxies, however, some studies using orientation-independent methods have found the black hole masses to be genuinely low (e.g., Publication II, Wang et al. 2016). This issue is further discussed in Section 2.2.

NLS1 galaxies exhibit an ensemble of considerably distinct characteristics when compared to other jetted AGN, but they are also remarkably diverse in their intra-class properties. The majority of NLS1 galaxies have never been detected at radio frequencies, making them seemingly radio-silent. On the other hand, the 15% fraction detected at radio frequencies includes a variety of sources spanning from radio-quiet to gamma-ray emitting individuals hosting relativistic jets. This apparent heterogeneity makes NLS1 studies challenging, and they are further complicated by a recent discovery that some radio-silent NLS1 galaxies are detectable at high radio frequencies, indicating that they host jets, and that an unknown fraction of NLS1 galaxies are misclassified (see Section 2.3). It seems clear that at least all NLS1 sources do not host jets, but it remains unclear whether these sources are similar when it comes to their other properties, for example, the black hole masses, the host galaxies, and the environments at different scales. If they are similar it raises a question about the triggering mechanism of the jet and the occurrence of the jet activity in general: is it something that the majority of NLS1 galaxies will undergo and is it a nonrecurring phase in their evolution or intermittent. If there are intrinsic disparities between NLS1 galaxies, the question is whether they are connected to each other, for example, via evolution, or do NLS1 sources with intrinsically different properties have separate evolutionary lines (see Sections 3.2 and 3.1).

2.1 Optical spectrum

NLS1 galaxies were first recognised as a distinct AGN class based on the properties of their optical spectra (Osterbrock & Pogge 1985), as described in the previous Section. While FWHM(Hβ) and the ratio between [O III] and Hβ form the official classification of NLS1 galaxies, it has been proposed that the strong Fe II emission should be considered as an additional classification criterion. In particular, in NLS1 galaxies Fe II/Hβ should be over 0.5 (Véron-Cetty et al. 2001). However, it seems that also lower values are common in sources that otherwise fulfill the NLS1 galaxy classification criteria (Cracco et al. 2016). The average optical spectrum of an NLS1 galaxy is shown in Figure 2.1. The most important emission lines and their properties are discussed below.

Permitted emission lines, for example, Balmer lines such as Hα and Hβ, and Mg II are unusually narrow. It is still not clear what is the origin of the this narrowness. One possibility is that the lines are not intrinsically narrow but appear to be so due to orientation effects (Decarli et al. 2008; Shen & Ho 2014). Emission lines arising from the virialised BLR can be broadened due to various mechanisms, for example, Doppler and rotational effects, turbulence in the line emitting gas, and gas outflows (Kollatschny & Zetzl 2013). These mechanisms lead to different line profiles, and line profile fitting can give us insight into the BLR dynamics, although most line profiles are usually a blend of various components. NLS1 galaxies are known to preferably be seen face-on at small inclination angles, and, if assuming that the geometry of the BLR is disk-like, we are able to observe only the velocity component pointing towards us, which causes the permitted emission lines to appear more narrow than what they actually are. Another possibility is that the rotational velocities in NLS1 galaxies are actually lower due to the less massive central black hole and the permitted lines are intrinsically narrow. The Hβ line profiles in NLS1 galaxies can usually be sufficiently modelled with Lorentzian line profiles, indicating that the turbulent motion of the BLR clouds is the main reason for the broadening (Kollatschny & Zetzl 2013; Cracco et al. 2016). Hα and Hβ are both produced in the inner part of the BLR.

Distinctly strong Fe II multiplets are usual in NLS1 galaxies and visible between ~4400–5500Å, around Hβ and [O III], in the composite spectrum in the lower panel of Figure 2.1. The strength of Fe II – integrated between 4434 and 4684 Å, and called Fe4570 – is usually defined in comparison with the total Hβ emission; this Fe II/Hβ ratio is denoted as R4570. The excitation mechanism of Fe II is still unclear; the photoionisation models or over-abundance of iron are not able to explain the characteristics, mainly the strength, of Fe II emission. Alternative explanations have been proposed, for example, collisional excitation (Cracco et al. 2016) or fluorescence by a variety of sources, for example, Lyα / Lyβ, or the continuum (Kovačević et al. 2010, and references therein). Studies of the location of the Fe II emitting clouds have arrived in contradicting results: some studies place it to the outer parts of the BLR, or ILR, relatively far away from the Hβ emitting lines (Marinello et al. 2016), whereas others find that both Fe II and Hβ are emitted by the same ionised gas (Hu et al. 2015; Cracco et al. 2016). Fe II and Hβ of the permitted emission lines in NLS1 sources

exhibit the so-called *inverse* Baldwin effect (Zhou et al. 2006; Cracco et al. 2016): the equivalent widths (EW) of these lines increase with the increasing continuum luminosity. The origin of the effect is still unknown.

BLRs in AGN exhibit two kinematically different groups of emission lines, high- and low-ionisation lines (Sulentic et al. 1995). The properties of these lines form a continuum from redshifted Hβ, seen preferably in radio-loud sources, to blueshifted C IV, usual in radio-quiet sources. NLS1 galaxies reside in one extreme of this continuum, with high C IV blueshifts.

High-ionisation lines, for example, C IV λ1549 and He II lines, consistently show broader line profiles than low-ionisation lines, and often exhibit blueshifts and blue asymmetries. These lines are thought to originate from a region of mostly optically thin, rather low-density clouds, possibly with a spherical-like geometry. The blueshifts have traditionally been explained by gas experiencing outward motions. Recently an alternative, successful explanation has been proposed: the blueshifts can be explained by electron and Rayleigh scattering off the inflowing gas (Gaskell & Goosmann 2013). In this scenario the blueshift correlates with the mass of the inflow, consistent with the high Eddington ratios of NLS1 galaxies requiring considerable amounts of gas flowing in.

Low-ionisation lines, for example, Fe II, Mg II λ2800, and Hβ, originate in the 'traditional' BLR following Keplerian motions around the black hole. The clouds emitting these lines are optically thick and dense with low temperatures and ionisation parameters. The abundant inflows in NLS1 galaxies can result in very high density gas in their BLRs. This could explain the high R4570 values seen in them: the Fe II emission is not particularly strong but the Balmer lines are unusually weak due to the high-density environment which allows hydrogen to thermalise (Gaskell 2000).

[O III] emission, most importantly the prominent [O III] $\lambda\,\lambda$ 4959, 5007 lines arise from the very low-density gas in the NLR. This region is located far away from the central engine and the obscuring matter around it, and emits isotropically. Since the NLR is photoionised by the central source, the intensity of [O III] is often considered to be proportional to the total intensity of the central source and the activity of the AGN (e.g., Heckman et al. 2004; Berton et al. 2015). The intensity of [O III] varies due to the intrinsic characteristics of the emitting gas, for example, the electron density and the ionisation parameter, but the most important factor seems to be the covering factor of the NLR clouds (Baskin & Laor 2005). Some studies propose that the increasing Eddington ratio might drive winds or outflows that increase the covering factor and thus decrease the [O III] intensity (Shen & Ho 2014), and, on the other hand, increase the Fe II intensity. Contradicting results also exist (Baskin & Laor 2005).

In NLS1 galaxies [O III] is relatively weak, Fe II strong, and their Eddington ratios are considerably high, fitting well to the aforementioned scenario. In addition NLS1 galaxies often show blue asymmetries in their [O III] line profiles. The profile consists of the very narrow [O III] component (FWHM $<$ 500 km s^{-1}), emitted by the NLR gas, and a broader (FWHM $\sim$500–1000 km s^{-1}), usually blueshifted component which is thought to originate in powerful gas outflows caused by high radiation pressure due to the high Eddington ratio (Cracco et al. 2016, and references

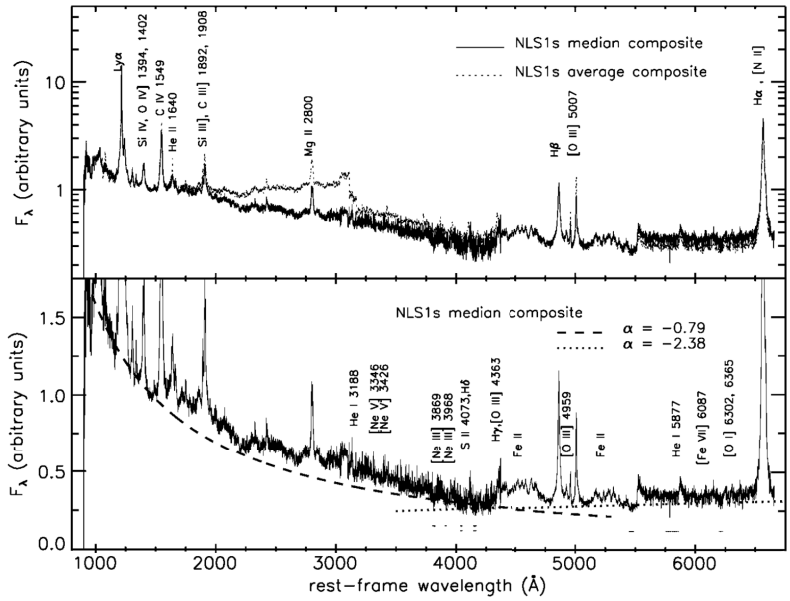

Figure 2.1. NLS1 composite spectrum (Constantin & Shields 2003).

therein). Another peculiarity seen in NLS1 galaxies are the so-called blue outliers; in these sources the whole line profile of [O III] is blueshifted compared to its rest wavelength, meaning that the bulk of the [O III] emitting gas is moving towards the observer. The mechanism behind this phenomenon is not yet known but alternatives include, for example, outflows associated with a disk wind (Zamanov et al. 2002) and the interaction of a relativistic jet with the NLR gas (Tadhunter et al. 2001; Komossa et al. 2008). Indeed, the properties of the [O III] line are found to be significantly different in radio-quiet and radio-loud sources: radio-loud sources exhibit considerably more signs of the jet/gas interaction, such as blue outliers, than radio-quiet sources (Berton et al. 2016). The number of blue outliers also seems to increase with the increasing continuum luminosity and Eddington ratio (Cracco et al. 2016). An alternative explanation for the blueshifts is scattering of photons off inflowing gas (Gaskell & Goosmann 2013). It has also been argued that the diversity seen in the [O III] properties is not due to jet interaction but orientation (Boroson 2011): [O III] originates in a polar flow. In this case sources with large [O III] blueshifts are seen pole-on and sources without a blueshifted [O III] component at larger angles. In this scenario radio-loud and radio-quiet NLS1 galaxies could intrinsically be similar sources but viewed at different angles.

2.2 Black hole masses

There has been much debate concerning the actual masses of the black holes in NLS1 galaxies and the issue remains unsolved. Virial methods consistently estimate the black hole masses in NLS1 galaxies to be in the range of $10^6 - 10^8 M_\odot$ (e.g., Xu et al. 2012; Rakshit et al. 2017, Publication I, Publication IV). However, Shen & Ho (2014) argued that the line width variations of the permitted emission lines in AGN are mainly due to the flattened geometry of the BLR and orientation effects. It has been suggested that if the BLR is flattened and an NLS1 galaxy is observed almost face-on, the emission lines would be extraordinarily narrow due to projection effects (Decarli et al. 2008). If taken into account it can explain the observed low black hole masses as well as the high Eddington ratios, both properties becoming comparable to the overall Seyfert population (e.g., Decarli et al. 2008; Liu et al. 2016; Rakshit et al. 2017). To get more insight into this issue, alternative methods to estimate the black hole masses in NLS1 galaxies have been used. Ryan et al. (2007) argued that when estimating the black hole masses in NLS1 galaxies using the $M_{\rm BH} - L_{\rm bulge}$ relation, their masses become comparable (average $\log M_{\rm BH} = 7.9\ M_\odot$) to the black hole masses in broad-line Seyfert 1 galaxies (BLS1). Calderone et al. (2013) modelled the optical/UV data of NLS1 galaxies using a standard Shakura–Sunyaev disk spectrum and estimated the black hole masses based on it. They found the black hole masses to be on the order of $> 10^8 M_\odot$. However, there is evidence that the accretion disks in NLS1 galaxies are not standard but slim disks (Mineshige et al. 2000b; Wang & Netzer 2003). On average slim disks are hotter than standard disks, exhibit a different temperature distribution (Crenshaw et al. 2003), and do not produce similar spectra. Models based on standard disk may not produce realistic results in case of NLS1 galaxies. Baldi et al. (2016) used spectropolarimetry to study the gamma-ray-detected NLS1 PKS 2004-447. They reported a detection of a very broad Hβ line in polarised light and argued that the black hole mass is well above $10^8 M_\odot$. Interestingly, it has been proposed that this source can be also classified as a CSS source (Gallo et al. 2006; Schulz et al. 2016). On the other hand, in Publication II the black hole mass estimates for a sample of flat-spectrum NLS1 galaxies were calculated using line dispersion (or the second moment of the line profile) that is less affected by orientation, the Eddington ratio, and the line profile than FWHM. The black hole masses were found to consistently be under $10^8 M_\odot$. Similar results were obtained in Publication VI. Also the black hole mass of the reverberation-mapped gamma-ray NLS1 1H 0323+342 was found to be only $3 \times 10^7 M_\odot$ (Wang et al. 2016), confirming that a supermassive black hole with an intermediate mass is able to launch a fully-developed relativistic jet (see also Rafter et al. 2013). Also other properties of NLS1 galaxies are in favour of the lower black hole masses. For example, NLS1 nuclei preferentially reside in evolutionarily young spiral galaxies with pseudobulges (Orban de Xivry et al. 2011; Ohta et al. 2007). If the black hole masses of NLS1 galaxies were comparable to those of BLS1 galaxies or even blazars, it would imply intrinsic differences because the observed properties, for example, the jet and the gamma-ray properties, are clearly different.

2.3 Radio properties

Only ∼7% of NLS1 galaxies are radio-loud and ∼3% percent very radio-loud ($R >$ 100, Komossa et al. 2006). An sdditional ∼5% of them are classified as radio-quiet ($R < 10$) and the rest have not so far been detected in radio at all and are considered radio-silent. Previously it was thought that radio loudness can be used as a proxy for the nuclear activity and that AGN could be divided to two separate types, radio-loud and radio-quiet that are clearly disparate in their properties. The reliability of radio loudness was questioned already in 2001 when Ho & Peng (2001) found that when measuring radio and optical flux densities using the nuclear region only – as is usually the case with high-redshift quasars with the nuclear region outshining the whole galaxy – most Sy1 galaxies should be classified as radio-loud. Evidence against the strict division to radio-loud and radio-quiet sources started to accumulate; instead of a bimodal radio loudness distribution, AGN seem to form a continuum in R values and the dividing number, R=10, is mostly arbitrary or slightly indicative at best (Padovani 2017, Publication IV, Publication VII). Also the variability seen in AGN has a considerable impact on the radio loudness parameter. As an example, NLS1 galaxy J1100+4421 exhibits extreme optical variability and the variance in R induced by this can be as high as 750% (Gabányi et al. 2018). Most sources are not this extreme but almost all AGN are known to be variable to some extent. For intermediate sources with $R \simeq 10$ even a slight change in the flux density might move them about the boundary, from radio-loud to radio-quiet and vice versa. R is usually calculated with non-simultaneous data and temporal variations are not taken into account. Ideally AGN should be classified based on their actual physical properties, in this case whether they host a powerful jet or not, but this is often impossible due to lack of data, and therefore R must be occasionally used as a proxy of the nuclear activity.

Most of the radio observations of NLS1 galaxies are from the Very Large Array (VLA) Faint Images of the Radio Sky at Twenty-Centimeters (FIRST) survey [1] at 1.4 GHz, and some from the National Radio Astronomy Observatory (NRAO) VLA Sky Survey (NVSS) [2] also at 1.4 GHz. At low radio frequencies the majority of NLS1 sources show flux densities around a few mJy, with only a handful of them showing flux densities higher than 10 mJy. The detection limit of FIRST is ∼1 mJy and based on these observations some very faint radio-quiet sources are probably classified as radio-silent. Higher radio frequency observations of NLS1 galaxies are scarce and usually concentrate on the brightest individuals. For example, *Fermi-GST* AGN Multi-frequency Monitoring Alliance (F-GAMMA [3]) monitored ∼60 *Fermi*-detected AGN of which seven are NLS1 galaxies between 2007 and 2015 at 12 frequencies between 2.64 and 345 GHz. The radio properties of four of these sources were extensively studied in Angelakis et al. (2015). They concluded that these sources show

[1] http://sundog.stsci.edu/
[2] http://www.cv.nrao.edu/nvss/
[3] http://www3.mpifr-bonn.mpg.de/div/vlbi/fgamma/fgamma.html

behaviour similar to what is seen in blazars. Generally, radio spectra of flat-spectrum[4] NLS1 sources exhibit strong variability due to the changes in the relativistic jet, as explained in Sections 1.2.1 and 1.4 (Publication II). The jet power in NLS1 galaxies is generally between 10^{42} and 10^{45} erg s^{-1}, but also jet powers as high as 10^{48} erg s^{-1} have been observed. The jet powers in NLS1 galaxies partly overlap with the less powerful BLOs, but are a few orders of magnitude below the jet powers seen in FSRQs. When the scaling of the jet power with the black hole mass is taken into account (Heinz & Sunyaev 2003), the jet powers in all of these source classes become roughly comparable, suggesting that they indeed are intrinsically similar (Publication II). However, some recent studies (Kynoch et al. 2018; Gardner & Done 2018) suggest that the situation might not be this simple and the jets in NLS1 galaxies seem to be less powerful than what is predicted by the scaling relations, indicating intrinsic differences between the jets in FSRQs and NLS1 galaxies. Jetted NLS1 galaxies represent a very small fraction of the whole NLS1 population and no comprehensive conclusions can be drawn from their properties. Overall the radio spectra of NLS1 sources are diverse. Radio-loud sources include flat- and steep-spectrum sources, whereas the majority of radio-quiet sources possess steep spectra, and most NLS1 galaxies have not even been detected at radio frequencies. To investigate the characteristics of the whole NLS1 population observations of larger and more diverse samples are needed.

2.3.1 Metsähovi NLS1 observing programme

An observing programme was launched at Aalto University Metsähovi Radio Observatory in Finland to amend the lack of high radio frequency observations of NLS1 galaxies . The observations are performed using the 13.7-metre radio telescope primarily at 37 GHz and secondarily at 22 GHz. Since the detection limit at 37 GHz is rather high, ∼0.2 Jy under optimal conditions, a detection can be considered as proof of the existence of a relativistic jet since no other phenomenon is able to generate emission at the level of several hundred mJy at high radio frequencies. The aim of the programme is to observe each source at least three to five times over a time period of one to two years, first, to see if they are detectable at all, and second, to study their high radio frequency characteristics, for example, variability. The Metsähovi NLS1 observing programme is currently the most extensive one concentrating on NLS1 sources at high radio frequencies. At the moment it consists of four Samples that include altogether ∼180 NLS1 galaxies, chosen based on diverse properties. The sample size is large enough to achieve statistically significant results. The observations of Sample 1 started in 2012, Sample 2 in 2013, and Samples 3 and 4 in 2014. The results were published in Publication III and Publication VII, and the main results are summarised here. In addition to providing novel high radio frequency data, Metsähovi observations are used to compile samples of the most intriguing individuals for follow-up observations.

[4] $S_\nu \propto \nu^\alpha$, $\alpha > -0.5$ for flat-spectrum sources, and $\alpha < -0.5$ for steep-spectrum sources.

Samples 1 and 2

The results for Samples 1 and 2 were published in Publication III. Sample 1 includes 45 sources (Foschini 2011; Komossa et al. 2006) that based on their radio properties, for example, extreme radio loudness or flat radio spectrum, could be detectable at 37 GHz. Observations of this sample started in February 2012 but three sources (SDSS J084957.97+510829.0, SDSS J094857.31+002225.4, and SDSS J150506.47+032630.8) had been observed before because they had been included in multifrequency campaigns. For example, the first observations of J084957.97+510829.0 were performed as early as January 1986. Sample 2 consists of 33 sources, chosen mostly based on their high radio loudness (Publication I; Foschini 2011; Komossa et al. 2006; Whalen et al. 2006). Its observations started in November 2013. 15 out of 78 sources in Samples 1 and 2 were detected at 37 GHz, giving a detection rate of 19% for the whole sample. Seven of 15 sources were detected only once indicating that they are variable, and that most of the time they stay below the rather high detection threshold of the Metsähovi telescope.

To build a more comprehensive picture of the higher radio frequency behaviour of NLS1 galaxies, additional quasi-simultaneous data from RATAN-600, Owens Valley Radio Observatory (OVRO), and the *Planck* satellite were used. RATAN-600 provides simultaneous data at 4.8, 8.2, 11.2, and 21.7 GHz with a detection limit of ∼8 mJy under favourable conditions. OVRO observes at 15 GHz and its detection limit is ∼10 mJy. *Planck* scanned the sky multiple times and provided observations at 30, 44, and 70 GHz with the Low Frequency Instrument, and at 100, 143, 217, 353, 545, and 857 GHz with the High Frequency Instrument. Additional data were available for 32, 15, and three sources by RATAN-600, OVRO (Richards et al. 2011), and *Planck*, respectively.

Comparison of Metsähovi and OVRO observations confirmed that the single detections of some of the sources at 37 GHz coincide with flaring episodes at 15 GHz, for example, as seen in the light curve of SDSS J164442.53+261913.2 in Figure 2.2, confirming that the 37 GHz detections are reliable and due to genuine variability. However, in two cases the 37 GHz detection does not coincide with 15 GHz activity and the 15 GHz light curves of are unusually uneventful over the whole observing period. If these detections are real it would indicate a very inverted spectrum. To study the radio properties in more detail, we compiled the radio spectra for all sources with detections at least at two frequencies (41 sources), and calculated spectral indices for sources with quasi-simultaneous data, that is, data taken within one month (20 sources). The spectral indices of NLS1 galaxies vary within a wide range from very steep to extraordinarily inverted. Significant variability can be seen in the radio spectra of individual sources at different epochs: the shape of the spectrum can change from steep to flat to inverted, and vice versa, which is a clear indication of flaring (Angelakis et al. 2015). In addition to changes in the spectral indices also achromatic variability (Angelakis et al. 2015; Planck Collaboration et al. 2016) is seen in some sources. Considerable changes in the spectral indices are visible also in sources that mostly maintain a steep spectral shape.

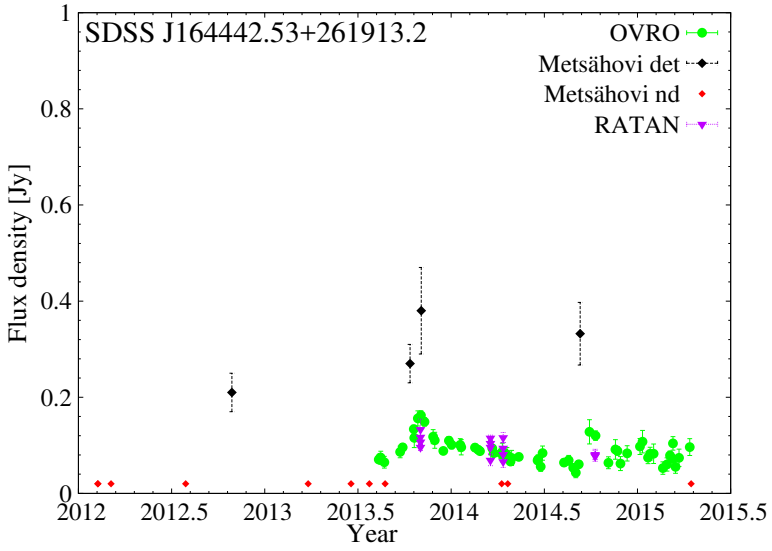

Figure 2.2. Flux density curve of SDSS J164442.53+261913.2 (Publication III). Metsähovi detections are denoted by black diamonds, and non-detections by red diamonds plotted at an arbitrary flux level. OVRO detections are marked with green circles and RATAN detections with purple triangles.

We further examined the variability at 15 and 37 GHz using the fractional variability equation (Aller et al. 1992). At both frequencies the variability of the brightest sources is the strongest. This could be expected since these are the sources that have been observed most frequently and have a higher probability to have been detected at extreme flux density values. Moreover, the variability of fainter sources gets dimished because due to the detection limit we detect them only when they are flaring and we do not see the fainter epochs at all. The obtained fractional variabilities are in line with Richards & Lister (2015), who note that the variability of NL1 galaxies is comparable to that of the blazar sample monitored at OVRO.

We compiled SEDs for all 78 sources using all available archival and new data. The SEDs were used to determine the synchrotron peak frequency, $\nu_{\rm peak}$. We fitted a third degree polynomial function individually for each source, carefully leaving out the disk component when visible, and confirmed the goodness of the fit by visual inspection, finally excluding 11 sources with possibly erraneous fits. The average log $\nu_{\rm peak}$ of the good fits is 13.20 GHz. This is exactly the same as for a large sample of the radio-brightest AGN, mostly blazars (Planck Collaboration et al. 2011).

The observations and the results, especially the behaviour of the radio spectra and the variability are similar to what is seen in blazars and strongly favour the relativistic jet as the main contributor to the high radio frequency esmission in NLS1 galaxies. It is likely that a subset of NLS1 galaxies in which low radio frequency emission is dominated by star formation processes exists (Caccianiga et al. 2015), but it is highly

improbable that these processes could be responsible for the variable emission at 37 GHz, thus the sources detected at high radio frequencies probably host powerful jets. Blazar-like behaviour was expected in the most radio-loud NLS1 sources, but it is interesting that some of the detected sources are borderline radio-loud/radio-quiet with very low 1.4 GHz flux densities. To investigate the predicting power of the low radio frequency observations we calculated the correlation between the 1.4 and 37 GHz flux densities, and whereas for some sources they seem to correlate, for the whole sample the correlation seems to be negligible or almost non-existent. Thus the 1.4 GHz emission cannot be considered as a good proxy for the detectability of a source at higher radio frequencies, and consequently for hosting a jet.

Samples 3 and 4

Encouraged by the success of the observations of Samples 1 and 2 and the results obtained, we decided to move past the ambiguous radio loudness parameter as a selection criterion. While it is probable that most radio-loud ($R > 100$) sources can be assumed to host a jet, these sources constitute only ~3% of NLS1 galaxies. This minority is not representative of the whole population. To remove the bias caused by selecting sources based on radio loudness and to diversify our NLS1 sample, we selected the sources for our Samples 3 and 4 following remarkably different criteria. Sample 3 includes 25 NLS1 galaxies residing in extraordinarily dense large-scale environments (Publication IV). For all these sources the surrounding large-scale luminosity-density is more than six times the average density, when more than three is the limit for a supercluster environment (see Section 2.5.2). We applied this selection criterion because based on the results in Publication IV it seems that the radio-louder NLS1 galaxies favour denser environments, and thus environment-based selection might reach some sources not selected based on conventional criteria. The 41 sources in Sample 4 were selected based on two multifrequency criteria. By extrapolating the SED by eye we estimated which sources could have high enough flux densities at 37 GHz to be detactable. Alternatively they should exhibit unusually high optical or X-ray emission compared to their archival, usually low frequency radio emission, possibly indicating that their radio emission level might increase to a detectable amount at high radio frequencies as well. The observations of these Samples started in March 2014.

The first results for the Samples 3 and 4 are published in Publication VII. Due to our unconventional selection criteria there are some radio-loud and radio-quiet sources in the samples as well, but the majority are radio-silent. Overall these 66 sources belong to the scarcely studied part of the NLS1 population, and multifrequency or any other additional data for them are rare and sporadic. The 37 GHz observations were performed similarly to Publication III, and we were able to detect eight of 66 sources. This yields a detection rate of 12% which is surprisingly high, taking into account that none of the sources were selected based on their radio properties. This result further questions the usefulness and credibility of using single-epoch low radio frequency observations as a proxy of the level of the nuclear activity. Four of the detected sources

are from the environment-selected and four from the multifrequency-selected sample. The levels of optical and X-ray emission of the detected, environment-selected sources are not particularly high, indicating that these properties are not a determining factor when predicting the level of radio emission at higher frequencies.

Based on their archival data, especially in radio, all eight detected sources are unlikely to host relativistic jets: one source is borderline radio-quiet/radio-loud, one is radio-quiet, and the rest six have previously been totally radio-silent, meaning that they were not detected by the FIRST or NVSS surveys – with detection limits of ∼1 mJy – even if they reside in the area of the sky covered by them. Two of the sources have been detected only once at 37 GHz but the remaining six more frequently. The detection percentages span from 2% to a remarkably high 37%, and the maximum flux densities from 0.27 Jy to 1.43 Jy.

This discovery has various implications. It diminishes the dominant role of the low radio frequency observations as an indicator of jet activity. Relativistic jets are not solely a curiosity seen in blazar-type NLS1 galaxies but seem to be a remarkably more widespread phenomenon among the NLS1 galaxies. Moreover, three of these sources were included in our host galaxy study (see Section 2.5.1 and Publication VI). Two of them, SDSS J151020.06+554722.0 and SDSS J152205.41+393441.3, were reliably fit; both of them are hosted by barred spiral galaxies with pseudo-bulges and additionally J152205.41+393441.3 is interacting with a smaller nearby galaxy. The black holes masses in the detected sources are intermediate, from $10^6 M_\odot$ to $2 \times 10^7 M_\odot$. While these are usual host galaxy characteristics for NLS1 sources, they are extraordinary for galaxies with AGN and relativistic jets; they contradict the conventional jet paradigm. As discussed in Section 1.2.2 there are only a few known spiral galaxies with relativistic jets, with properties resembling ellipticals and dissimilar to NLS1 galaxies.

In addition to the Metsähovi radio observations we reduced all the available *Fermi* gamma-ray data of the detected sources. Applying the usual detection limit of maximum-likelihood test statistic, TS > 25, we discovered one new gamma-ray emitting NLS1 galaxy: SDSS J164100.10+345452.7, with TS = 39. Its photon flux, $S_\gamma = 12.5 \times 10^{-9}$ ph cm^{-2} s^{-1}, and photon index, Γ_γ = -2.5, are in line with other gamma-detected NLS1 galaxies. In addition to J164100.10+345452.7 we found another three sources for which 9 < TS < 25. They are strong candidates for future gamma-ray detections. So far less than 20 NLS1 galaxies, all of which are radio-loud, have been detected in gamma-rays (e.g., Abdo et al. 2009a,b; D'Ammando et al. 2012; Paliya et al. 2018). The jet luminosities of NLS1 sources are lower than those of FSRQs but become comparable when scaled to take into account the lower black hole masses. This and other similarities, for example, in the characteristics of their radio and optical spectra, have led to the proposition that NLS1 galaxies are the low black hole mass tail of the high-excitation type jetted AGN.

We checked the large-scale environments of the detected sources using data from Publication IV. The four environment-selected sources naturally reside in supercluster environments, and of the remaining four sources, two reside in voids and two in intermediate-density regions (filaments or supercluster-to-void transition regions).

Interestingly it seems that the sources residing in more diffuse regions show on average higher 37 GHz flux densities, lower black hole masses, and more pronounced variability than the sources that reside in superclusters. These sources also reside at the lowest redshifts, which might indicate that the observed differences are of evolutionary origin. The sample size is too small to make further conclusions at this point, but it will be interesting to see if this trend exists in larger samples.

The most interesting question evoked by this extraordinary discovery is that of the 'missing' low radio frequency emission. Since all six of the radio-silent sources reside in the area covered by the VLA FIRST survey their 1.4 GHz flux densities at the time of the FIRST observations, approximately 20 years ago, have had to be less than $\sim$1 mJy. Unfortunately there are no recent low radio frequency data available for these sources. One possibility is that a less powerful, non-relativistic jet was present but in an inactive state and thus not detectable or very faint at 1.4 GHz (Mundell et al. 2009). Since then the activity would have increased so that the jet is now detectable at 37 GHz. An alternative is that the sources really were non-jetted at the time of the last observations and we are now seeing the onset of the nuclear activity and the triggering of a relativistic jet. Since NLS1 galaxies do not generally exhibit relic radio emission (however, exceptions do exist, e.g., Congiu et al. 2017) it has been suggested that short timescale intermittent activity might be common in them. The activity periods could be caused by radiative instability in the accretion disk and occur at timescales of the order of only tens-to-hundreds of years (Czerny et al. 2009). The third explanation is that the level of the activity has remained similar but these sources exhibit unusually inverted radio spectra. Assuming a 1.4 GHz flux density of 1 mJy for the radio-silent sources and using the archival observations for the detected sources, the spectral indices between 1.4 and 37 GHz would have to be 1.7 – 2.1 to explain the 37 GHz detections. If true, the nature of these sources is extreme, even among the more powerful blazars. Low radio frequency observations are needed to distinguish between these alternative scenarios. Additionally, very long baseline interferometry (VLBI) observations will be essential to confirm the existence of relativistic jets and to investigate their properties.

Samples 5 and 6

The next samples, 5 and 6, were added to the observing programme in Spring 2017. Sample 5 consists of 16 sources with radio-loudness parameters between 50 and 100 selected from Publication I. Based on sample 3 it seems that the large-scale environment density can successfully be utilised to select good candidates for high radio frequency observations. Therefore we selected sources residing in the densest large-scale environments based of the Sloan Digital Sky Survey (SDSS) Baryon Oscillation Spectroscopic Survey (BOSS) luminosity-density field (LDF) to form our sample 6. Compared to Sample 3 these sources reside at higher redshifts. We have also prepared a sample of southern NLS1 sources selected from the Six-degree Field Galaxy Survey (6dFGS) (Chen et al. 2018) to be added to the Metsähovi observing programme shortly. New sources will be added to the observing programme whenever

suitable candidates are found. In addition to increasing the total sample size, we continue monitoring the older samples, especially the sources detected at 37 GHz. The Metsähovi NLS1 galaxy observing programme is unique in its extent, duration, and flexibility, and will continue to provide valuable information for these sources.

2.3.2 Radio morphologies

The resolution of a single radio telescope is too low to resolve any structures in a non-local radio source. However, a technique combining the observed signals from multiple radio telescopes, called interferometry, can be utilised to achieve even (sub-)milliarcsecond resolution, which for low-redshift sources, for example, NLS1 galaxies, translates to ability to resolve parsec-scale structures. Different interferometer set-ups are sensitive to different scales, thus it is important to observe a source at different resolutions to achieve a compherensive picture of its radio structure, and also perform single-dish observations which are able to obtain the total flux of a source.

VLBI can be used to infer intrinsic jet parameters such as the Lorentz and Doppler factors (see Section 1.2.1), and at least the projected extent of the jet. If the angle of the jet to the line of sight can be estimated, for example, if the counter-jet is visible, the deprojected dimensions of the jet can be calculated. Additional important parameter, usually calculated using high-resolution images of the radio core, is the brightness temperature, T_B. It is defined as the temperature that a source emitting a black body spectrum would need to have to account for the observed intensity at a given wavelength:

$$T_B = 1.8 \times 10^9 (1+z) \frac{S_{\nu,p}}{\nu^2 \theta_{maj} \theta_{min}} [\mathrm{K}] \tag{2.1}$$

where $S_{\nu,p}$ is the peak flux density in mJy beam^{-1}, ν is the observing frequency in GHz, and θ_{maj} and θ_{min} are the major and minor axes of the source in milliarcseconds, deconvolved from the beam. The brightness temperature can almost unambiguously be used to identify non-thermal emission originating from an AGN compared to other processes emitting at radio frequencies. Normal stars ($T_B = 10^3 - 10^4$ K) cannot produce brightness temperatures high enough to be detected using interferometry, but certain stellar-related processes, for example, stellar jets, X-ray binaries, and young supernovae and supernova remnants can occasionally produce brightness temperatures of the order of $10^5 - 10^7$ K, detectable using VLBI (e.g., Pérez-Torres et al. 2009). Non-thermal synchrotron radiation from supernovae and their remnants is the most relevant alternative origin of the radio emission in star-forming galaxies such as NLS1 galaxies. However, this is a rare phenomenon; only ~50 radio supernovae have been detected during about 30 years of observations and all of them are Galactic or in the very local Universe (Lien et al. 2011). Moreover, AGN cores usually show brightness temperatures around $10^{10} - 10^{12}$ K, clearly separating them from other possible radio emission sources.

Due to the discovery of gamma-ray emission from NLS1 galaxies, it was expected that they would show extended radio jet structures similar to blazars. This has proven

to be partially true: NLS1 galaxies do show extended radio emission but overall they exhibit a wide range of diverse pc- and kpc-scale radio structures that often are not similar to what is seen in blazars.

Parsec-scale radio mophologies

Richards et al. (2015) studied a sample of 15 radio-loud NLS1 galaxies and reported that at pc-scale they show core-dominated, blazar-like structures, with 13 of them showing one-sided pc-scale radio jets. Lister et al. (2016) confirmed that some, preferentially gamma-ray-loud, NLS1 galaxies host relativistic jets exhibiting superluminal speeds ($\sim 10c$), Lorentz factors ($\gamma \sim 10$) and viewing angles ($\theta < 10^{\circ}$) comparable to what is seen in blazars but not quite as extreme (Lister et al. 2016). Gu et al. (2015) examined the pc-scale structure of 14 radio-loud NLS1 galaxies, and found seven of them to show only the radio core, five to have a compact one-sided core–jet structure, and two to exhibit an extended one-sided core–jet structure. Typically for NLS1 galaxies, 12 out of 14 sources are core-dominated. In their sample half of the sources are flat- and half steep-spectrum, but interestingly the radio structure and the spectral shape do not correlate. They find these sources to show quite low brightness temperatures and argue that the jets are not strongly beamed and are only mildly relativistic. An interesting discovery was made by Doi et al. (2013) who investigated seven radio-quiet NLS1 galaxies at pc-scales. The five sources they were able to detect all show brightness temperatures too high to be explained by any thermal processes, and they conclude that these radio-quiet sources host central engines similar to radio-loud sources and that the radio emission is generated by non-thermal processes near the nucleus. Moreover, they were able to detect pc-scale jets in three of the sources. However, they find that much of the radio power originates in diffuse emission within the innermost 300 pc, indicating that the jets terminate and dissipate at a quite small radius and are not powerful enough to break out from the host galaxy.

Kiloparsec-scale radio mophologies

Also kpc-scale jets in NLS1 galaxies exhibit considerable diversity. Richards & Lister (2015) examined three radio-loud NLS1 galaxies and found all of them to show asymmetric two-sided kpc-scale jets, with lengths from 20 to 70 kpc. They found the sources to be core-dominated and the radio lobes to be diffuse, terminating in hotspots and resembling FR-II radio morphology. Two of the sources show a pc-scale jet aligned with the apparently approaching kpc-scale jet. From these they were able to infer that the jets are mildly relativistic with viewing angles of 10–15 °. In contrast to their findings Gliozzi et al. (2010) and Doi et al. (2015) found kpc-scale jets with approximately the same extent but resembling FR-I radio morphology. Aligned pc-scale jets were found also in these studies. Intriguingly, the source studied in Doi et al. (2015) is a radio-quiet NLS1 galaxy, strengthening the idea that the radio loudness parameter does not necessarily correlate with the actual radio properties of a source. Both core- and lobe-dominated sources were found in a study by Doi et al. (2012). The results so far seem to indicate that generally NLS1 galaxies do not have a favoured

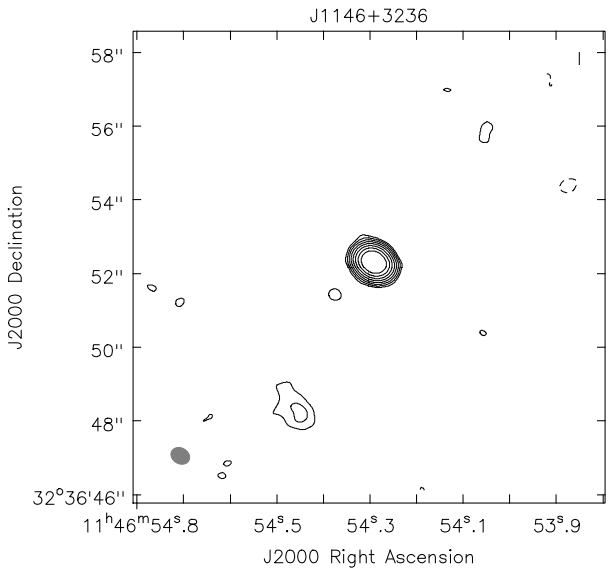

Figure 2.3. SDSS J114654.28+323652.3, a flat-spectrum NLS1 galaxy with a compact kpc-scale radio morphology. Rms = 11 μJy, contour levels at -3, 3×2^n, $n \in$ [0,9], beam size 3.11×2.52 kpc. (Publication V).

kpc-scale radio morphology type. Caccianiga et al. (2017) examined a radio-loud, steep-spectrum NLS1 galaxy and found it to show an asymmetric two-sided jet with a deprojected linear size of some kiloparsecs. They propose that this source is similar to flat-spectrum NLS1 galaxies but seen at a larger inclination, belonging to the so far elusive parent population of flat-spectrum NLS1 galaxies. Many of its properties are reminiscent of a CSS source, and they further argue that this discovery strengthens the role of CSS sources as a viable parent population candidate for NLS1 sources (see Section 3.1).

The majority of the observations at kpc-scale come from the FIRST survey (Becker et al. 1995), in which only sources larger than 2 arcmin are resolved (White et al. 1997). On the other hand, VLBI enables radio imaging at milliarcsecond scale, leaving a wide gap between these two resolutions unexplored. To investigate the scales in-between, a diverse sample of 74 NLS1s – radio-quiet and radio-loud – was observed with the Karl G. Jansky Very Large Array (JVLA) at 5 GHz in A-configuration (Publication V). The sources were mainly selected from Publication II and Berton et al. (2015), with some additions from Tarchi et al. (2011); Moran (2000); Wadadekar (2004); Komossa et al. (2006) and Gallo et al. (2013). This is so far the largest survey aimed at radio imaging of NLS1 sources at this frequency. All of the sources have been previously detected at 1.4 GHz in either the FIRST or the NVSS survey.

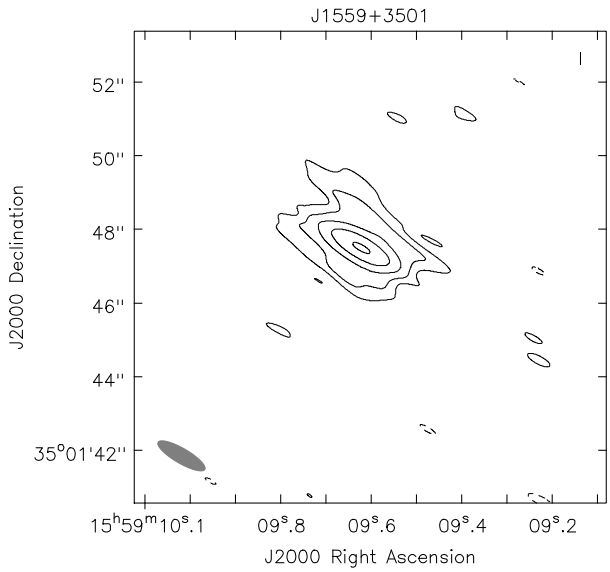

Figure 2.4. Mrk 493, a steep-spectrum NLS1 galaxy with an extended kpc-scale radio morphology. Rms = 11 μJy, contour levels at -3, 3×2^n, $n \in$ [0,4], beam size 0.91×0.25 kpc (Publication V).

The sources were divided into three groups based on their in-band spectral indices; radio-loud flat-spectrum (F-NLS1, $\alpha >$ -0.5, N = 28), radio-loud steep-spectrum (S-NLS1, $\alpha <$ -0.5, N = 19), and radio-quiet sources (Q-NLS1, N = 27) which all were steep-spectrum. There is a clear trend of F-NLS1 sources residing at highest redshifts, Q-NLS1 sources at lowest redshifts, and S-NLS1 sources in between, with median redshift values of 0.437, 0.048, and 0.225, respectively. Another division was made based on their morphologies using the ratio between the peak and the total flux density, $\mathscr{R} = S_{\rm peak} / S_{\rm total}$. Sources for which $\mathscr{R} \geq 0.95$ were classified as compact (N = 27), sources with $0.75 \leq \mathscr{R} < 0.95$ as intermediate (N = 26), and sources with $\mathscr{R} < 0.75$ as extended (N = 21). Subsamples based on spectral indices and morphologies correlate to some extent: most F-NLS1 sources are compact, one third intermediate, and only 11% extended, whereas almost half of Q-NLS1 sources show extended morphology and only 22% are compact. S-NLS1 sources do not have a preferred morphological type. Examples of compact and extended morphologies are shown in Figures 2.3 and 2.4, respectively.

As could be expected, the total luminosity is on average lowest in the Q-NLS1 sample, highest in the F-NLS1 sample, and between them in the S-NLS1 sample. The brightness temperatures were estimated using Equation 2.1. It should be noted that since T_B is usually calculated using higher resolution observations, these estimates are

lower limits since the estimates for the size of the core are upper limits. However, since it is estimated in a similar manner for all sources in this study, they are comparable with each other. The mean logarithmic T_B and the standard deviation for F-, Q- and S-NLS1 subsamples are 5.33±1.00, 3.15±0.98, and 3.51±0.98, respectively. T_B among F-NLS1 sources is on average significantly higher than in Q- and S-NLS1 subsamples. The results are similar for the subsamples based on morphology: compact sources exhibit on average higher brightness temperatures than intermediate or extended sources. The average logarithmic black hole masses (in units of $M_\odot$) of F-, Q- and S-NLS1 subsamples are 7.46±0.61, 7.13±0.46, and 7.76±0.41, respectively. Based on the Kolmogorov-Smirnov test, F- and S-NLS1 sources are drawn from the same black hole mass distribution, that is different than the black hole mass distribution of Q-NLS1 sources. Interestingly, the morphology-based subsamples all have similar average black hole masses.

All three subsamples exhibit disparate properties. F-NLS1 sources are characterised by compact radio morphologies, high luminosity, and consequently high brightness temperatures. Q-NLS1 sources are almost opposite to F-NLS1 sources: they consistently show extended and intermediate radio morphologies, and low brightness temperatures. S-NLS1s seem to be intermediate between F- and Q-NLS1 sources: they show no preferred morphology type, and they show luminosities and brightness temperatures lower than F-NLS1 but higher than Q-NLS1 sources. The differences between F- and S-NLS1 sources can be explained by the different orientation of these sources. F-NLS1 sources are most similar to blazars, with relativistic jets viewed at small angles, and their luminosities and brightness temperatures are enhanced by relativistic effects. S-NLS1 sources are intrinsically similar to F-NLS1 sources but observed at larger angles, diminishing the relativistic effects. None of our F- or S-NLS1 sources show a fully-developed, one-sided large-scale relativistic jet, similar to what was found in, e.g., Richards & Lister (2015). Instead many of the intermediate and extended sources possess smaller projected sizes, possibly suggesting smaller inclinations angles.

Q-NLS1 sources on the other hand do not necessarily fit into this orientation-based unification scenario. There are some examples of radio-quiet NLS1 sources with jet producing central engines (Doi et al. 2013), pc-scale jets (Doi et al. 2015), and high brightness temperatures, indicating that they might indeed be misaligned F-NLS1 sources. However, the radio luminosities and brightness temperatures are very low in the majority of Q-NLS1 sources. As discussed earlier, radio emission can alternatively be produced by star formation processes and this might be the case for Q-NLS1 sources. Caccianiga et al. (2015) showed that the radio emission even in some radio-loud sources can be dominated by, or at least have a significant contribution from star formation. Many of these sources, identified in Caccianiga et al. (2015), are included in this study, and they consistently show quite low brightness temperatures, supporting star formation as a possible explanation for the radio emission production in the Q-NLS1 sources.

Many of the sources in this sample have previously been included in radio imaging studies with another resolution scale, usually scoping smaller spatial scales. The

kpc-scale structures found in this study mostly agree, in terms of position and position angle, with the smaller-scale structures found in the earlier studies (e.g., Doi et al. 2013; Gu et al. 2015). Interestingly, Doi et al. (2013) argue that the jets in the radio-quiet NLS1 sources they studied terminate and dissipate at a radius of a few hundred pc, but in this study all of those sources are found to exhibit intermediate or extended morphology. This indicates that the jets indeed are able to reach kpc-scales and that this emission is probably resolved out by higher resolution observations.

In radio images blazars and their higher inclination counterparts, radio galaxies, show powerful relativistic jets and significant radio lobes at kpc-scales (Antonucci & Ulvestad 1985; Murphy et al. 1993; Cooper et al. 2007; Kharb et al. 2010). Similar intense extended emission, with luminosities comparable to the core luminosity, is not seen in the sample of F-NLS1 sources; their extended emission is more diffuse and overall they are less luminous than blazars. This discrepancy suggests that F-NLS1 sources are intrinsically disparate in their physical properties when compared to other AGN with relativistic jets. However, it has been suggested that the jet phenomena in F-NLS1 galaxies and FSRQs can be unified based on the scalability of the jet power as a function of the mass of the central black hole (Heinz & Sunyaev 2003; Foschini 2014). F-NLS1 sources represent the low-mass, less evolved version of FSRQs. Consequently, due to their young age they may not have yet had time to produce prominent radio lobes (Berton et al. 2015).

It has been proposed that CSS sources could be misaligned F-NLS1 sources and therefore a part of their parent population, along with S-NLS1 sources (e.g., Komossa et al. 2006; Gu et al. 2015; Caccianiga et al. 2015, 2017; Berton et al. 2016). However, on average the radio luminosities of F-NLS1 sources are lower than the luminosities of CSS sources, mostly because they lack the intense extended emission seen in the latter. Also the radio morphologies of CSS sources seem to be more complex than those seen in F-NLS1 sources (Dallacasa et al. 2013; Gu & Chen 2010). When considering only the low-power CSS sources the differences with F-NLS1 sources seem to diminish (Kunert-Bajraszewska et al. 2010), as they are less luminous and show simpler radio morphologies than more luminous CSS sources (Kunert-Bajraszewska et al. 2006).

Another viable alternative is that the radio-silent and radio-quiet NLS1 galaxies form the parent population of radio-loud NLS1 sources. Relativistic beaming can cause an object, that would otherwise be classified as radio-quiet or even radio-silent, appear as radio-loud when observed at a small angle. However, in this sample Q-NLS1 sources, when compared to S-NLS1 sources and to some extent to F-NLS1 sources, show disparities that are hard to explain as orientation effects; the black hole mass distributions are different as are the radio luminosities. Furthermore, in Q-NLS1 sources the contribution of star formation to radio emission seems to be more important than in F- or S-NLS1 sources. It should be noted that the redshift distributions of the subsamples are different and might induce bias. A comparison sample of higher redshift radio-quiet and radio-silent sources will be needed to perform a proper comparison. The parent population of NLS1 galaxies is discussed in more detail in Section 3.1.

2.4 Statistical multiproperty studies

2.4.1 Multifrequency correlations

Multifrequency correlations performed with large enough samples to be statistically significant can offer us insight into via which processes and where in the AGN, or its host galaxy, the emission at different frequencies is generated and how these processes are related. If emission in two or more frequency bands is strongly correlated it can be assumed that also their origins are connected –and vice versa for uncorrelated frequency bands. However, performing multifrequency correlations can be challenging. AGN tend to be variable, in some cases at all frequencies, but usually single-epoch observations are used for the correlation studies. Additionally, simultaneous data are rarely available and the observations in different bands may be decades apart. Even if the observations were simultaneous, variability might drastically change the flux density levels and a single-epoch observation may not necessarily represent the characteristic state of the source. Variations at different frequencies may also show lags compared to each other. To account for the variability, longer term quasi-simultaneous monitoring at several frequencies is needed but this is often impossible. Furthermore, the origin of emission at any given frequency may be different not only between different AGN classes but also within a class. For example, the low-frequency radio emission may be produced by star formation related processes, such as radio supernovae and supernova remnants, or by the jet, or any combination of the two, as is the case for many NLS1 galaxies. The effect of these issues can be reduced by using large enough, carefully selected samples, so that the properties of single sources are not so pronounced.

Extensive statistical multifrequency studies of AGN are scarce, and for NLS1 galaxies practically nonexistent. A correlation between $L_{\rm R} - L_{\rm O}$ has been found for a sample of ∼100 quasars, and between $L_{\rm R,\,jet} - L_{\rm O}$ for a small sample of BLOs (N=18) (Arshakian et al. 2010). Ballo et al. (2012) discovered a $L_{\rm R} - L_{\rm X}$ correlation but found no $L_{\rm O} - L_{\rm X}$ correlation in a sample of 852 quasars and 14 Seyfert galaxies, whereas Brinkmann et al. (2000) found a correlation for both in a mixed sample. Correlation between $L_{\rm R} - L_{\rm X}$ has been found in several studies with samples of varying sizes and properties (Panessa et al. 2007; Bianchi et al. 2009; Younes et al. 2012). However, radio and gamma-ray emission in radio-loud AGN have been found to be connected in many studies (e.g., Jorstad et al. 2001; Lähteenmäki & Valtaoja 2003; Nieppola et al. 2011; León-Tavares et al. 2012).

The study in Publication I was essentially the first multifrequency correlation analysis of a large sample of NLS1 galaxies. A sample of 292 radio-detected NLS1 sources, of which 97 were radio-quiet and 195 radio-loud, was studied. The correlations among the whole sample and the radio-loud and radio-quiet subsamples were examined using Pearson product-moment correlation coefficient (Pearson's r), Spearman's rank correlation coefficient (Spearman's ρ), and corresponding partial correlation coefficients to account for the possible false correlations induced by redshift. However, all correlation

analyses were in agreement.

No correlation between $L_R - L_O$ for the whole sample was found, and the correlation among the radio-quiet and radio-loud subsamples is generated by the division to these subsamples. There is a strong correlation between $L_O - L_{IR}$, especially in the radio-quiet sample. This correlation can be expected since a fraction of the optical emission generated by the accretion disk is absorbed by the surrounding molecular clouds and re-emitted in infrared. Also the $L_O - L_X$ relation is rather strong in both subsamples and the whole sample. The connection can be explained by the IC scattering of optical/UV accretion disk photons to X-rays in the hot corona above the accretion disk. A correlation between L_R and L_X was not found, suggesting that their production mechanisms are not connected. L_R and L_{IR} show a considerable correlation in the radio-quiet sample, indicating that radio and infrared emission share a common origin. It is probable that infrared and radio emission in radio-quiet sources originate from star formation processes (Caccianiga et al. 2015). This correlation does not exist among the radio-loud sample, suggesting a different origin compared to the radio-quiet sources. A plausible explanation is that the radio emission in radio-loud sources is mostly generated by the jet; if not a fully-developed relativistic jet then at least a mildly relativistic jet or a jet base. The infrared emission originates mostly from the molecular torus, and possibly partly from the star formation processes.

2.4.2 Principal component analysis

Principal component analysis (PCA, Abdi & Williams 2010) is a comprehensive way for investigating how the various properties of AGN are connected. It is a statistical procedure that can be used to effectively study large amounts of data which include multiple variables. PCA can reveal underlying relations that may include multiple parameters and do not show up in conventional correlation analyses. It uses an orthogonal transformation to convert a set of possibly correlated variables into a set of linearly uncorrelated variables called principal components or eigenvectors (EV). The number of EVs is the same as the number of variables. The transformation is performed so that the first EV has as large a variance as possible and thus accounts for as much of the variability in the data as possible. The subsequent EVs are constructed so that also they have the highest possible variance while still being orthogonal to the preceding EVs. PCA makes it possible to find the most dominant variable or an ensemble of variables in a data set. However, PCA is sensitive to the properties of the original data set. In case some variables are already tightly connected, PCA emphasises this connection and these variables might dominate the results. The variables used should therefore be selected carefully. If the original variables have very different scales, the variables with the most extensive scale tend to show the most variability and skew the results. This can be avoided by normalising the data. A similar bias might occur if the variables are in different units, in which case the variables should be weighted using the inverse of their variances. In addition, it must be remembered that the results of PCA depend on the properties of the input data set. When these possible pitfalls are taken into account, PCA is a powerful tool to

examine and systematise extensive data sets, and in case of AGN, to search for sets of connected properties and to identify common physical drivers behind them.

PCA has been rather widely used in AGN research. The first comprehensive analysis was done in Boroson & Green (1992) who used the optical properties of a sample of 87 quasi-stellar objects (QSO). They found that the EV1 is dominated by the anticorrelation between the strength of Fe II, and the strength of [O III] λ5007 and $FWHM$(Hβ). EV2 distinguished between the optical luminosity and the strength of He II λ4686. In a follow-up study 75 sources were added to the sample (Boroson 2002). The results were consistent with the previous study and they suggested that the physical driver behind EV1 is the Eddington ratio [5], and EV2 is driven by the accretion rate. Grupe (2004) examined a sample of 110 soft X-ray selected AGN, about half of them being NLS1 galaxies, and concluded that their EV1 is similar to the previously found EV1. EV2 of their study strongly correlated with the black hole mass. EVs similar to Boroson (2002) were also found in a study by Xu et al. (2012) using a sample of NLS1 and BLS1 galaxies. In their study it is also evident that NLS1 and BLS1 galaxies occupy different regions in the EV1 – EV2 plane.

Based on several subsequent studies the correlation space defined by $FWHM$(Hβ), [O III] λ5007 vs. R4570, the velocity shift of the C IV λ1549 profile, and the soft X-ray photon index ($\Gamma_{\rm soft}$) has been established as the 4DE1 parameter space of AGN (e.g., Marziani et al. 2006; Sulentic et al. 2007) that can be used to explain a host of diverse properties observed in them. The most relevant correlation exists between $FWHM$(Hβ), [O III] λ5007, and R4570. Instead of using radio loudness as a dividing factor, $FWHM$(Hβ) is used to divide sources to populations A and B since prominent changes in the spectroscopic features appear at $FWHM$(Hβ) $\approx$ 4000 km s^{-1}. By definition, FWHM(Hβ) in population A sources is $<$ 4000 km s^{-1}, and they generally show strong Fe II, and soft X-ray excess. Their emission lines are best modelled with Lorentzian profiles, indicating that the broadening is due to the turbulent motion in the BLR. Most of population A sources are radio-quiet. On the other hand, $FWHM$(Hβ) in population B sources is $>$ 4000 km s^{-1}, they show weak Fe II, and their emission line profiles are Gaussian, suggesting a rotational origin (Doppler broadening, however, see Kollatschny & Zetzl 2013). These sources are generally radio-loud but also some radio-quiet sources fall into this category (Zamfir et al. 2010). The changes in the 4DE1 properties correspond to the changes of intrinsic physical properties, for example, the black hole mass, the ionization parameter, and the accretion rate. This continuum of properties indicates that the 4DE1 space might represent an evolutionary sequence of AGN, driven by the Eddington ratio. NLS1 galaxies occupy the high Eddington ratio extreme of the 4DE1 space with characteristic narrow $FWHM$(Hβ) and strong Fe II.

The number of NLS1 galaxies included in the previous PCA studies has been quite small. We performed PCA of a large and pure sample of 292 NLS1 sources in Publication I. Since this was the first PCA study that includes only NLS1 galaxies it especially highlights the variables that drive the changes in the properties within the NLS1 class. The variables included in our study were $FWHM$(Hβ), $M_{\rm BH}$, R4570,

[5] $L_{\rm Bol}/L_{\rm Edd}$, where $L_{\rm Edd} = 3.2 \times 10^4 (M/M_\odot) L_\odot$

$S_{\rm O}$, $S_{\rm R}$, $S_{\rm IR}$, and $S_{\rm X}$. PCA was performed separately for the whole sample, and radio-quiet and radio-loud subsamples. For most parts the results of the whole sample and the subsamples agree.

Anticorrelation of $S_{\rm O}$ and $S_{\rm IR}$ versus $M_{\rm BH}$ dominates the EV1 in this study. In the radio-quiet sample the radio emission contributes almost as much as the optical and infared emission, which is in agreement with the multifrequency correlations (Publication I), supporting their connected origins. Since the optical emission and the black hole mass have the strongest contribution to the EV1, it is quite similar to EV2 found in previous studies. However, including both $S_{\rm O}$ and $S_{\rm IR}$, which are rather strongly linearly correlated, might emphasise their significance in EV1. EV1 does not correlate with the Eddington ratio. On the contrary, EV2 of this study represents the 'traditional' EV1 and is dominated by the anticorrelation between R4570 and $FWHM(\mathrm{H}\beta)$. In the radio-quiet subsample also the contribution of the black hole mass is strong and it correlates with the $FWHM(\mathrm{H}\beta)$. EV2 is strongly correlated with the Eddington ratio as expected.

Since the study in Publication I included only radio-detected sources and thus concerned only a limited part of the NLS1 population, we decided to do a follow-up study with a larger sample that includes also radio-silent sources. In Publication IV we used PCA to analyse ∼1300 NLS1 galaxies. The sources were split into two samples according to the origin of the large-scale environment density parameter that was introduced as a new variable. Since the density values are from two different surveys, they are not directly comparable. This study was the first ever to include a parameter describing the large-scale environment density in the PCA of AGN. Our first sample consisted of 960 NLS1 galaxies of which 799, 73, and 87 were radio-silent, radio-quiet, and radio-loud, respectively. The large-scale environment density data come from a luminosity-density field (LDF) constructed using a sample of luminous red galaxies (LRG) in the SDSS Data Release 7 (Abazajian et al. 2009; Lietzen et al. 2011; Liivamägi et al. 2012). The second sample included 323 NLS1 sources: 266 radio-silent, 6 radio-quiet, and 51 radio-loud sources. The environment data for these are from an LDF constructed using the SDSS BOSS Constant MASS (CMASS) sample from Data Release 12 (Alam et al. 2015). For a more detailed description of the large-scale environment density parameter see Section 2.5.2. These surveys do not spatially overlap due to their different redshift ranges and thus could not be scaled to be directly comparable; therefore we performed PCA separately for the two samples. Additionally, we analysed subsamples of radio-detected sources and X-ray-detected sources. The final variables included were R4570, $S(\text{[O III]})$, $S_{\rm O}$, $FWHM(\mathrm{H}\beta)$, and the large-scale environment parameter, and $S_{\rm R}$ and $S_{\rm X}$ for the radio-detected and X-ray-detected subsamples, respectively.

The results for EV1 are rather similar for all of the subsamples in both LRG and BOSS samples. EV1 of the whole sample and the radio-detected subsample is dominated by the anticorrelation of R4570 versus $S(\text{[O III]})$ and $S_{\rm O}$. $FWHM(\mathrm{H}\beta)$ also correlates with $S(\text{[O III]})$ and $S_{\rm O}$, but its contribution is less significant. Interestingly, in the X-ray-detected subsample R4570 is insignificant and the contribution of $S_{\rm X}$, which correlates with $S(\text{[O III]})$ and $S_{\rm O}$, is strong. In the LRG sample EV1 correlates

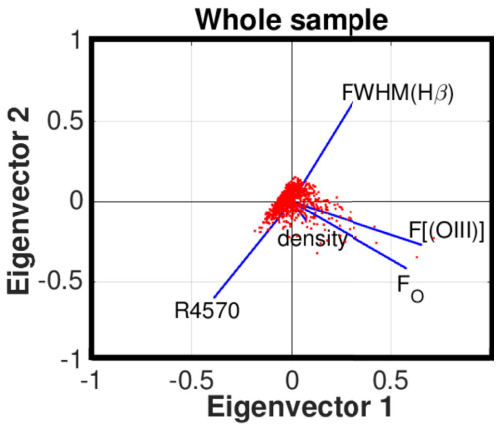

Figure 2.5. EV1 and EV2 of the PCA of the whole LRG sample. Individual sources are marked with red points, and the contribution of variables to each EV with blue lines. $F_{\rm O}$ is the optical flux density and F([O III]) the flux density of the [O III] emission line (Publication IV).

with the Eddington ratio to some extent in the whole sample and the radio-detected subsample, but not in the X-ray-detected subsample. There is a weak but significant correlation with the black hole mass in all samples. In the BOSS sample EV1 correlates strongly with $M_{\rm BH}$. This EV clearly seems to be comparable to the EV2 found in previous studies.

EV2 is similar for the whole sample and the radio-detected subsample, and is dominated by R4570, $S_{\rm O}$ which anticorrelate with $FWHM$(Hβ). $S_{\rm R}$ shows a significant contribution among the radio-detected sample and correlates with $FWHM$(Hβ). X-ray-detected sources otherwise agree with the other samples but the contribution of the optical emission is negligible, and in the BOSS sample the large-scale environment density contributed significantly and correlates with $FWHM$(Hβ). It seems that EV2 of this study is similar to the 'traditional' EV1, dominated by the anticorrelation between R4570 and $FWHM$(Hβ) (Boroson & Green 1992; Boroson 2002; Xu et al. 2012). Indeed, despite the minor differences in the variable strengths in EV2, it correlates strongly with the Eddington ratio among all samples.

Practically in all cases EV3 is dominated by the density parameter, with the other variables being negligible. Only in the radio-detected subsample of the LRG sample also $S_{\rm R}$ has a considerable contribution and it correlates with the density parameter. The emergence of radio emission together with the large-scale environment density in this EV supports the scenario that the environment affects the radio properties of AGN. The fact that EV3 is almost completely dominated by the large-scale environment parameter, with the other variables being insignificant, indicates that there exists no tight connection between the large-scale environment density and the intrinsic properties of NLS1 galaxies included in this study. EV3 does not correlate with the Eddington ratio or the black hole mass either.

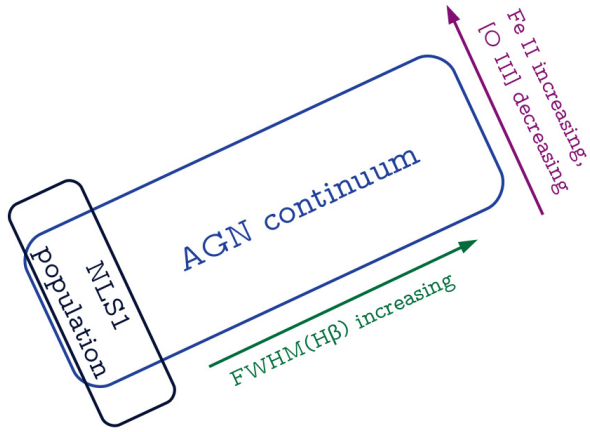

Figure 2.6. Schematic AGN continuum.

As Figure 2.5 shows, EV1 and EV2 are dominated by the interplay between R4570, $FWHM(\mathrm{H}\beta)$ and S([O III]), the components that are also the most dominant in the 4DE1 space. This result fits NLS1 population nicely in the narrow $FWHM(\mathrm{H}\beta)$, strong Fe II, and weak [O III] extreme of the AGN continuum. When using a sample of only NLS1 galaxies, the first EVs seem to be reversed, a phenomenon seen already in Publication I. This is due to using a pure sample inside which there is much less variance in certain variables, for example, in the case of NLS1 galaxies $FWHM(\mathrm{H}\beta)$ is limited to 0–2000 km s^{-1}. This causes the variance of other variables to be emphasised in the PCA. Figure 2.6 explains this with a simplified graph; when taking only a slice of the whole AGN continuum, the variance is more pronounced along the 'secondary' properties and thus they are also more dominant in the PCA.

2.5 Environment

2.5.1 Host galaxies

The host galaxy is the closest environment of an AGN and directly affects its activity level because the black hole feeds on the gas reservoirs of its host galaxy. For the AGN to stay active the gas must be efficiently transferred from the outer parts of the galaxy towards its center. In spiral galaxies non-axisymmetric structures such as bars are able to bring gas within the innermost 1 kpc (Sakamoto et al. 1999). The gas forms nuclear spirals which further transfer it closer to the nucleus (van de Ven & Fathi 2010). The accumulating gas often triggers nuclear star formation, or even starburst, frequently seen in AGN (LaMassa et al. 2013). The AGN might be triggered simultaneously

or at a later time. Mass loss from the evolving young stars provides additional fuel for the black hole. Star formation gradually decreases, leaving an intermediate-age stellar population behind while the AGN activity can continue for tens to hundreds of mega-years (Storchi-Bergmann 2008).

The active nucleus in turn affects the host galaxy via various feedback machanisms, for example, radiation pressure, jets, and winds and outflows. This feedback is thought to be responsible for establishing the black hole mass – galaxy scaling relations, for example, the $M_{\rm BH} - \sigma$ relation. The feedback is stronger in jetted AGN. Two main feedback modes have been recognised; quasar mode and radio mode, corresponding to the accretion modes of AGN, HERG and LERG, respectively. The quasar mode works mainly through radiative feedback and winds, whereas in radio mode the jet is the predominant source of feedback. The feedback connected to the quasar mode can be either positive or negative. Positive feedback can enhance or even induce star formation in the host galaxy (e.g., Ishibashi & Fabian 2012), whereas negative feedback can slow down or entirely suppress star formation in the host galaxy (Pović et al. 2012). Radio mode feedback is usually associated with quenching of the star formation via heating the gas in the galaxy, and is believed to be responsible for turning galaxies into red and 'dead' galaxies. A review of these processes can be found in Fabian (2012).

The dynamics of the feedback processes between the host galaxy and the AGN are complicated and not yet well understood, but the AGN clearly considerably affects the galaxy evolution. Since significant AGN feedback is mostly associated with powerful jets – rare in NLS1 galaxies – it probably does not play a major role in shaping the properties of the NLS1 population. On the other hand, the host galaxy properties are likely to affect the nuclear activity and characteristics of NLS1 sources.

The intrinsic host galaxy morphology and properties can be affected by its local environment. In fact, studies indicate that galaxy – galaxy interactions may play a crucial role in AGN activity. A galaxy residing in a dense environment, for example, in a galaxy cluster, may undergo a number of minor and major mergers, and close encounters. Minor mergers can replenish the gas reservoirs of the more massive galaxy, and in addition distort its gas dynamics and cause gas infall, subsequently triggering circumnuclear star formation and feeding the black hole (Taniguchi 1999; Barth et al. 2008; Kaviraj 2016). Minor mergers are more frequent than major mergers (Lotz et al. 2011), and usually leave the morphology of the more massive galaxy unchanged. Also major mergers can bring more gas into the galaxy and cause similar gas infall than what is seen in minor mergers (Urrutia et al. 2008; Ellison et al. 2011), but they may also strip the galaxy of its gas reservoirs, quenching or preventing future star formation and severely limiting the gas supply of the black hole, and consequently impacting its future activity. Either way, in major mergers the morphologies of the participating galaxies are transformed and usually they form a massive early-type galaxy. It has been argued that the most luminous AGN are predominantly triggered by major mergers (Treister et al. 2012; Villforth et al. 2014). Merging is also an effective way to grow a black hole when the central black holes of the merging galaxies coalesce. The effects of a close encounter depend strongly on the initial parameters of the system,

but like minor mergers it may cause gas infall leading to enhanced star formation and triggering of the AGN activity. However, there are also studies which do not find mergers and AGN activity connected at all (Corbin 2000; Cisternas et al. 2011; Kocevski et al. 2012).

Host galaxy studies of NLS1 galaxies have so far concentrated on the radio-quiet and radio-silent sources, mostly because in the radio-loud sources the AGN contribution is considerable also in the optical and infrared bands, and complicates or prevents the modelling of the morphology. Most but not all radio-quiet NLS1 sources reside in late-type galaxies (Ohta et al. 2007).

Generally the host galaxies of NLS1 sources seem to exhibit an ensemble of properties that support the secular growth scenario of the central black hole. Large-scale stellar bars outside the innermost 1 kpc are frequently seen in NLS1 galaxies; Crenshaw et al. (2003) found 65% and Ohta et al. (2007) 80% of the disk-like hosts of NLS1 galaxies to possess bars. Deo et al. (2006) found that in their NLS1 sample 83% of the host galaxies show nuclear dust spirals within the innermost 1 kpc and most of them are grand-design (80%). Evidence of enhanced circumnuclear star formation in NLS1 galaxies has also been found in several studies (e.g., Deo et al. 2006; Sani et al. 2010).

Quite a small fraction, 8%–16%, of NLS1 galaxies show signs of interaction or merging (Ohta et al. 2007). It seems that it is rarer in NLS1 galaxies than in Seyfert galaxies in general (20%–30%, Schmitt et al. 2001). Ohta et al. (2007) also found that the frequency of interacting or merging increases with increasing FWHM(Hβ). This could at least partly explain the discovery by Crenshaw et al. (2003) that the frequency of bars is anticorrelated with FWHM(Hβ), since a merger is able to disturb or even destroy the bar structure. The absence of interaction or merging in NLS1 galaxies (e.g., Ryan et al. 2007; Ohta et al. 2007) indicates that the evolution of the host galaxy as well as the growth of the central black hole have been and are dominated by secular processes. The prevalence of pseudo-bulges in NLS1 host galaxies supports this scenario (Orban de Xivry et al. 2011), since pseudo-bulges are formed via internal secular processes, whereas classical bulges are usually formed as a consequence of a merger.

The favourable combination of properties seen in NLS1 galaxies might be able to efficiently fuel the central black hole. Sufficient fuel supply via secular processes seems to be able to maintain the high activity levels seen in them and at least partly explain the high observed Eddington ratios. However, even if most NLS1 sources are radio-quiet or radio-silent and preferentially non-jetted, the small fraction of jetted NLS1 galaxies is becoming increasingly important in attempts to understand the nature of the whole NLS1 population as well as the triggering and maintaining of relativistic jets in young AGN.

So far the host galaxy morphologies of only four jetted NLS1 sources have been investigated. Zhou et al. (2007) claimed the host galaxy of 1H0323+342 to be a one-armed spiral galaxy. However, it has been later argued that it is an elliptical galaxy whose morphology is disturbed due to merging (Antón et al. 2008; León Tavares et al. 2014). According to Olguín-Iglesias et al. (2017) the host galaxy of FBQS

J1644+2619 is a barred lenticular galaxy with a pseudo-bulge. They argue that the host shows clear signs of strong bar-driven secular evolution which efficiently feeds the black hole and maintains the nuclear activity. There are also signs of recent minor mergers which could replenish the gas reservoirs of the host galaxy. On the contrary, D'Ammando et al. (2017) claim that the host galaxy of FBQS J1644+2619 is an elliptical galaxy. The third studied jetted NLS1 galaxy, PKS 2004-447, resides in a barred disk-like galaxy (Kotilainen et al. 2016), and has a pseudo-bulge, indicating that its evolution and growth have been dominated by secular processes. According to D'Ammando et al. (2018), the fourth studied jetted NLS1 galaxy, PKS 1502+036, is hosted by an elliptical galaxy. All of these four NLS1 galaxies are gamma-ray detected sources with powerful relativistic jets, so it is remarkable that the secular evolution seems to be dominant at least in some of them. This discovery goes against the conventional view of only highly-evolved massive elliptical galaxies being able to launch and maintain relativistic jets.

However, no definite conclusions can be drawn from four galaxies, a considerably larger sample is needed. We observed the host galaxies of nine NLS1 sources using the NOTCam at the Nordic Optical Telescope (NOT, Publication VI). All the sources are included in the Metsähovi NLS1 observing programme (Publication III and Publication VII), but their properties are otherwise diverse. They are also included in our ongoing e-VLBI programme that aims to study the differences in the pc-scale radio morphologies of steep- and flat-spectrum NLS1 galaxies. These nine NLS1 galaxies were selected for near-infrared observations to enable comparison of radio morphologies and spectra, and host galaxy morphologies, and to study their possible connection. The sample includes sources detected and not detected at 37 GHz, radio-silent, radio-quiet, and radio-loud sources, and both flat- and steep-spectrum sources.

The observations were performed in J-band using the NOTCam with high resolution imaging (0.078"/px). We also observed a separate point spread function (PSF) star with very high S/N for each of our sources to properly model the AGN and remove its contribution. To perform a photometric decomposition of the images we used a 2D fitting algorithm GALFIT version 3 (Peng et al. 2010). Most sources were sufficiently fit with variations of the Sérsic profile (Graham & Driver 2005). In addition to modelling the host galaxy morphologies we obtained their radial surface brightness profiles using IRAF task *ELLIPSE*.

Our results are summarised in Table 2.1. We were not able to model four of our sources reliably. This was probably due to the non-optimal weather conditions combined with some of the highest redshifts of our sample; the data quality was not good enough to properly perform the photometric decomposition. However, the remaining five host galaxies were modelled successfully, and all of them are late-type galaxies. Four of them host pseudo-bulges, and the fifth does not seem to have a distinguishable bulge component. Four out of five also have bars. Three of these five sources have been detected at 37 GHz and possibly host jets. We estimated the black hole masses of the successfully modelled sources using the Hβ line dispersion, and the mean black hole mass is $\log M_{\rm BH} = 6.8\ M_{\odot}$. Whereas these morphologies and black hole masses are typical for NLS1 galaxies, they are unusual for jetted AGN.

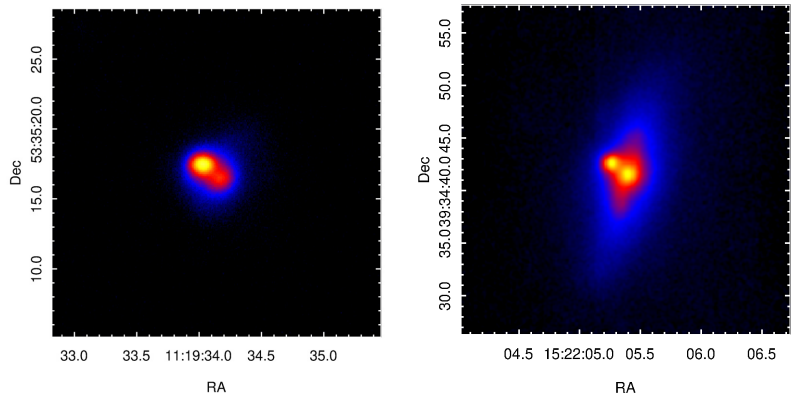

Figure 2.7. *J*-band images of interacting NLS1 galaxies. *Left panel:* SDSS J111934.01+533518.7. The field of view is 23.4" / 44.1 kpc. *right panel:* SDSS J152205.41+393441.3. The field of view is 31.2" / 43.5 kpc (Publication VI).

The high fraction of interacting or perturbed galaxies is also remarkable: three out of five properly modelled sources have a disturbed morphology. Examples of such sources are shown in Figure 2.7. Due to the characteristics of late-type galaxies, for example, pseudo-bulges, it seems that secular processes have dominated their evolution so far. Two of these three have been detected at 37 GHz. If they really are jetted, this result could indicate that in NLS1 galaxies the instabilities caused by a merger are able to trigger the nuclear activity and eventually lead to the launching of a jet. One source also exhibits star formation at starburst level (Caccianiga et al. 2015), which could be due to the interaction causing gas infall, triggering the starburst, and also feeding the black hole. Mathur et al. (2001) argued that NLS1 galaxies could be sources rejuvenated by mergers. Whereas this scenario seems not to hold for the NLS1 population in general, it might be true for the jetted sources.

Indeed, compared to the radio-quiet/radio-silent NLS1 population, the host galaxy properties seem to be similar with the exception of the significantly higher percentage of interaction among the jetted sources. However, even if it seems likely that interaction is connected to the launching of jets in NLS1 galaxies, there are also sources that possess jets but do not show signs of interaction – or possible signs have passed unnoticed – requiring an alternative explanation. In general, however, interaction seems to be a dividing factor between the jetted and non-jetted NLS1 galaxies. This scenario is supported by the result that jetted NLS1 galaxies reside in denser large-scale environments, where also interaction is more probable, than the non-jetted NLS1 galaxies (Publication IV). The heterogeneity seen in the NLS1 population could also be explained by different evolutionary stages, induced by interaction and mergers.

Our results more than double the number of jetted NLS1 sources with known host galaxy morphologies and provide additional proof that evolving young spiral galaxies with unusually low black hole masses can indeed launch and maintain powerful jets.

Table 2.1. Summary of the host galaxy observation results.

source	morph.	components	notes
J091313.73+365817.2	spiral	PB, bar, disk	enhanced SF
J111934.01+533518.7	spiral	PB	interacting, RL
J122749.14+321458.9†	unclear		enhanced SF
J123220.11+495721.8†	unclear		
J125635.89+500852.4†	unclear		
J133345.47+414127.7†	unclear		SB
J151020.06+554722.0†	spiral	bar, disk	
J152205.41+393441.3†	spiral	PB, bar, disk	interacting
J161259.83+421940.3†	spiral	PB, bar	disturbed, SB

† = jetted, PB = pseudo-bulge, RL = radio-loud, SF = star formation, SB = starburst.

This highlights the uniqueness of jetted NLS1 galaxies among the jetted AGN, and further challenges the conventional view that only highly-evolved massive elliptical galaxies with black hole masses exceeding $10^8 M_\odot$ are able to launch relativistic jets.

2.5.2 Local and large-scale environments

The local environment of a galaxy spans from its close satellite and neighbour galaxies to the group or cluster it resides in. ∼15% of massive galaxies[6] ($M_{\rm gal} > 10^{11} M_\odot$) have at least one satellite galaxy whose mass is 10% of the mass of the more massive galaxy, and 30% a satellite galaxy whose mass is 1% of the mass of the primary. Elliptical galaxies are two to three times more likely to possess satellites than disk-like galaxies, and are therefore more likely to undergo minor mergers with their satellite galaxies (Mármol-Queraltó et al. 2012). The fraction of galaxies in close pairs is found to be ∼1–4% (Keenan et al. 2014; Man et al. 2012; Robotham et al. 2014; Fu et al. 2018), but it remains unclear whether significant evolution with redshift exists. However, in general, a galaxy can be expected to have undergone ∼1 major merger at $z < 3$, and 0.2 – 0.8 mergers since $z = 1$. The number of major mergers depends on the environment as the fraction of non-isolated galaxies strongly increases with the increasing density of the local environment (Ideue et al. 2009).

Only ∼5% of galaxies reside in rich clusters which are the largest gravitationally bound structures in the Universe. Rich clusters typically consist of 30–300 members within a radius of 1–2 h^{-1} Mpc. The largest fraction of galaxies, ∼55%, are in groups and poor clusters with 3–30 galaxies (Bahcall 1996) and a radius of 0.1–1 h^{-1} Mpc . A minor fraction of the rest are in pairs, and almost 40% are singular field galaxies.

The environment has an ability to shape and steer the evolution and properties of a galaxy. Galaxy – galaxy interactions, discussed in the previous Section, can radically impact the galaxy and the AGN. In denser environments, for example,

[6]For comparison, the mass of the Galaxy is $5.8 \times 10^{11} M_\odot$.

in galaxy groups or clusters, the probability of interaction is higher. There is a relation between the cluster-scale environment and the galaxy morphology (Hubble & Humason 1931; Dressler 1980; Park & Choi 2009; Chen et al. 2017): galaxies residing in clusters are more likely to show an early-type morphology than field galaxies. This tendency can be explained by more frequent galaxy – galaxy interactions in denser regions. Mergers transform the galaxy morphology from late-type towards early-type and the speed of this evolution greatly depends on the galaxy density of the local environment. Ellipticals being more frequent in denser environments may also explain the higher fraction of satellite galaxies around them, when compared to late-type galaxies (Mármol-Queraltó et al. 2012). A galaxy can also interact with a galaxy cluster and due to ram-pressure stripping it might lose a fraction or almost all of its gas in the process, which in turn quenches the star formation in the galaxy and transforms it to a red, inactive galaxy (Ebeling et al. 2014; Steinhauser et al. 2016).

At the largest scale galaxies are not distributed evenly in space but form a cosmic web of superclusters, filaments, and voids. Superclusters are collections of galaxy clusters and groups, and their sizes vary from tens to hundreds of Mpc. Most superclusters are not gravitationally bound, and the member clusters and groups shift away from each other due to the expansion of the Universe. Superclusters are connected to each other by filaments, regions containing an overdensity of galaxies but not as dense as superclusters. The axial ratios of these thread-like filaments are close to 1 and their radii is of the order of $\sim 0.5\ h^{-1}$ Mpc (Tempel et al. 2014a), with typical lengths of $50 - 80\ h^{-1}$ Mpc (Bharadwaj et al. 2004). Superclusters and filaments surround large regions of considerable underdensity called voids. Voids are generally spherical in shape and span from 20 to $100\ h^{-1}$ Mpc in diameter (Alpaslan et al. 2014). The matter density in a void is $\sim 10\%$ of the typical matter density in the Universe, and there are very few, usually isolated galaxies. However, structures similar to filaments but much more sparse have been found. Park & Lee (2009) found 'void filaments' with approximate lengths of $10\ h^{-1}$ Mpc and further speculated that since the gas flow is enhanced along these filamentary structures they might explain surprisingly high star formation and AGN activity in voids. Alpaslan et al. (2014) also found 'tendrils' of void galaxies branching from the actual filaments. These tendrils host on average six galaxies and are $10\ h^{-1}$ Mpc long. A relation similar to the one seen in cluster-scale environment also applies for the large-scale environments: the galaxies that reside close to or in filaments and superclusters have a higher probability of showing spheroid morphology, whereas the percentage of late-type galaxies increases the further inside the void they reside in (Lietzen et al. 2012; Einasto et al. 2014; Chen et al. 2017; Kuutma et al. 2017; Pandey & Sarkar 2017). Moreover, the large-scale environment density affects the properties of galaxy groups and thus indirectly the evolution of their member galaxies (Poudel et al. 2017).

AGN are found in all environments in the Universe, but their properties substantially differ depending on the environment. Ellison et al. (2011) found the fraction of AGN in close pairs to be higher than in isolated galaxies, and the AGN fraction seems to increase with the decreasing distance between the galaxy pair. In addition they found the number of binary AGN to be too high to be explained with random pairing of

galaxies, and argue that the pair galaxies exhibit correlated activity: an AGN paired with a normal galaxy is able to turn on the non-active galaxy. On the other hand, Fu et al. (2018) did not find an excess of single AGN in pairs but also they found a surprisingly high fraction of binary AGN.

Krongold et al. (2001) investigated the local environments of samples of NLS1, BLS1, and Sy2 galaxies by mapping their neighbour galaxies. They were able to confirm the results by Dultzin-Hacyan et al. (1999) who found Sy2 galaxies to have an excess of bright companion galaxies. However, they did not find any differences between the local environments of NLS1 and BLS1 galaxies. They found that NLS1 galaxies have fewer companions residing farther away from them when compared to a matching sample of non-active galaxies. Moreover, they found the host galaxies of NLS1 nuclei to be smaller than the hosts of BLS1 or non-active galaxies.

After Krongold et al. (2001) the local environments of NLS1 galaxies have not been investigated. However, the disparity between the local environments of BLS1 and Sy2 galaxies has been quite widely researched and the results are in good agreement. Generally, Sy2 galaxies have more close companion galaxies than BLS1 galaxies (Koulouridis et al. 2006, 2013). The companions of Sy2 galaxies also seem to be systematically bluer and exhibit more star formation than the companions of Sy1 galaxies. This is not compatible with the simple orientation-based AGN unification model. An alternative scheme evoked to explain this speculates an evolutionary line from starburst galaxies to Sy2 galaxies, and further to Sy1 galaxies (see Section 3.2). Agreeing results have been found when investigating the neighbouring galaxies of Type 1 and Type 2 AGN in general: companion galaxies of Type 1 AGN exhibit less star formation and have older stellar populations than the companion galaxies of Type 2 AGN (Villarroel & Korn 2014). If Type 2 AGN really are interacting or merging sources in which the AGN activity has been recently triggered, the heavy obscuration seen in them can be at least partly explained by star-forming circumnuclear molecular clouds.

The group- and cluster-scale environments of NLS1 galaxies have not been previously investigated, and studies including any Seyfert galaxies are scarce. Constantin & Vogeley (2006) concluded that Seyfert galaxies are less clustered than average galaxies and usually reside in smaller groups or in the outskirts of clusters. This kind of an environment could provide Seyfert galaxies with the ample cold gas needed to maintain their nuclear activity and high Eddington ratios. In general, significantly diverse AGN characteristics can be seen depending on the group- or cluster-scale environment. It seems that the radio-loudest AGN are consistently found in rich galaxy clusters (however, see McLure & Dunlop 2001), whereas radio-quiet AGN prefer less dense environments and reside mostly in groups (Kauffmann et al. 2008; Ramos Almeida et al. 2013; Hatch et al. 2014). This discrepancy seems to hold at least up to $z = 3$ and suggests that an exceptionally dense environment is required for an AGN to reach extraordinarily high radio luminosity, in other words, to be able to launch and maintain a relativistic jet. However, interesting differences have been observed among the radio-loud AGN. Ramos Almeida et al. (2013) found that 82% of radio galaxies with weak emission lines, that is, LERGs, reside in clusters, whereas the percentage

for radio galaxies with strong emission lines is only 31%. The result was similar also when comparing the environments of FR I and FR II galaxies. This discovery is in agreement with other observed properties of these AGN, the host galaxies of LERGs are preferably red, inactive ellipticals, but HERGs are often hosted by green or blue star-forming galaxies (Janssen et al. 2012). In the context of the morphology – environment relation this would place LERGs in the inner regions of rich clusters, which is also consistent with their accretion mode, and HERGs to considerably lower density environments with more abundant cold gas reservoirs to feed them.

Lietzen et al. (2011) used a sample of non-active LRGs in the SDSS Data Release 7 to construct a low-resolution three-dimensional LDF at $z < 0.3$ to investigate how various AGN classes are distributed in the large-scale structures of the Universe. They divided the LDF to superclusters, intermediate-density regions – filaments and outskirts of superclusters – and voids. As expected, FR I galaxies have, on average, the densest large-scale environments of all AGN classes included in their study: they mostly reside in superclusters and intermediate-density regions. In contrast BLOs, which are supposed to be unifiable with FR I sources, are found in significantly less dense environments. Similar and even more pronounced discrepancy is seen when comparing the environments of FR II galaxies and radio-loud quasars. The authors argue that the results may be due to small sample sizes. Their results may also be affected by the fact that the divisions to FR I/II and BLO/radio-loud quasar classes do not always go hand in hand. On average, the Sy 1 and Sy2 galaxies in their sample mostly reside in intermediate-density regions as do radio-quiet quasars. This is an expected result since these classes of AGN are probably rather similar, as explained in Section 1.3, and the environment in the filaments and the outer parts of superclusters can provide the gas needed for the intense accretion. Their Sy1 sample does not include NLS1 galaxies because they used a cut-off [O III]/H$\beta > 3$.

Constantin et al. (2008) used SDSS Data Release 2 data to study AGN activity in voids and compared the results with samples of wall (supercluster and filament) AGN. Their results show that AGN are common also in voids. There even seems to be more intermediate-luminosity AGN in voids than in walls, especially among the weakly accreting AGN. They do not find the properties of weakly accreting massive galaxies, mostly low-ionization nuclear emission-line region galaxies, to be correlated with their local environments, and propose that they were formed in massive halos to begin with and have since 'cleaned' their nearby environments in the voids. Instead, they find young galaxies such as H II and Seyfert galaxies to be preferentially located in small-scale strcutures or groups, and argue that their activity is triggered, or ar least affected, by the environment that enables galaxy – galaxy interaction. The wall AGN in their study seem to have significantly higher probabilities to be detectable at low radio frequencies (1.4 GHz) and, on average, they exhibit higher flux densities than void AGN.

The large-scale environment studies of NLS1 galaxies are practically nonexistent. Ermash (2014) compared the spatial densities of samples of NLS1 and BLS1 galaxies as a function of the large-scale galaxy density using the SDSS Data Release 7. They found the ratio of NLS1 and BLS1 galaxies to remain constant over different local

galaxy densities, implying that there are no differences between the large-scale environments of NLS1 and BLS1 galaxies. They also argue that since the fraction does not change with increasing density the evolution of NLS1 galaxies is dominated by secular processes in all environments. Generally the large-scale environment reflects the morphology – density relation; galaxies in denser large-scale environments have a higher probability to reside in a group or a cluster.

The properties of the local and large-scale environments of NLS1 galaxies are poorly known, but they could offer us an additional parameter in studying the nature of the NLS1 population and their connections to other AGN classes. We looked at the local and large-scale environments of a large and diverse sample of NLS1 galaxies in Publication IV. We used three environment data sets covering different redshift ranges between $z = 0 - 0.62$ and studied the large-scale environment trends within the NLS1 population, as well as compared their large-scale environment properties to the large-scale environments of other AGN samples. We also studied whether the large-scale environment significantly affects any of the intrinsic properties of NLS1 galaxies.

To achieve statistically significant results we compiled a large seed sample of 2049 NLS1 galaxies (Zhou et al. 2006; Komossa et al. 2006; Whalen et al. 2006; Yuan et al. 2008; Foschini 2011) without any selection criteria to be able to study the whole population. 1341 of these sources reside in the LDFs we use for this study. We used radio loudness to divide our sample into radio-silent, radio-quiet, and radio-loud subsamples. It is not an optimal method to categorise AGN, as discussed in Sections 1.3 and 2.3, but due to the lack of appropriate data it was the only proxy for nuclear activity available. In addition it allows the comparison with earlier results. Ambiguity of the radio loudness parameter, and an unknown fraction of misclassifications, for example, previously radio-silent sources hosting jets (Publication VII) can be expected to affect our results and to cause obscurity to some extent. We used the $FWHM(\mathrm{H}\beta)$ – luminosity mass scaling relation (Greene & Ho 2005) to estimate the black hole masses of our sources with adequate data (1312 sources). Depending on the case this method might underestimate (inclination effects caused by the possibly disk-like BLR, Decarli et al. 2011), or overestimate (unknown amount of jet contribution to the monochromatic luminosity at 5100Å, Wu et al. 2004) the black hole mass. However, when used mostly in statistics for a large sample it serves well as an order of magnitude estimate.

To extend the redshift coverage of our study we use three separate sets of environment data in our analyses. 1) SDSS Main Galaxy sample is a low-redshift catalogue of galaxies, limited to $z \leq 0.2$. We cross-matched the NLS1 galaxies with the galaxy and group catalogues (Tempel et al. 2014b) and filament catalogues (Tempel et al. 2014a) constructed using the Main Galaxy sample, and found 229 matches. In addition to local environment data, Tempel et al. (2014a) provides LDF data with 1, 2, 4, and 8 h^{-1} Mpc smoothing for each galaxy. 2) SDSS LRG LDF is the same LDF that was used in Lietzen et al. (2011), where also a more detailed description can be found (see also Liivamägi et al. 2012). The LDF spans from redshift of ∼0.07 to 0.4, and has a smoothing scale of 16 h^{-1} Mpc. The mean density around each galaxy is calculated

in a volume of 3 h^{-1} Mpc, essentially reflecting the supercluster scale environment surrounding it. We were able to obtain SDSS LRG LDF data for 960 sources, 171 of which overlap with the SDSS Main Galaxy sample. 3) The third LDF we used is constructed using the SDSS BOSS CMASS sample, and is limited to z = 0.43–0.62. The grid size is 3 h^{-1} Mpc, and the used smoothing scale was 8 h^{-1} Mpc. A detailed description of the BOSS LDF can be found in Lietzen et al. (2016). We have BOSS LDF data for 323 sources.

The local environment and filament data are available only for the sources in the Main Galaxy sample. Large-scale environment density data are available for all sources, but due to the different construction methods and smoothing scales they are not straightforwardly comparable and we analyse them separately. It should be noted that the luminosity-density is based on mean density, and whereas supercluster and void environments probably correlate well with the actual physical large-scale structures, the intermediate-density regions can coincide either with the physical filaments or regions similar in density between the superclusters and voids.

Of the NLS1 galaxies in the Main Galaxy sample only 23% (N=52) reside in groups, 10% in pairs (N=22), and the rest are field galaxies (N=155). The percentage in groups is significantly lower than for galaxies in general, for example, Bahcall (1996) found 60%, and Tempel et al. (2014b) 48% of galaxies to reside in groups or clusters. Moreover, the groups NLS1 galaxies are members of are generally poor. This result is in agreement with their young, unevolved nature. There is no difference in the group richness between radio-silent and radio-detected sources, but compared to radio-silent sources, radio-detected sources seem to reside in groups with smaller radii, meaning that they have higher number density. This may indicate that the density of the group has an impact on the radio properties of NLS1 galaxies possibly via galaxy – galaxy interactions. The comparison of the group richness and the large-scale environment density shows that groups with more members prefer denser large-scale environments, as was also found in Poudel et al. (2017).

In the LRG and BOSS LDFs the different density regions are based on their overdensity compared to the mean density. In the LRG LDF the density in a supercluster is more than three times the mean density, in an intermediate-density region the density is between one and three, and in a void less than the mean density (Lietzen et al. 2011). In the BOSS LDF only supercluster and non-supercluster environments have been defined, and the dividing density is six times the mean density. The average luminosity-densities for the different samples and their distribution to the large-scale environments for the LRG LDF are shown in Table 2.2 and for the BOSS LDF in Table 2.3.

The main results for both LDFs are consistent with each other: radio loudness increases with the increasing large-scale environment density. The large-scale environment seems to be able to transform the radio properties of NLS1 galaxies, probably via interaction and merging. Interestingly, the black hole masses of the different subsamples in a limited redshift range are similar, indicating that radio loudness is not a product of more massive black holes. The masses are similar in all environments. Thus the large-scale environment does not seem to affect the black hole mass at all,

suggesting that, on average, the accretion histories of all NLS1s have so far been similar, probably dominated by secular processes.

As a consequense of the large-scale environment affecting the radio characteristics of NLS1 galaxies also their spatial distribution to superclusters, intermediate-density regions, and voids changes as the radio loudness increases. The changes are not drastic but they are distinct nonetheless, for example, the fraction of sources residing in voids is largest among the radio-silent sources, and radio-louder sources are more often found in superclusters. An interesting exception to this are the radio-silent sources, of which a surprisingly large fraction – much larger than of the radio-quiet sources – reside in supercluster environments. This may be due to the severe misclassification of some radio-silent sources, as already seen in the Metsähovi 37 GHz observations of NLS1 galaxies (Section 2.3 Publication VII).

Since the SDSS LRG LDF we use is the same as in Lietzen et al. (2011), a comparison with their AGN samples is easy. Compared to any of their samples, NLS1 galaxies, on average, reside in less dense large-scale environments and the spatial distributions are distinct. The large-scale environments properties of NLS1 galaxies do not coincide with any of the samples used in Lietzen et al. (2011). Particularly interesting, and in contradiction with the results in Ermash (2014), is the fact that the large-scale environments and spatial distribution of NLS1 galaxies significantly differ from BLS1 and Sy2 galaxies. This is in disagreement with the orientation-based unification model of NLS1 and BLS1 galaxies (Decarli et al. 2008; Rakshit et al. 2017), and based on this result it seems improbable that BLS1 galaxies would be the parent population of NLS1 galaxies. This issue is discussed in more detail in Section 3.1.

We wanted to investigate whether using division to jetted and non-jetted NLS1 galaxies, instead of using the ambiguous radio loudness parameter (Padovani 2016), would affect the results. We collected all NLS1 galaxies that based on their properties, for example, gamma-ray or 37 GHz detections – can be assumed to host relativistic jets. Comparison samples include sources in which the radio emission is believed to be generated solely by star formation processes, or is a mixture of the jet and star formation emission. The number of NLS1 galaxies known to host jets is still small and only 15[7] of those lie in the LRG LDF. Their average density is similar to that of the radio-loud sample and higher than the average density of the star formation dominated or mixed sample. Interestingly, the average density of the star formation dominated sources is similar to that of radio-silent and radio-quiet sources. This is understandable since the star formation dominated sources probably do not have a jet and are radio-silent when only the jet emission is considered.

Even when selecting only the jetted NLS1 galaxies their average large-scale environment density (1.75±0.31) is considerably lower compared to the jetted AGN samples in Lietzen et al. (2011) (BLOs 2.50±0.20, flat-spectrum radio galaxies 2.60±0.07, FR I radio galaxies 3.01±0.07, and FR II radio galaxies 3.20±0.04). This is not surprising since the sources in their samples, for example, FR I and II galaxies, and BLOs and radio-loud quasars, are typically massive, highly-evolved galaxies that in

[7] Originally 17, but two sources were removed since they were initially selected for 37 GHz observations based on their dense large-scale environments and are thus biased.

the framework of the morphology – density relation should indeed reside in denser regions. However, this emphasises the disparity of NLS1 galaxies among the jetted AGN, and confirms that jets can be triggered in diverse environments, spanning from voids to superclusters. The triggering mechanism still remains unclear, but based on these results it seems that the environment, probably via galaxy – galaxy interactions, may play a role in the triggering of the jet.

In addition to the large-scale environment analysis we performed PCA using a parameter defining the large-scale environment density in the PCA of AGN for the first time ever. This study is described in Section 2.4.2. We did not find the density to correlate with any intrinsic properties of NLS1 galaxies included in the study. This is probably because the effect of the large-scale environment is subtle and works over long timescales steering the evolution of the whole galaxy. On the other hand, the nuclear activity in AGN varies at much shorter timescales and can be intermittent. The possible impacts of the large-scale environment can also easily pass unnoticed in a sample consisting of similar sources, such as the pure NLS1 galaxy sample in this study.

Table 2.2. Average density of the whole SDSS LRG sample and the NLS1 subsamples, and percentage in voids, intermediate density regions, and superclusters.

	N	Average density	LD[a] < 1 (%)	1 < LD < 3 (%)	LD > 3 (%)
all	960	1.50 ± 0.04	44	44	12
RS	799	1.48 ± 0.05	45	43	12
RD	161	1.61 ± 0.10	40	47	13
RQ	73	1.48 ± 0.08	40	52	8
RL + VRL	87	1.71 ± 0.14	40	43	17

(a) LD = mean luminosity-density of the LDF.

Table 2.3. Average density of the whole SDSS BOSS sample and the NLS1 subsamples, and the fraction outside of and in superclusters.

	N	Average density	LD[a] < 6 (%)	LD > 6 (%)
all	323	2.29 ± 0.15	92	8
RS	266	2.13 ± 0.15	93	7
RD	57	3.05 ± 0.54	86	14
RQ	6	1.12 ± 0.51	100	0
RL + VRL	51	3.27 ± 0.60	84	16

(a) LD = mean luminosity-density of the LDF.

3. Discussion on the nature of narrow-line Seyfert 1 galaxies

3.1 Heterogeneity, unification, and parent population

NLS1 galaxies are Type 1 AGN, probably seen almost face-on, and require not only a numerous parent population of Type 2 sources but also Type 1 sources seen at larger angles. The size of the parent population can be estimated based on the number of beamed NLS1 sources and their average Lorentz factor, γ. For each beamed source there should exist about $2\gamma^2$ misaligned sources. Taking the number of beamed NLS1 galaxies to be ∼20 at the moment and assuming γ is ∼10, the unbeamed parent population should consist of ∼4000 sources. The unbeamed NLS1 population offers a natural candidate for the parent population, but some studies indicate that all NLS1 sources are not intrinsically similar and thus cannot be unified to form one homogeneous class. If this is true, alternative parent population candidates from other AGN classes will be needed. After the discovery of relativistic jets in NLS1 galaxies also their role in the AGN unification scheme became more complicated. Traditionally they were placed into the unification scheme of radio-quiet, non-jetted AGN along with other Seyfert galaxies, but in the light of our current knowledge this idea has to be revised. These issues are discussed in more detail in this section.

3.1.1 Are NLS1 galaxies a homogeneous class?

As proof of the varied properties of the NLS1 population accumulates, the words of Pogge (2011):" – while NLS1s are a fairly well-defined and distinctive subclass of AGN, they are also a *diverse* subclass", could not be more true. The simplest division between NLS1 galaxies can be made based on their radio properties: radio-loud, radio-quiet, and radio-silent. Radio-loud sources can be further divided into flat- and steep-spectrum sources, whereas radio-quiet sources seem to mostly have steep spectra. The majority of NLS1 sources are radio-silent, and the absence of detected radio emission in them and their connection to radio-detected NLS1 sources is unclear.

In the simplest scenario all NLS1 sources are intrinsically similar, and the observed differences caused by external factors and some changing intrinsic properties, for

example, the intermittency of the nuclear activity. As estimated before the whole parent population needed at the moment consists of a few thousand sources –a number easily covered by the unbeamed NLS1 population. The various subclasses could be unified based on orientation. Gamma-detected sources are seen at very small angles and their radiation is greatly enhanced due to relativistic effects. Flat-spectrum radio-loud NLS1 sources would be seen at slightly larger angles so that the impact of relativistic effects is dimished, or their jets could be less powerful. When moving to even larger inclinations, the extended radio emission starts to dominate and the sources appear as steep-spectrum radio-loud NLS1 galaxies (Berton et al. 2015). The distributions of properties in the samples of flat- and steep-spectrum radio-loud NLS1 galaxies have been found to be statistically similar and point to their uniformity (Berton et al. 2015, Publication V). The discovery of jets in radio-quiet NLS1 galaxies (see Section 2.3) suggests that also they are a part of this unification scheme. Their radio quietness can be explained by the increasing contamination from the host galaxy; indeed, Ho & Peng (2001) found that most Sy1 nuclei are radio-loud when the host galaxy contamination is removed. However, studies comparing the properties of NLS1 subsamples defined based on their radio properties have not yielded conclusive results (Publication IV, Berton et al. 2015, Publication V).

There is evidence of enhanced star formation in NLS1 galaxies (Sani et al. 2010), even at levels where it could dominate the radio emission in some NLS1 sources (Caccianiga et al. 2015). Consequently, some radio-quiet and even radio-loud sources might be intrinsically radio-silent when considering only the AGN. Seemingly radio-silent sources could in turn belong to the parent population when taking into account the beaming effects. The intrinsic radio flux density at sub-mJy level, which would have been gone undetected, for example, in the FIRST survey, can due to beaming be enhanced hundredfold, to the radio emission levels seen in gamma-ray detected NLS1 sources (Publication V). Some observed differences between the radio-loud and radio-quiet/radio-silent sources, for example, the [O III] emission line blueshifts could also be explained by orientation (Boroson 2011, and see Section 2.1). The observed difference in the black hole masses may be partly due to the disparate radio luminosity distributions of the subsamples causing an observational bias that the radio-quiet sources are preferentially observed at lower redshifts (due to the faint radio emission they would appear radio-silent at higher redshifts), possibly causing the tendency of lower-luminosity radio-quiet sources seemingly harbouring also lower-mass black holes.

An additional factor able to explain the radio-loud – radio-quiet/radio-silent disparity might be intermittent jet activity at short timescales (tens-to-hundreds of years, Czerny et al. 2009): radio-quiet and radio-silent sources would currently be experiencing an inactive state. Intermittent jet activity, along with lower kinetic jet power, and high density nearby environment (gas-rich young spiral galaxies) could explain the general lack of blazar-like luminous extended radio structures and prominent relic radio emission. Some hints of possible intermittent jet activity have been seen in NLS1 galaxies, for example, a decrease of several magnitudes in their X-ray flux densities and the lack of gamma-ray detections in sources whose SEDs otherwise indicate the

dominance of a relativistic jet (Publication II). Also an aborted jet model has been proposed to account for the differences seen in the radio properties. In some sources – mostly radio-quiet – the initial velocity of the material launched into the jet is smaller than the escape velocity from the central potential well, and thus after reaching a certain radius the material falls back, colliding with newly ejected blobs and producing at least some of the observed X-ray radiation in these sources (Ghisellini et al. 2004). The conditions that in this case determine the success of the jet launch remain unclear.

Despite the multiple scenarios aimed at unifying NLS1 galaxies, there is also ample evidence against their simple unification. The statistically significant disparity in the black hole mass distributions is what seems to set radio-quiet and radio-loud sources apart, even when limiting the subsamples to low redshifts (Publication V). Additional arguments against the simple unification scenario come from radio imaging. The radio cores of radio-quiet sources are consistently found to fall at the less luminous end, and their extended emission seems to be faint and diffuse instead of intense radio emission indicating the presence of a proper relativistic jet. Moreover, the contribution of star formation seems to be more important in radio-quiet sources. It is possible that star formation activity is enhanced in all NLS1 galaxies, but in radio-loud sources the (beamed) radio emission from the jet dominates whereas in unbeamed radio-quiet and radio-silent sources the intrinsic radio emission from the jet is so weak that the contribution of the star formation becomes significant. The impact of distinct redshift distributions is, however, unknown, and the results remain inconclusive. Interestingly, the steep-spectrum NLS1 galaxies seem to harbour more massive black holes than the flat-spectrum sources. This could be explained by a disk-like BLR, leading to underestimated black hole masses in flat-spectrum sources, preferentially viewed at smaller angles.

In contrast the average black hole masses among radio-silent, radio-quiet, and radio-loud subsamples in different LDFs (and thus redshift ranges) in Publication IV seem to be similar. The tendency of radio-loud sources residing at higher redshifts is clear but this is probably an observational bias. However, the large-scale environment properties of the subsamples differ – a denser large-scale environment seems to be connected to a higher probability of radio loudness – and support the heterogeneity of the population (Publication IV). Similar black hole masses indicate that the disparate radio properties must be due to some other factor. The surprisingly high fraction of radio-silent sources residing in superclusters and the 37 GHz detections of radio-silent sources suggest that there is still a considerable number of misclassified NLS1 sources with powerful jets hiding among the radio-quiet and radio-silent populations. The inability to correctly classify NLS1 sources, or even determine the origin of the radio emission, is a considerable issue that leads to mixed subsamples, and inconsistent and inconclusive results in statistical studies. However, the large-scale environment differences remain even when considering more carefully selected samples of jetted and star formation dominated samples, indicating that these sources are actually not intrinsically similar[1].

[1]Caution must be exercised when using the 1.4 GHz radio flux density as a proxy for the possible jettedness (Publication VI).

Studies using smaller samples, for example, host galaxy studies, also point to the disparate intrinsic properties of the NLS1 subsamples. The results suggest differences in the host galaxy properties of jetted and non-jetted NLS1 sources. The higher fraction of interaction and mergers in jetted NLS1 galaxies is striking, possibly indicating that non-jetted and jetted sources are at different evolutionary stages. Indeed, the intraclass evolution could be a viable explanation for the observed heterogeneity among the NLS1 population (see Section 3.2 for more details).

It is also possible that the various subsamples are actually not connected at all and there exists separate evolutionary lines inside the NLS1 class. This requires that some of their intrinsic properties are different in a way that under similar internal and external conditions some NLS1 sources are able to launch a relativistic jet whereas some are not. What these properties could be remains unanswered. At the moment this scenario is not needed to explain the diverse characteristics of the NLS1 population, and it lacks observational proof that could not be explained by evolution.

3.1.2 Unification with blazars

Observations clearly show that (jetted) NLS1 galaxies are intrinsically different from blazars. Almost all of the observational characteristics can be explained by their lower black hole masses. Jetted NLS1 galaxies are less luminous but accrete at higher Eddington ratios, and they show shorter time-scale variability and generally more compact radio morphologies. In case of extended emission they show diffuse radio morphologies, probably due to their low-power jets. They also show intermittent nuclear activity and reside in dense accretion environments. As discussed in Section 2.2 it has been argued that the black holes in NLS1 galaxies are not genuinely low-mass but a product of orientation effects. However, it this were true their characteristics should be similar to those of FSRQs – which seems not to be true – or the mechanism that maintains the jet would need to be intrinsically different.

In addition to the properties of the AGN, for example, the disparate large-scale environments (Lietzen et al. 2011, Publication IV) and luminosity functions (Berton et al. 2016) further support the distinct nature of NLS1 galaxies when compared to blazars. The luminosity function of an FSRQ sample shows evolution in accordance with the cosmic downsizing: their number increases with increasing redshift (Berton et al. 2016). Their dense large-scale environments agree with this in the context of hierarchical galaxy evolution. Galaxies and also AGN in the denser areas are more evolved and therefore host more massive black holes than the galaxies residing in less dense areas. Interestingly the flat-spectrum radio-loud NLS1 sample in Berton et al. (2016) does not show any significant evolution with redshift, at least up to redshift z=0.6.

The jet powers of NLS1 galaxies are comparable with those of BLOs but for a different reason. In BLOs the jet power is low due to their photon-poor environments and ineffective electron cooling, whereas in NLS1 sources it is due to the lower-mass black holes. In contrast, the accretion environments of NLS1 galaxies are similar to the photon-rich environments of FSRQs. When taking into account the jet power

scaling with the black hole mass, $P_{\rm jet} \sim M_{\rm BH}^{1.4}$ (Heinz & Sunyaev 2003), the jets in NLS1 galaxies can be unified with the jets in FSRQs (Publication II). NLS1 sources seem to represent the lower black hole mass end of the FSRQ-type jetted AGN. Also their radio luminosity function seems to be the low-luminosity continuation of the radio luminosity function of FSRQs (Berton et al. 2016). In reality, however, the situation may be more complicate and the mass-based unification may need some finetuning as discussed in Section 2.

3.1.3 Parent population candidates

Even if the unbeamed NLS1 population could constitute the misaligned parent population of beamed NLS1 sources, they are Type 1 sources and an additional Type 2 parent population is needed. Since NLS1 galaxies are thought to be seen at small inclination angles (smaller than BLS1 galaxies), there are multiple Type 1 larger-inclination parent population candidates. If the NLS1 population includes separate – either evolutionarily or otherwise – subpopulations these require separate parent populations, which further complicates the picture. The most relevant Type 1 and 2 parent population candidates, and arguments for and against them, are discussed in this Section.

BLS1 galaxies

BLS1 galaxies, as another Sy1 class seemingly differing from NLS1 galaxies only in emission line widths, are a natural larger inclination angle candidate for the parent population. The largest discrepancy between BLS1 and NLS1 galaxies seems to be the black hole mass – generally more than $10^8 M_\odot$ in BLS1 and less than $10^8 M_\odot$ in NLS1 galaxies. This issue was discussed in more detail in Section 2.2. As a summary, some studies support the scenario that the narrow permitted emission lines are a projection effect caused by the small viewing angle and a flattened BLR, and the black hole masses and Eddington ratios become comparable to those of BLS1 galaxies when this is taken into account (e.g., Decarli et al. 2008; Rakshit et al. 2017). Other studies, estimating the black hole masses in NLS1 galaxies using alternative methods, do not agree with this and argue that the black hole masses are genuinely low (e.g., Publication II, Wang et al. 2016). However, definitive conclusions cannot yet be drawn.

Differences in optical properties have been confirmed in many studies (e.g., Xu et al. 2012; Rakshit et al. 2017), the most prominent being the considerably (factor of two in Rakshit et al. 2017) stronger relative Fe II emission in NLS1 galaxies. Rakshit & Stalin (2017) studied the optical variability of large samples of BLS1 and NLS1 sources, and confirmed the previous results (Klimek et al. 2004; Ai et al. 2013) that NLS1 galaxies show lower-amplitude variability than BLS1 galaxies. Also their X-ray properties are different: NLS1 sources show more prominent variability and have steeper X-ray spectra than BLS1 galaxies (Boller et al. 1996; Fabian et al. 2013). Host galaxy studies offer an opportunity to compare BLS1 and NLS1 galaxies based on properties that are not affected by orientation. Several studies have found considerable

differences in the host galaxy characteristics of BLS1 and NLS1 sources. The host galaxies of NLS1 galaxies were found to be smaller than those of BLS1 galaxies (Krongold et al. 2001). There are more large-scale stellar bars in NLS1 than BLS1 galaxies (they are ∼2–3 times more frequent, Crenshaw et al. 2003; Ohta et al. 2007). In addition Crenshaw et al. (2003) found an anticorrelation between the frequency of bars and the FWHM(Hβ). Nuclear dust spirals, especially of grand design, are much more common in NLS1 galaxies (Deo et al. 2006) and they exhibit higher rates of nuclear star formation (Deo et al. 2006; Sani et al. 2010) than BLS1 galaxies. NLS1 galaxies show less signs of merging and interaction than the Seyfert population in general (Ohta et al. 2007; Schmitt et al. 2001), and the probability of interaction seems to increase with increasing FWHM(Hβ). This could in part explain, for example, the absence of bars in BLS1 galaxies, since they could have been destroyed due to past interaction or mergers. In agreement with these results is also the discovery that the bulges in NLS1 galaxies are mostly pseudobulges, whereas the bulges in BLS1 galaxies come in all flavours, pseudo, classical, and composite bulges (Orban de Xivry et al. 2011).

A comparison of the local and large-scale environments of galaxies can be effectively utilised to study large, statistically significant samples and to reveal population-wide trends. In principle sources belonging to the same population should, on average, reside in similar environments. For example, were BLS1 galaxies the parent population of NLS1 galaxies their local and large-scale environments should be similar. Krongold et al. (2001) compared the environments of NLS1 and BLS1 galaxies by searching for close companions, but found no difference between them. The large-scale environments of a large sample of BLS1 galaxies (N=1095) were studied in Lietzen et al. (2011). Using the same data and methods this was done for an NLS1 sample of comparable size (N=960) in Publication IV. The average large-scale luminosity densities of BLS1 and NLS1 galaxies, and their spatial distributions, were found to be statistically significantly different. NLS1 sources preferentially reside in less dense large-scale environments than BLS1 sources, which agrees well with their presumably younger age. These results do not support the orientation-based unification of NLS1 and BLS1 sources. However, the diversity of BLS1 galaxies might affect the results, for example, the variety of bulges seen in them may indicate that the BLS1 population is not uniform. This heterogeneity has not been taken into account in any of the host galaxy or environment studies.

A similar issue was encountered with BLS1 and Sy2 galaxies before it was realised that Sy2 galaxies are actually a heterogeneous class, consisting of Type 2 counterparts of BLS1 galaxies with hidden BLRs (HBLR Sy2) and of 'pure' Sy2 sources genuinely without a BLR (non-HBLR Sy2, Heisler et al. 1997; Tran 2001, 2003; Marinucci et al. 2012). When some of the previous studies were reanalysed taking this into account, the BLS1 and Sy2 galaxies with hidden BLRs were found to be similar, and non-HBLR Sy2 galaxies different when compared to them. This could also be the case with NLS1 and BLS1 galaxies; it is possible that a subset of BLS1 galaxies is a part of the parent population of NLS1 galaxies.

Non-HBLR Sy2 galaxies

Sy2 galaxies without a hidden BLR were proposed as a possible Type 2 parent population of NLS1 galaxies (Zhang & Wang 2006). Zhang & Wang (2006) found non-HBLR Sy2 and NLS1 galaxies to have similar black hole masses, Eddington ratios, and [O III], infrared and radio luminosities, and argue that the sources could be unified based on orientation. They suggest that the non-detected polarised emission lines in non-HBLR Sy2 sources are due to the low-mass black holes and high accretion rates. Tran et al. (2011) studied these sources in more detail and confirmed that there is no evidence of broad emission lines in their polarised spectra, suggesting that the BLR is not just 'weak' but that these sources do not intrinsincally have a BLR. Therefore this scenario is probably not realistic.

CSS sources

The extreme radio loudness and flat radio spectra of some NLS1 galaxies were the first hints of the presence of relativistic jets in them. After the gamma-ray detections it became evident that a jetted, misaligned parent population is needed. Since NLS1 galaxies are thought to be young sources, young radio galaxies could constitute a natural parent population. A relation between NLS1 and CSS sources was suggested early on and evidence has since accumulated in favour of their close connection (e.g., Oshlack et al. 2001; Komossa et al. 2006; Yuan et al. 2008; Caccianiga et al. 2014; Schulz et al. 2016). CSS sources are powerful ($P_{1.4\mathrm{GHz}} > 10^{25}$ W Hz^{-1}) radio galaxies with radio spectra peaking around ∼100 MHz. They often exhibit double-sided jets that are confined inside the host galaxy (extent 1–20 kpc). The jets cross the interstellar medium but are probably powerful enough to break out from it. This is thought to be evidence of their young age, which according to estimates is $\sim 10^5$ yr or less (O'Dea 1998, and references therein). Similarly to more evolved radio galaxies they can be classified as LERG or HERG, and it is the HERG CSS sources that could form a part of the parent population of jetted NLS1 galaxies.

Berton et al. (2016) compared samples of F-NLS1 and HERG CSS sources (with a control sample of FSRQs). They found the black hole mass and Eddington ratio distributions of the NLS1 and HERG CSS samples to be similar at a statistically significant level: both sources generally harbour black holes with masses between 10^7 and $10^8 M_\odot$, and have high Eddington ratios. Neither of these samples show considerable density and/or luminosity evolution up to z=0.6, whereas the control sample of FSRQs shows positive evolution with increasing redshift. They also point out that signs of intermittent activity has been observed in both F-NLS1 and HERG CSS sources, further supporting their similar nature. However, the results are not yet conclusive and there are problems with the NLS1 / HERG CSS unification. On average CSS sources are considerably more luminous than NLS1 sources and exhibit more complex radio morphologies (Dallacasa et al. 2013). Interestingly, the lower-luminosity tail of CSS sources seem to be more alike to F-NLS1 sources: their radio morphologies are simpler and may indeed be products of intermittent jet activity (Kunert-Bajraszewska et al. 2010). This indicates that also the HERG CSS class is

heterogeneous and only the lower radio power HERG CSS sources could be unified with F-NLS1 sources. This scenario is supported by other results as well, for example, FWHM(Hβ) in some HERG CSS sources is < 2000 km s^{-1}. HERG CSS sources as radio galaxies should by definition be hosted by elliptical galaxies, but studies of their host galaxies are almost nonexistent. However, the black hole masses in CSS sources are quite low, and lower-mass black holes are usually found in disk-like host galaxies.

CSS sources are a promising parent population candidate for F-NLS1 galaxies. They fit well into the unification scenario of F- and S-NLS1 sources providing at least a part of the missing high inclination Type 1 and Type 2 parent population. Indeed, many S-NLS1 sources closely resemble CSS sources (Caccianiga et al. 2014; Gu et al. 2015; Schulz et al. 2016). The role of the radio-quiet NLS1 sources in this scenario is unclear. If CSS sources can actually be unified with F- and S-NLS1 sources, it suggests that the radio lobes should be prominent also in misaligned NLS1 sources, in contradiction to the faint, diffuse emission seen in radio-quiet NLS1 sources (Publication V). Most radio-quiet NLS1 galaxies could then belong to the evolutionarily younger NLS1 population discussed earlier.

Disk-hosted radio galaxies

Another possibility for the misaligned, jetted parent population are disk-hosted radio galaxies, especially those classified as HERGs. However, since their emission lines are broad (if the BLR is visible), this option requires the BLR to be flat and the lines in NLS1 galaxies to be narrow due to the projection effects. The properties of broad-line and narrow-line disk-hosted radio galaxies in comparison to flat-spectrum NLS1 galaxies were studied in Berton et al. (2015). They found that according to the Kolmogorov-Smirnov test the black hole mass distributions of disk-hosted radio galaxies and F-NLS1 sources could be drawn from the same population. However, the disk-hosted radio galaxies span a wider range of black hole masses and show a high-mass tail similar to 'normal' radio galaxies that are hosted by massive ellipticals. They also argue that the disk radio galaxies with low black hole masses and preferentially with pseudobulges could be part of the parent population of F-NLS1 sources. In general the disk-hosted radio galaxies seem to be an intermediate population between low black hole mass and high Eddington ratio sources such as NLS1 galaxies, and high black hole mass and low Eddington ratio sources such elliptical radio galaxies. While a fraction of disk-hosted radio galaxies might belong to the parent population of the jetted NLS1 galaxies, their number is still low, and as such cannot explain the whole missing parent population. Further studies, especially of their host galaxy properties, and of statistically significant extent will be needed to estimate the contribution of these sources to the parent population of jetted NLS1 galaxies.

3.2 Evolution

The evolution of the most luminous AGN show a trend called *cosmic downsizing* (Barger et al. 2005). Their number density and luminosity peak at $z \sim 2$–3, and have

been decreasing after that (Fanidakis et al. 2011; Rigby et al. 2015). Essentially it means that the most massive black holes, mostly residing in massive ellipticals, were more active in the past with the activity peaking at $z \sim 2$–3. These sources prefer the densest large- and cluster-scale environments where the galaxy could initially evolve fast to a massive elliptical through mergers, and the black hole could effectively increase its mass through coalescence with other black holes and efficient radiative mode feeding (HERG). The decrease in their luminosity and number density is thought to be due to a change in their accretion mode. Instead of efficient cold gas accretion in a radiatively efficient mode, continuously larger fraction of them started accreting via a radiatively inefficient hot gas mode (Babić et al. 2007, LERG).

Recent studies indicate that the AGN population at high redshifts is twofold. In addition to the aforementioned population of very luminous, probably merger-triggered AGN there exists a more numerous population of mainly disk-hosted, undisturbed AGN with moderate luminosities (Schawinski et al. 2011; Kocevski et al. 2012). Interestingly this 'general' AGN population seems to be quite similar to the AGN population of the local Universe (Schawinski 2012). The number densities and luminosities of moderate- and low-luminosity AGN populations do not show similar behaviour to the luminous population (in fact the number of moderate- and low-luminosity AGN may be increasing, Cowie et al. 2003), but since the contribution of the once extraordinarily luminous AGN is diminishing, the overall population at $z < 1$ is dominated by these less luminous AGN with less massive black holes. These AGN and their mainly disk-like host galaxies are still evolving, mostly via secular processes. NLS1 galaxies belong to this population but seem to be evolving rapidly.

3.2.1 Intraclass evolution

Based on host galaxy studies most NLS1 galaxies reside in undisturbed, often barred spiral galaxies with pseudobulges. These properties indicate that the evolution of the host galaxy as well as the central black hole is, and has been, dominated by secular processes.

Assuming that the black holes in NLS1 galaxies have been accreting since $z \sim 1$ – when bars became a common component in spirals – with a duty cycle of ∼9% (for details, see Orban de Xivry et al. 2011), seed black holes of $10^3 - 10^4 M_\odot$ would have reached masses of $10^9 - 10^{10} M_\odot$ assuming a 'standard' value for the radiative efficiency, $\epsilon = 0.1$, and masses of $5 \times 10^5 - 5 \times 10^6 M_\odot$ with $\epsilon = 0.2$. NLS1 galaxies would have thus needed to accrete with a higher radiative efficiency than the general AGN population. If they continued accreting in a similar manner, it would take them ∼2.8 Gyr to increase their mass another order of magnitude, highlighting that NLS1 activity is not just a flick but a long-lasting phase in galaxy evolution. However, the mass accretion efficiency greatly depends on ϵ that depends on the spin of the black hole: black holes with larger spin have larger ϵ. To speed up the black hole in an NLS1 nucleus, infalling matter would need to have a favoured direction over long periods of time. This can be achieved if the properties of the infalling matter were related to the structure of the host and hence have, for example, a preferred angular

momentum direction. Results concerning the spins of black holes in NLS1 nuclei ar contradictory. Some studies indicate that they might be maximally rotating (Fabian et al. 2009; Gallo et al. 2015; Fabian et al. 2013), whereas others find the spins to be low or intermediate (Done et al. 2013; Liu et al. 2015). Large spins could explain the presence of relativistic jets in NLS1 galaxies in the context of the spin paradigm (see Section 1.2.2). However, this issue remains unsolved until more data are obtained.

As discussed in Section 3.1.1 it seems that NLS1 galaxies may not form a uniform class. In the emerging picture it is the radio properties that separate the different NLS1 subpopulations. Flat- and steep-spectrum radio-loud NLS1 galaxies share similar characteristics and could be unified by orientation, whereas the majority of radio-quiet NLS1 galaxies seem to belong to a different subpopulation. Radio-silent sources could in principle belong to either population. If the bulk of NLS1 galaxies were intrinsically similar and had evolved similarly, for example, via secular processes, they should show similar properties. Since this is not the case, there must be something that affected the evolution of a fraction of them and is responsible for the diversity we observe. Based on the largely undisturbed host galaxy morphologies of the radio-quiet sources, and the higher black hole masses of the F-NLS1 sources and their parent population, it seems that the latter are the more evolved sources. If their nuclei and host galaxies initially were similar to the radio-quiet population, we need to look for external factors that affected their evolution and set them apart.

A natural cause are events disturbing the host galaxy morphology, for example, minor and major mergers, and interaction, which are known to be capable of causing gas infall in galaxies and thus enhancing nuclear activity (see Section 2.5.1). As discussed in Section 2.5.1, the host galaxies of jetted NLS1 sources indeed seem to differ from the host galaxies of radio-quiet NLS1 sources by showing a considerably higher fraction of interaction and mergers. The higher merger rate could be a result of their environments; in a denser environment the probability of a merger is higher than in a less dense environment. Comparisons between the local environments of radio-loud and radio-quiet sources have not been performed, but in Publication IV their large-scale environments were found to be different, with radio-loud – and also jetted – sources favouring denser large-scale environments. Large-scale environment is not a proxy of their local environment, for example, the number and proximity of neighbouring galaxies, but the large-scale environment correlates with the evolution of the general galaxy population. The most evolved, old galaxies are found in the densest large-scale environments, whereas the younger galaxies reside in less dense large-scale environments. This supports the scenario in which jetted NLS1 galaxies are more evolved than radio-quiet ones, and the evolution is triggered by interaction and mergers. It is likely that not all NLS1 galaxies follow this evolutionary path and some of them, especially in the less dense regions, continue evolving via secular processes. Whether this evolution can lead to the triggering of relativistic jets during their NLS1 phase is unknown. Overall, our understanding of the diversity of the NLS1 population and the disparity between the possible subclasses is still incomplete.

3.2.2 Interclass evolution

Another important aspect is the place of the NLS1 galaxies among other AGN. There are various scenarios explaining the evolution of NLS1 galaxies prior to the NLS1 phase, as well as hypotheses concerning their future after it. If NLS1 galaxies were initially similar it can be assumed that they evolved from the same seed population. However, if during the NLS1 phase they can take separate evolutionary paths, for example, due to the interaction of only a fraction of the population, their characteristics after the NLS1 phase may diverge and they probably evolve into very different directions.

It has been proposed that NLS1 galaxies evolve from ultraluminous infrared galaxies (ULIRG, Kawakatu et al. 2007). However, this seems unlikely since ULIRGs are formed in mergers, whereas the majority of NLS1 galaxies are undisturbed spirals. A more plausible alternative is that before becoming active they were part of the ordinary non-active galaxy population with properties similar to NLS1 sources (Ermash & Komberg 2013). Simulations also show that galaxies with a dominant disk and low-luminosity bulge have quiet pasts, and have not undergone significant mergers since z = 2 (Martig et al. 2012). The third proposed alternative, based on similar host galaxy properties, is that they evolve from H II/starburst galaxies once the nuclear activity is triggered via a secular process, for example, the bar transporting matter to the nuclear region (Ohta et al. 2007).

Assuming that the emission lines in NLS1 galaxies are narrow due to the low-mass black holes efficiently accreting matter, they will in the future evolve to be broad-line AGN. The natural next step in their evolution will then be BLS1 galaxies and this has been proposed by many authors (e.g., Kawakatu et al. 2007; Wang & Zhang 2007; Zhu et al. 2009; Orban de Xivry et al. 2011). It should be noted again that BLS1 sources do not seem to be a uniform class and, for example, their bulges show diverse properties indicating that the evolution of a fraction of BLS1 galaxies with pseudobulges has been dominated by secular processes, whereas some seem to be products of merging and possess classical bulges. Then again, it is becoming evident that the NSL1 population is not homogeneous either. In the simple evolutionary scenario, NLS1 galaxies that do not experience mergers continue growing their black holes until they reach masses high enough to turn them into broad-line AGN. They then emerge as BLS1 galaxies with pseudobulges. The small fraction of NLS1 sources that undergo mergers could similarly evolve into BLS1 galaxies with classical and composite bulges. However, the fraction of classical bulges in BLS1 galaxies is higher than the estimated merger fraction of NLS1 galaxies (Ohta et al. 2007; Orban de Xivry et al. 2011), indicating that not all BLS1 galaxies have been NLS1 galaxies in the past –unless the merger fraction of NLS1 galaxies used to be significantly higher in the past, for example, due to the denser environments. In fact, as BLS1 galaxies do reside in denser large-scale environments than NLS1 galaxies, they should be more evolved than NLS1 galaxies and should have had a higher probability of interaction and merging in the past (Publication IV). Whether they had an NLS1 phase before turning into BLS1 galaxies is unclear. An important question is asked in Orban de Xivry et al.

(2011): "– when NLS1s evolve into BLS1s, will they be distinguishable from systems classified as BLS1s?" This can be examined by studying, for example, BLS1 sources with pseudobulges and comparing them to NLS1 galaxies with pseudobulges.

The future of the jetted NLS1 galaxies is even more uncertain. If they stay active longer than it takes for the black hole to grow to masses comparable to BLS1 galaxies, they probably would not be classified as such since relativistic jets do not occur in BLS1 galaxies. Mathur (2000) argue that they are low-redshift equivalents of luminous quasars and follow a separate but similar evolutionary path. They argue that NLS1 galaxies are in a phase comparable to low-ionisation broad absorption line quasars, when the winds from the nucleus are blowing away the matter surrounding it, and which is thought to precede the luminous quasar phase. Some results seem to support this scenario, for example, the metallicities in high-z quasars and NLS1 galaxies are equally high (Hamann & Ferland 1993), they share similar optical spectral properties (e.g., Lawrence et al. 1997; Elston et al. 1994), and outflows and winds are observed also in NLS1 galaxies. According to this scenario, after blowing away the interstellar medium, NLS1 galaxies reach the quasar phase that lasts as long as there is fuel left in the vicinity of the black hole. After depleting the remaining gas reservoirs they become dormant black holes, similar to what is seen in the centres of massive ellipticals in the local Universe. However, Mathur (2000) further argue that NLS1 nuclei reside in galaxies rejuvenated in mergers that would have also triggered the nuclear activity. According to our current knowledge this is not true for the majority of NLS1 galaxies, but since it seems that the interacting/merging fraction is significantly higher among the jetted NLS1 galaxies, this scenario could be realistic for them.

Observations support the connection of the jetted NLS1 galaxies to the higher-redshift, more luminous quasars. Jetted NLS1 galaxies seem to be very similar to FSRQs. They both exhibit HERG-type accretion and, when taking into account the scaling with the black hole mass, their jet powers are comparable (Publication II) possibly indicating that the environment near the black hole is similar as are the properties of the jets (Zhu et al. 2016). NLS1 galaxies seem to form the low-luminosity tail of FSRQs (Berton et al. 2016), which further supports their close connection. Berton et al. (2016) argue that NLS1 galaxies are the young, evolving versions of FSRQs, and suggest an evolutionary scenario in which jetted NLS1 galaxies will grow and evolve to become FSRQs. The HERG CSS sources of their parent population will evolve to HERG FR radio galaxies. NLS1 galaxies offer us an unprecedented view to the first stages of the evolution of powerful quasars, and may help us address the issues concerning the triggering and launching of jets as well as the conditions necessary to maintain them.

4. Conclusions

Astronomers have been intrigued by NLS1 galaxies since their discovery over 30 years ago, and their extraordinary properties challenge our understanding of AGN. An unexpected discovery were the fully-developed relativistic jets in a fraction, probably still increasing, of NLS1 galaxies. The presence of powerful jets in sources which were believed to be unable to host them has several implications on our understanding of the triggering and maintaining mechanisms of jets, and proved that the jet phenomenon is more diverse than previously thought. Jetted NLS1 sources clearly do not fit into the current evolutionary path leading to massive jetted ellipticals through major mergers, thus an alternative evolution scenario is needed to explain the relativistic jets in NLS1 galaxies. Unification schemes also need revision or, more likely, a new unification scheme for young, jetted AGN needs to be crafted. The heterogeneity of the NLS1 population further complicates these issues, because the subpopulations are not yet well defined and their relationship to other AGN classes is unclear. While examining the most exceptional individual jetted NLS1 galaxies is important and might help us to understand the jet phenomenon better, studying the whole diverse population is crucial for understanding the place of NLS1 galaxies in the big picture of AGN.

The aim of this thesis was to study the characteristics of the whole NLS1 population. This was achieved by executing statistical studies of unprecedentedly large samples of NLS1 galaxies, carrying out the high radio frequency observing programme at Metsähovi, and performing studies of smaller samples of NLS1 galaxies targeted to provide information about their previously poorly known properties.

In Publication II multifrequency data, from radio to gamma-rays, of 42 radio-loud flat-spectrum NLS1 galaxies were collected and analysed. Extreme spectral and flux density variability strongly favours the presence of relativistic jets in these sources, and indicates that the central engine of flat-spectrum NLS1 galaxies is alike to that of blazars, even if the jets in NLS1 galaxies are less powerful. The black hole mass was found to be $< 10^8 M_\odot$ for all sources, and once the jet power is scaled by the black hole mass, the jet powers in NLS1 galaxies and blazars become comparable, suggesting that the observed disparities are due to scaling.

In Publication I we performed the first PCA of a pure sample of almost 300 radio-detected NLS1 galaxies. It was followed by Publication IV in which the larger sample consisted of almost 1000 radio-detected and radio-silent NLS1 galaxies. In Publication

IV the large-scale environments of NLS1 galaxies were studied for the first time, and a parameter describing the large-scale environment was included in the PCA of AGN for the first time. The PCA in Publication I and Publication IV are in agreement, and place NLS1 galaxies in one extreme of the 4DE1 continuum as expected. The first two EVs in this pure NLS1 sample are reversed, probably due to the limited range of FWHM(Hβ). The statistical multifrequency and large-scale environment studies in Publication I and Publication IV support the heterogeneous nature of the NLS1 population. The radio-loud/jetted and the radio-quiet/radio-silent/non-jetted sources are distinct in terms of multifrequency emission, and the jettedness and radio loudness are connected to the large-scale environment density. However, on average, the large-scale environments of NLS1 galaxies are significantly less dense when compared to other jetted AGN, and some jetted NLS1 galaxies clearly reside in voids proving that the triggering of relativistic jets is possible in diverse environments. Comparison of large-scale environments further indicates that NLS1 galaxies cannot be unified with BLS1 galaxies simply based on their orientation. In the future carefully executed multifrequency and large-scale environment studies offer an effective tool for studying, for example, the parent population candidates of NLS1 galaxies and more generally the whole young AGN population.

A surprisingly high fraction of radio-silent NLS1 galaxies residing in superclusters hinted towards possibly misclassified sources. This proved to be true when two samples of NLS1 galaxies, selected based on other than their radio properties, were observed at Metsähovi Radio Observatory at 37 GH, published in Publication VII. The fraction of detected sources was nearly comparable to the detection rate of the two previous samples consisting of gamma-ray detected and the radio-loudest sources published in Publication III. This discovery highlights the ambiguity of the use of the low radio frequency observations, and the radio loudness parameter derived from them, as an indicator of the activity level of NLS1 nuclei. It further implies that powerful jets in NLS1 galaxies are more common than what was previously assumed and that high radio frequency observations offer an alternative tool for identifying them. The Metsähovi 37 GHz observations published in Publication III and Publication VII already constitute the largest data set of high radio frequency observations of NLS1 galaxies. The ongoing observation programme will continue to provide frequent NLS1 galaxy monitoring data at 37 GHz, and with the addition of new targets identification of new jetted NLS1 galaxies is expected. In the near future observations of these samples also at 22 GHz will be started.

Based on the Metsähovi observations a sample of mostly jetted NLS1 sources were observed in near-infrared to examine their host galaxy morphologies. The results, published in Publication VI, more than doubled the number of jetted NLS1 galaxies with known host morphologies. All NLS1 nuclei in our sample are hosted by preferentially barred spiral galaxies with pseudobulges and have black hole masses of $< 10^8 M_{\odot}$, confirming that powerful jets can be launched also in spiral galaxies with lower-mass black holes. Two out of three jetted sources show clearly disturbed morphology. The merger fraction is considerably higher than among the radio-quiet/radio-silent NLS1 population, indicating that interaction may have a role in initially triggering the

jet in NLS1 galaxies. In this framework the heterogeneity of the NLS1 population can be explained by different evolutionary stages due to interaction. The number of jetted NLS1 galaxies with known host morphologies is still small, and these results need to be confirmed with larger samples.

Publication V was so far the largest study, with 74 sources, concentrating on the kpc-scale radio morphologies of NLS1 galaxies. The results confirm the existence of the distinct NLS1 subclasses seen in previous studies. The extended kpc-scale radio morphologies seen in NLS1 galaxies are consistently quite diffuse and thus significantly different compared to blazars or radio galaxies, or the majority of CSS sources. This implies that the jetted NLS1 galaxies are not straightforwardly unifiable with CSS sources that have been proposed as their parent population. A more detailed study of the characteristics of CSS sources, for example, their host galaxies, will be needed to clarify their connection to NLS1 galaxies.

In the future NLS1 galaxies should be examined together with other young AGN classes. Studying the characteristics of diverse young AGN samples may help us to understand the initial triggering mechanism of the jet, and the circumstances needed to launch and maintain them. Investigating comprehensive samples of young AGN is a step towards a grand scheme of unification and evolution of young AGN. Additionally, it may give insights into their future evolution. They seem to be the scaled-down versions of FSRQs as concluded in Publication II, but it is unclear whether they will evolve to match them in black hole mass and jet power.

Future observatories and instruments are expected to greatly increase the number of NLS1 galaxies. Deeper, extensive optical surveys, for example, J-PAS[1], will scope the fainter NLS1 population and provide spectra also for sources not included in the SDSS spectroscopic survey. Even more important is to extend spectroscopic surveys towards near-infrared so that more NLS1 galaxies at higher redshifts could be found. Currently the SDSS BOSS allows the detection of the Hβ line up to z=1.05, slightly extending the range, but to study the cosmic evolution of NLS1 galaxies it will be essential to be able to identify them at even higher redshifts. Once operational, the James Webb Space Telescope[2] will enable spectroscopy in near- and mid-infrared bands, practically covering NLS1 galaxies over all cosmic time. Considerable advancements can also be expected in radio astronomy. The Square Kilometre Array[3] (SKA) will offer unprecedented sensitivity, flexibility, and speed. The sensitivity of SKA is well below mJy level and it will be able to detect most of the NLS1 sources currently classified as radio-silent. Its precursors, some of which might be later integrated to SKA, Australian Square Kilometre Array Pathfinder[4], MeerKAT[5], and the Murchison Widefield Array[6] are already performing high sensitivity observations. Next generation X-ray observatories, for example, the Advanced Telescope for High-

[1] http://www.j-pas.org/
[2] https://jwst.nasa.gov/index.html
[3] https://www.skatelescope.org/
[4] https://www.atnf.csiro.au/projects/askap/index.html
[5] http://www.ska.ac.za/gallery/meerkat/
[6] http://www.mwatelescope.org/

ENergy Astrophysics[7] will enable detailed observations of the innermost parts of the AGN. These observations are expected to reveal the geometry and position of the X-ray corona, and increase our knowledge about the properties of accretion disks and the disk-jet coupling. It will be possible to compare the X-ray data with the radio monitoring data now being collected at Metsähovi Radio Observatory. The search for gamma-ray emitting NLS1 galaxies must also continue, even though a replacement for *Fermi* seems not, unfortunately, to be imminent. NLS1 sources are also potential TeV targets. With new and more sensitive instruments in the near future, such as the Cherenkov Telescope Array[8], statistical studies and the comparison of TeV data to radio light curves become possible.

The knowledge of NLS1 galaxies was scarce for long, and the lack of data prevented their effective research or proper understanding. Recently samples of NLS1 galaxies have been included in various observing programmes, and extensive studies of the whole population as well as detailed studies of individual sources have been performed. Our new results allow performing well-planned and appropriate studies to form a comprehensive picture of NLS1 galaxies as a class and to study their place in the AGN family.

[7] http://www.the-athena-x-ray-observatory.eu/
[8] https://www.cta-observatory.org/

References

Abazajian, K. N., Adelman-McCarthy, J. K., Agüeros, M. A., et al. 2009, ApJS, 182, 543

Abdi, H. & Williams, L. J. 2010, Wiley Interdisciplinary Reviews: Computational Statistics, 2

Abdo, A. A., Ackermann, M., Ajello, M., et al. 2009a, ApJ, 699, 976

Abdo, A. A., Ackermann, M., Ajello, M., et al. 2009b, ApJ, 707, 727

Abramowicz, M. A., Czerny, B., Lasota, J. P., & Szuszkiewicz, E. 1988, ApJ, 332, 646

Ackermann, M., Ajello, M., Allafort, A., et al. 2011, ApJ, 743, 171

Adhikari, T. P., Hryniewicz, K., Różańska, A., Czerny, B., & Ferland, G. J. 2018, ApJ, 856, 78

Ai, Y. L., Yuan, W., Zhou, H., et al. 2013, AJ, 145, 90

Alam, S., Albareti, F. D., Allende Prieto, C., et al. 2015, ApJS, 219, 12

Allen, S. W., Dunn, R. J. H., Fabian, A. C., Taylor, G. B., & Reynolds, C. S. 2006, MNRAS, 372, 21

Aller, M. F., Aller, H. D., & Hughes, P. A. 1992, ApJ, 399, 16

Alpaslan, M., Robotham, A. S. G., Obreschkow, D., et al. 2014, MNRAS, 440, L106

Angelakis, E., Fuhrmann, L., Marchili, N., et al. 2015, A&A, 575, A55

Angelakis, E., Fuhrmann, L., Nestoras, I., et al. 2012, in Journal of Physics Conference Series, Vol. 372, Journal of Physics Conference Series, 012007

Antón, S., Browne, I. W. A., & Marchã, M. J. 2008, A&A, 490, 583

Antonucci, R. R. J. & Ulvestad, J. S. 1985, ApJ, 294, 158

Arshakian, T. G., Torrealba, J., Chavushyan, V. H., et al. 2010, A&A, 520, A62

Babić, A., Miller, L., Jarvis, M. J., et al. 2007, A&A, 474, 755

Bagchi, J., Vivek, M., Vikram, V., et al. 2014, ApJ, 788, 174

Bahcall, J. N., Kirhakos, S., Saxe, D. H., & Schneider, D. P. 1997, ApJ, 479, 642

Bahcall, N. A. 1996, ArXiv: 9611148

Baldi, R. D., Capetti, A., Robinson, A., Laor, A., & Behar, E. 2016, MNRAS, 458, L69

Ballo, L., Heras, F. J. H., Barcons, X., & Carrera, F. J. 2012, A&A, 545, A66

Barger, A. J., Cowie, L. L., Mushotzky, R. F., et al. 2005, AJ, 129, 578

Barth, A. J., Bentz, M. C., Greene, J. E., & Ho, L. C. 2008, ApJ, 683, L119

Baskin, A. & Laor, A. 2005, MNRAS, 358, 1043

Becker, R. H., White, R. L., & Helfand, D. J. 1995, ApJ, 450, 559

Beckmann, V. & Shrader, C. R. 2012, Active Galactic Nuclei (Wiley-VCH Verlag GmbH)

Berton, M., Caccianiga, A., Foschini, L., et al. 2016, A&A, 591, A98

Berton, M., Foschini, L., Ciroi, S., et al. 2015, A&A, 578, A28

Berton, M., Liao, N. H., La Mura, G., et al. 2017, ArXiv: 1707.07681

Best, P. N. & Heckman, T. M. 2012, MNRAS, 421, 1569

Bharadwaj, S., Bhavsar, S. P., & Sheth, J. V. 2004, ApJ, 606, 25

Bianchi, S., Bonilla, N. F., Guainazzi, M., Matt, G., & Ponti, G. 2009, A&A, 501, 915

Blandford, R. D. & Znajek, R. L. 1977, MNRAS, 179, 433

Boettcher, M. 2010, ArXiv: 1006.5048

Boissay, R., Ricci, C., & Paltani, S. 2016, A&A, 588, A70

Boller, T. 2000, NewAR, 44, 387

Boller, T., Brandt, W. N., Fabian, A. C., & Fink, H. H. 1997, MNRAS, 289, 393

Boller, T., Brandt, W. N., & Fink, H. 1996, A&A, 305, 53

Boroson, T. A. 2002, ApJ, 565, 78

Boroson, T. A. 2011, ApJ, 735, L14

Boroson, T. A. & Green, R. F. 1992, ApJS, 80, 109

Brinkmann, W., Laurent-Muehleisen, S. A., Voges, W., et al. 2000, A&A, 356, 445

Butler, A., Huynh, M., Delvecchio, I., et al. 2018, ArXiv: 1804.05983

Caccianiga, A., Antón, S., Ballo, L., et al. 2014, MNRAS, 441, 172

Caccianiga, A., Antón, S., Ballo, L., et al. 2015, MNRAS, 451, 1795

Caccianiga, A., Dallacasa, D., Antón, S., et al. 2017, MNRAS, 464, 1474

Calderone, G., Ghisellini, G., Colpi, M., & Dotti, M. 2013, MNRAS, 431, 210

Capetti, A., Axon, D. J., Macchetto, F. D., Marconi, A., & Winge, C. 1999, ApJ, 516, 187

Chen, S., Berton, M., La Mura, G., et al. 2018, ArXiv: 1801.07234

Chen, Y.-C., Ho, S., Mandelbaum, R., et al. 2017, MNRAS, 466, 1880

Chiaberge, M. & Marconi, A. 2011, MNRAS, 416, 917

Cirasuolo, M., Magliocchetti, M., Celotti, A., & Danese, L. 2003, MNRAS, 341, 993

Cisternas, M., Jahnke, K., Inskip, K. J., et al. 2011, ApJ, 726, 57

Collmar, W., Böttcher, M., Krichbaum, T. P., et al. 2010, A&A, 522, A66

Congiu, E., Berton, M., Giroletti, M., et al. 2017, A&A, 603, A32

Constantin, A., Hoyle, F., & Vogeley, M. S. 2008, ApJ, 673, 715

Constantin, A. & Shields, J. C. 2003, PASP, 115, 592

Constantin, A. & Vogeley, M. S. 2006, ApJ, 650, 727

Cooper, N. J., Lister, M. L., & Kochanczyk, M. D. 2007, ApJS, 171, 376

Corbin, M. R. 2000, ApJ, 536, L73

Cowie, L. L., Barger, A. J., Bautz, M. W., Brandt, W. N., & Garmire, G. P. 2003, ApJ, 584, L57

Cracco, V., Ciroi, S., Berton, M., et al. 2016, MNRAS, 462, 1256

Cracco, V., Ciroi, S., di Mille, F., et al. 2011, MNRAS, 418, 2630

Crenshaw, D. M., Kraemer, S. B., & Gabel, J. R. 2003, AJ, 126, 1690

Czerny, B., Siemiginowska, A., Janiuk, A., Nikiel-Wroczyński, B., & Stawarz, Ł. 2009, ApJ, 698, 840

Dallacasa, D., Orienti, M., Fanti, C., Fanti, R., & Stanghellini, C. 2013, MNRAS, 433, 147

D'Ammando, F., Acosta-Pulido, J. A., Capetti, A., et al. 2018, MNRAS, 478, L66

D'Ammando, F., Acosta-Pulido, J. A., Capetti, A., et al. 2017, MNRAS, 469, L11

D'Ammando, F., Orienti, M., Finke, J., et al. 2012, MNRAS, 426, 317

Decarli, R., Dotti, M., Fontana, M., & Haardt, F. 2008, MNRAS, 386, L15

Decarli, R., Dotti, M., & Treves, A. 2011, MNRAS, 413, 39

Deo, R. P., Crenshaw, D. M., & Kraemer, S. B. 2006, AJ, 132, 321

Doi, A., Asada, K., Fujisawa, K., et al. 2013, ApJ, 765, 69

Doi, A., Nagira, H., Kawakatu, N., et al. 2012, ApJ, 760, 41

Doi, A., Wajima, K., Hagiwara, Y., & Inoue, M. 2015, ApJ, 798, L30

Done, C., Jin, C., Middleton, M., & Ward, M. 2013, MNRAS, 434, 1955

Dotti, M., Colpi, M., Pallini, S., Perego, A., & Volonteri, M. 2013, ApJ, 762, 68

Dressler, A. 1980, ApJ, 236, 351

Dultzin-Hacyan, D., Krongold, Y., Fuentes-Guridi, I., & Marziani, P. 1999, ApJ, 513, L111

Ebeling, H., Stephenson, L. N., & Edge, A. C. 2014, ApJ, 781, L40

Einasto, M., Lietzen, H., Tempel, E., et al. 2014, A&A, 562, A87

Ellison, S. L., Patton, D. R., Mendel, J. T., & Scudder, J. M. 2011, MNRAS, 418, 2043

Elston, R., Thompson, K. L., & Hill, G. J. 1994, Nature, 367, 250

Ermash, A. A. 2014, ARep, 58, 205

Ermash, A. A. & Komberg, B. V. 2013, Ap, 56, 569

Fabian, A. C. 2012, ARA&A, 50, 455

Fabian, A. C., Kara, E., Walton, D. J., et al. 2013, MNRAS, 429, 2917

Fabian, A. C., Zoghbi, A., Ross, R. R., et al. 2009, Nature, 459, 540

Fanaroff, B. L. & Riley, J. M. 1974, MNRAS, 167, 31P

Fanidakis, N., Baugh, C. M., Benson, A. J., et al. 2011, MNRAS, 410, 53

Fath, E. A. 1909, Lick Observatory Bulletin, 5, 71

Foschini, L. 2011, in Narrow-Line Seyfert 1 Galaxies and their Place in the Universe, https://pos.sissa.it/126/024/pdf

Foschini, L. 2014, in International Journal of Modern Physics Conference Series, Vol. 28, International Journal of Modern Physics Conference Series, 1460188

Fu, H., Steffen, J. L., Gross, A. C., et al. 2018, ApJ, 856, 93

Gabányi, K. É., Frey, S., Paragi, Z., et al. 2018, MNRAS, 473, 1554

Gallo, L. C., Edwards, P. G., Ferrero, E., et al. 2006, MNRAS, 370, 245

Gallo, L. C., Fabian, A. C., Grupe, D., et al. 2013, MNRAS, 428, 1191

Gallo, L. C., Wilkins, D. R., Bonson, K., et al. 2015, MNRAS, 446, 633

Gardner, E. & Done, C. 2018, MNRAS, 473, 2639

Gaskell, C. M. 2000, NewAR, 44, 563

Gaskell, C. M. & Goosmann, R. W. 2013, ApJ, 769, 30

Ghisellini, G., Haardt, F., & Matt, G. 2004, A&A, 413, 535

Ghisellini, G., Tavecchio, F., Foschini, L., Bonnoli, G., & Tagliaferri, G. 2013, MNRAS, 432, L66

Gliozzi, M., Papadakis, I. E., Grupe, D., et al. 2010, ApJ, 717, 1243

Goodrich, R. W. 1989, ApJ, 342, 224

Graham, A. W. & Driver, S. P. 2005, PASA, 22, 118

Greene, J. E. & Ho, L. C. 2005, ApJ, 630, 122

Grupe, D. 2004, AJ, 127, 1799

Gu, M. & Chen, Y. 2010, AJ, 139, 2612

Gu, M., Chen, Y., Komossa, S., et al. 2015, ApJS, 221, 3

Hamann, F. & Ferland, G. 1993, ApJ, 418, 11

Hardcastle, M. J., Evans, D. A., & Croston, J. H. 2006, MNRAS, 370, 1893

Harrison, C. 2014, PhD thesis, Durham University

Hatch, N. A., Wylezalek, D., Kurk, J. D., et al. 2014, MNRAS, 445, 280

Heckman, T. M., Kauffmann, G., Brinchmann, J., et al. 2004, ApJ, 613, 109

Heinz, S. & Sunyaev, R. A. 2003, MNRAS, 343, L59

Heisler, C. A., Lumsden, S. L., & Bailey, J. A. 1997, Nature, 385, 700

Ho, L. C. & Peng, C. Y. 2001, ApJ, 555, 650

Hota, A., Sirothia, S. K., Ohyama, Y., et al. 2011, MNRAS, 417, L36

Hu, C., Du, P., Lu, K.-X., et al. 2015, ApJ, 804, 138

Hu, C., Wang, J.-M., Ho, L. C., et al. 2008, ApJ, 683, L115

Hubble, E. 1926a, Contributions from the Mount Wilson Observatory / Carnegie Institution of Washington, 324, 1

Hubble, E. & Humason, M. L. 1931, ApJ, 74, 43

Hubble, E. P. 1926b, ApJ, 64, 321

Hutchings, J. B., Janson, T., & Neff, S. G. 1989, ApJ, 342, 660

Ichimaru, S. 1977, ApJ, 214, 840

Ideue, Y., Nagao, T., Taniguchi, Y., et al. 2009, ApJ, 700, 971

Ilić, D., Popović, L. Č., Shapovalova, A. I., et al. 2015, JApA, 36, 433

Ishibashi, W. & Fabian, A. C. 2012, MNRAS, 427, 2998

Janssen, R. M. J., Röttgering, H. J. A., Best, P. N., & Brinchmann, J. 2012, A&A, 541, A62

Jorstad, S. G., Marscher, A. P., Mattox, J. R., et al. 2001, ApJ, 556, 738

Kauffmann, G., Heckman, T. M., & Best, P. N. 2008, MNRAS, 384, 953

Kaviraj, S. 2016, in IAU Symposium, Vol. 319, Galaxies at High Redshift and Their Evolution Over Cosmic Time, ed. S. Kaviraj, 130–136

Kaviraj, S., Shabala, S. S., Deller, A. T., & Middelberg, E. 2015, MNRAS, 454, 1595

Kawakatu, N., Imanishi, M., & Nagao, T. 2007, ApJ, 661, 660

Keenan, R. C., Foucaud, S., De Propris, R., et al. 2014, ApJ, 795, 157

Kellermann, K. I., Sramek, R., Schmidt, M., Shaffer, D. B., & Green, R. 1989, AJ, 98, 1195

Kharb, P., Lister, M. L., & Cooper, N. J. 2010, ApJ, 710, 764

Kharb, P., O'Dea, C. P., Baum, S. A., Colbert, E. J. M., & Xu, C. 2006, ApJ, 652, 177

Kharb, P. & Shastri, P. 2004, A&A, 425, 825

Kinney, A. L., Schmitt, H. R., Clarke, C. J., et al. 2000, ApJ, 537, 152

Klimek, E. S., Gaskell, C. M., & Hedrick, C. H. 2004, ApJ, 609, 69

Kocevski, D. D., Faber, S. M., Mozena, M., et al. 2012, ApJ, 744, 148

Kollatschny, W. & Zetzl, M. 2013, A&A, 549, A100

Komossa, S., Voges, W., Xu, D., et al. 2006, AJ, 132, 531

Komossa, S., Xu, D., Zhou, H., Storchi-Bergmann, T., & Binette, L. 2008, ApJ, 680, 926

Kormendy, J. & Gebhardt, K. 2001, in American Institute of Physics Conference Series, Vol. 586, 20th Texas Symposium on relativistic astrophysics, ed. J. C. Wheeler & H. Martel, 363–381

Kotilainen, J. K., León-Tavares, J., Olguín-Iglesias, A., et al. 2016, ApJ, 832, 157

Koulouridis, E., Plionis, M., Chavushyan, V., et al. 2013, A&A, 552, A135

Koulouridis, E., Plionis, M., Chavushyan, V., et al. 2006, ApJ, 639, 37

Kovačević, J., Popović, L. Č., & Dimitrijević, M. S. 2010, ApJS, 189, 15

Krongold, Y., Dultzin-Hacyan, D., & Marziani, P. 2001, AJ, 121, 702

Kunert-Bajraszewska, M., Gawroński, M. P., Labiano, A., & Siemiginowska, A. 2010, MNRAS, 408, 2261

Kunert-Bajraszewska, M., Marecki, A., & Thomasson, P. 2006, A&A, 450, 945

Kuutma, T., Tamm, A., & Tempel, E. 2017, A&A, 600, L6

Kynoch, D., Landt, H., Ward, M. J., et al. 2018, MNRAS, 475, 404

Lähteenmäki, A. & Valtaoja, E. 2003, ApJ, 590, 95

LaMassa, S. M., Cales, S., Moran, E. C., et al. 2015, ApJ, 800, 144

LaMassa, S. M., Heckman, T. M., Ptak, A., & Urry, C. M. 2013, ApJ, 765, L33

Landt, H., Padovani, P., Perlman, E. S., & Giommi, P. 2004, MNRAS, 351, 83

Laor, A. 2000, ApJ, 543, L111

Lawrence, A., Elvis, M., Wilkes, B. J., McHardy, I., & Brandt, N. 1997, MNRAS, 285, 879

Leipski, C., Falcke, H., Bennert, N., & Hüttemeister, S. 2006, A&A, 455, 161

León Tavares, J., Kotilainen, J., Chavushyan, V., et al. 2014, ApJ, 795, 58

León-Tavares, J., Valtaoja, E., Giommi, P., et al. 2012, ApJ, 754, 23

Lien, A., Chakraborty, N., Fields, B. D., & Kemball, A. 2011, ApJ, 740, 23

Lietzen, H., Heinämäki, P., Nurmi, P., et al. 2011, A&A, 535, A21

Lietzen, H., Tempel, E., Heinämäki, P., et al. 2012, A&A, 545, A104

Lietzen, H., Tempel, E., Liivamägi, L. J., et al. 2016, A&A, 588, L4

Liivamägi, L. J., Tempel, E., & Saar, E. 2012, A&A, 539, A80

Lisakov, M. M., Kovalev, Y. Y., Savolainen, T., Hovatta, T., & Kutkin, A. M. 2017, MNRAS, 468, 4478

Lister, M. L., Aller, M. F., Aller, H. D., et al. 2016, AJ, 152, 12

Liu, X., Yang, P., Supriyanto, R., & Zhang, Z. 2016, IJAA, 6, 166

Liu, Z., Yuan, W., Lu, Y., & Zhou, X. 2015, MNRAS, 447, 517

Lohfink, A. M., Reynolds, C. S., Mushotzky, R. F., & Nowak, M. A. 2013, MmSAI, 84, 699

Lorenz, E. & Wagner, R. 2012, EPJH, 37, 459

Lotz, J. M., Jonsson, P., Cox, T. J., et al. 2011, ApJ, 742, 103

Lynden-Bell, D. 1969, Nature, 223, 690

Man, A. W. S., Toft, S., Zirm, A. W., Wuyts, S., & van der Wel, A. 2012, ApJ, 744, 85

Marinello, M., Rodríguez-Ardila, A., Garcia-Rissmann, A., Sigut, T. A. A., & Pradhan, A. K. 2016, ApJ, 820, 116

Marinucci, A., Bianchi, S., Nicastro, F., Matt, G., & Goulding, A. D. 2012, ApJ, 748, 130

Markarian, B. E. 1967, Afz, 3, 24

Markaryan, B. E. 1969, Ap, 5, 206

Mármol-Queraltó, E., Trujillo, I., Pérez-González, P. G., Varela, J., & Barro, G. 2012, MNRAS, 422, 2187

Marscher, A. P. & Gear, W. K. 1985, ApJ, 298, 114

Martig, M., Bournaud, F., Croton, D. J., Dekel, A., & Teyssier, R. 2012, ApJ, 756, 26

Marziani, P., Dultzin-Hacyan, D., & Sulentic, J. W. 2006, Accretion onto Supermassive Black Holes in Quasars: Learning from Optical/UV Observations, ed. P. V. Kreitler (Nova Science Publishers), 123

Mathur, S. 2000, MNRAS, 314, L17

Mathur, S., Kuraszkiewicz, J., & Czerny, B. 2001, NewA, 6, 321

McLure, R. J. & Dunlop, J. S. 2001, MNRAS, 321, 515

McLure, R. J., Kukula, M. J., Dunlop, J. S., et al. 1999, MNRAS, 308, 377

Mineshige, S., Kawaguchi, T., & Takeuchi, M. 2000a, NewAR, 44, 435

Mineshige, S., Kawaguchi, T., Takeuchi, M., & Hayashida, K. 2000b, PASJ, 52, 499

Moran, E. C. 2000, NewAR, 44, 527

Mundell, C. G., Ferruit, P., Nagar, N., & Wilson, A. S. 2009, ApJ, 703, 802

Murphy, D. W., Browne, I. W. A., & Perley, R. A. 1993, MNRAS, 264, 298

Narayan, R. & Yi, I. 1994, ApJ, 428, L13

Nardini, E., Fabian, A. C., Reis, R. C., & Walton, D. J. 2011, MNRAS, 410, 1251

Nieppola, E., Tornikoski, M., Valtaoja, E., et al. 2011, A&A, 535, A69

O'Dea, C. P. 1998, PASP, 110, 493

Ohta, K., Aoki, K., Kawaguchi, T., & Kiuchi, G. 2007, ApJS, 169, 1

Olguín-Iglesias, A., Kotilainen, J. K., León Tavares, J., Chavushyan, V., & Añorve, C. 2017, MNRAS, 467, 3712

Orban de Xivry, G., Davies, R., Schartmann, M., et al. 2011, MNRAS, 417, 2721

Oshlack, A. Y. K. N., Webster, R. L., & Whiting, M. T. 2001, ApJ, 558, 578

Osterbrock, D. E. & Pogge, R. W. 1985, ApJ, 297, 166

Padovani, P. 2016, A&A Rev., 24, 13

Padovani, P. 2017, Nature Astronomy, 1, 0194

Paliya, V. S., Ajello, M., Rakshit, S., et al. 2018, ApJ, 853, L2

Pandey, B. & Sarkar, S. 2017, MNRAS, 467, L6

Panessa, F., Barcons, X., Bassani, L., et al. 2007, A&A, 467, 519

Park, C. & Choi, Y.-Y. 2009, ApJ, 691, 1828

Park, D. & Lee, J. 2009, MNRAS, 400, 1105

Peng, C. Y., Ho, L. C., Impey, C. D., & Rix, H.-W. 2010, AJ, 139, 2097

Penston, M. V. & Perez, E. 1984, MNRAS, 211, 33P

Pérez-Torres, M. A., Romero-Cañizales, C., Alberdi, A., & Polatidis, A. 2009, A&A, 507, L17

Peterson, B. M., McHardy, I. M., Wilkes, B. J., et al. 2000, ApJ, 542, 161

Planck Collaboration, Aatrokoski, J., Ade, P. A. R., et al. 2011, A&A, 536, A15

Planck Collaboration, Ade, P. A. R., Aghanim, N., et al. 2016, A&A, 596, A106

Pogge, R. W. 2011, in Narrow-Line Seyfert 1 Galaxies and their Place in the Universe, https://pos.sissa.it/126/002/pdf

Poudel, A., Heinämäki, P., Tempel, E., et al. 2017, A&A, 597, A86

Pović, M., Sánchez-Portal, M., Pérez García, A. M., et al. 2012, A&A, 541, A118

Rafter, S. E., Kaspi, S., Chelouche, D., et al. 2013, ApJ, 773, 24

Rakshit, S. & Stalin, C. S. 2017, ApJ, 842, 96

Rakshit, S., Stalin, C. S., Chand, H., & Zhang, X.-G. 2017, ApJS, 229, 39

Ramos Almeida, C., Bessiere, P. S., Tadhunter, C. N., et al. 2013, MNRAS, 436, 997

Reber, G. 1944, ApJ, 100, 279

Richards, J. L. & Lister, M. L. 2015, ApJ, 800, L8

Richards, J. L., Lister, M. L., Savolainen, T., et al. 2015, in IAU Symposium, Vol. 313, Extragalactic Jets from Every Angle, ed. F. Massaro, C. C. Cheung, E. Lopez, & A. Siemiginowska, 139–142

Richards, J. L., Max-Moerbeck, W., Pavlidou, V., et al. 2011, ApJS, 194, 29

Rigby, E. E., Argyle, J., Best, P. N., Rosario, D., & Röttgering, H. J. A. 2015, A&A, 581, A96

Robotham, A. S. G., Driver, S. P., Davies, L. J. M., et al. 2014, MNRAS, 444, 3986

Ryan, C. J., De Robertis, M. M., Virani, S., Laor, A., & Dawson, P. C. 2007, ApJ, 654, 799

Sakamoto, K., Okumura, S. K., Ishizuki, S., & Scoville, N. Z. 1999, ApJ, 525, 691

Sani, E., Lutz, D., Risaliti, G., et al. 2010, MNRAS, 403, 1246

Schawinski, K. 2012, ArXiv: 1206.2661

Schawinski, K., Treister, E., Urry, C. M., et al. 2011, ApJ, 727, L31

Schmidt, M. 1963, Nature, 197, 1040

Schmidt, M. & Green, R. F. 1983, ApJ, 269, 352

Schmitt, H. R., Antonucci, R. R. J., Ulvestad, J. S., et al. 2001, ApJ, 555, 663

Schulz, R., Kreikenbohm, A., Kadler, M., et al. 2016, A&A, 588, 146

Seyfert, C. K. 1943, ApJ, 97, 28

Shakura, N. I. & Sunyaev, R. A. 1973, A&A, 24, 337

Shakura, N. I. & Sunyaev, R. A. 1976, MNRAS, 175, 613

Shen, Y. & Ho, L. C. 2014, Nature, 513, 210

Sikora, M., Stawarz, Ł., & Lasota, J.-P. 2007, ApJ, 658, 815

Singh, V., Ishwara-Chandra, C. H., Sievers, J., et al. 2015, MNRAS, 454, 1556

Steinhauser, D., Schindler, S., & Springel, V. 2016, A&A, 591, A51

Storchi-Bergmann, T. 2008, in Revista Mexicana de Astronomia y Astrofisica Conference Series, Vol. 32, Revista Mexicana de Astronomia y Astrofisica Conference Series, 139–146

Sulentic, J. W., Bachev, R., Marziani, P., Negrete, C. A., & Dultzin, D. 2007, ApJ, 666, 757

Sulentic, J. W. & Marziani, P. 1999, ApJ, 518, L9

Sulentic, J. W., Marziani, P., Dultzin-Hacyan, D., Calvani, M., & Moles, M. 1995, ApJ, 445, L85

Szuszkiewicz, E., Malkan, M. A., & Abramowicz, M. A. 1996, ApJ, 458, 474

Tadhunter, C. 2016, A&A Rev., 24, 10

Tadhunter, C., Wills, K., Morganti, R., Oosterloo, T., & Dickson, R. 2001, MNRAS, 327, 227

Taniguchi, Y. 1999, ApJ, 524, 65

Tarchi, A., Castangia, P., Columbano, A., Panessa, F., & Braatz, J. A. 2011, A&A, 532, A125

Tchekhovskoy, A., Narayan, R., & McKinney, J. C. 2010, ApJ, 711, 50

Tempel, E., Stoica, R. S., Martínez, V. J., et al. 2014a, MNRAS, 438, 3465

Tempel, E., Tamm, A., Gramann, M., et al. 2014b, A&A, 566, A1

Tran, H. D. 2001, ApJ, 554, L19

Tran, H. D. 2003, ApJ, 583, 632

Tran, H. D., Lyke, J. E., & Mader, J. A. 2011, ApJ, 726, L21

Treister, E., Schawinski, K., Urry, C. M., & Simmons, B. D. 2012, ApJ, 758, L39

Türler, M. 2011, MmSAI, 82, 104

Urrutia, T., Lacy, M., & Becker, R. H. 2008, ApJ, 674, 80

Urry, C. M. & Padovani, P. 1995, PASP, 107, 803

Urry, M. 2003, in Astronomical Society of the Pacific Conference Series, Vol. 290, Active Galactic Nuclei: From Central Engine to Host Galaxy, ed. S. Collin, F. Combes, & I. Shlosman, 3

van de Ven, G. & Fathi, K. 2010, ApJ, 723, 767

Véron-Cetty, M.-P., Véron, P., & Gonçalves, A. C. 2001, A&A, 372, 730

Villarroel, B. & Korn, A. J. 2014, Nature Physics, 10, 417

Villforth, C., Hamann, F., Rosario, D. J., et al. 2014, MNRAS, 439, 3342

Volonteri, M., Madau, P., Quataert, E., & Rees, M. J. 2005, ApJ, 620, 69

Wadadekar, Y. 2004, A&A, 416, 35

Wadadekar, Y. & Kembhavi, A. 1999, AJ, 118, 1435

Wang, F., Du, P., Hu, C., et al. 2016, ApJ, 824, 149

Wang, J.-M. & Netzer, H. 2003, A&A, 398, 927

Wang, J.-M. & Zhang, E.-P. 2007, ApJ, 660, 1072

Whalen, D. J., Laurent-Muehleisen, S. A., Moran, E. C., & Becker, R. H. 2006, AJ, 131, 1948

White, R. L., Becker, R. H., Helfand, D. J., & Gregg, M. D. 1997, ApJ, 475, 479

Wilson, A. S. & Colbert, E. J. M. 1995, ApJ, 438, 62

Wu, X.-B., Wang, R., Kong, M. Z., Liu, F. K., & Han, J. L. 2004, A&A, 424, 793

Xu, D., Komossa, S., Zhou, H., et al. 2012, AJ, 143, 83

Yang, H., Yuan, W., Yao, S., et al. 2018, MNRAS, 477, 5127

Yang, Q., Wu, X.-B., Fan, X., et al. 2017, ArXiv: 1711.08122

Younes, G., Porquet, D., Sabra, B., Reeves, J. N., & Grosso, N. 2012, A&A, 539, A104

Yuan, W., Zhou, H. Y., Komossa, S., et al. 2008, ApJ, 685, 801

Zamanov, R., Marziani, P., Sulentic, J. W., et al. 2002, ApJ, 576, L9

Zamfir, S., Sulentic, J. W., & Marziani, P. 2008, MNRAS, 387, 856

Zamfir, S., Sulentic, J. W., Marziani, P., & Dultzin, D. 2010, MNRAS, 403, 1759

Zel'dovich, Y. B. & Novikov, I. D. 1964, SPhD, 9, 246

Zhang, E.-P. & Wang, J.-M. 2006, ApJ, 653, 137

Zhou, H., Wang, T., Yuan, W., et al. 2006, ApJS, 166, 128

Zhou, H., Wang, T., Yuan, W., et al. 2007, ApJ, 658, L13

Zhu, L., Zhang, S. N., & Tang, S. 2009, ApJ, 700, 1173

Zhu, Y.-K., Zhang, J., Zhang, H.-M., et al. 2016, RAA, 16, 170

Zwicky, F., Herzog, E., & Wild, P. 1963, Catalogue of galaxies and of clusters of galaxies, Vol. 2 (California Institute of Technology)

Zwicky, F., Herzog, E., Wild, P., Karpowicz, M., & Kowal, C. T. 1961, Catalogue of galaxies and of clusters of galaxies, Vol. I (California Institute of Technology)

.

Narrow-line Seyfert 1 (NLS1) galaxies are young active galactic nuclei (AGN) that harbour low-mass black holes and are preferentially hosted by spiral galaxies. The detection of NLS1 galaxies at gamma-rays confirmed the presence of powerful relativistic jets in them. This discovery contradicts the traditional view that only supermassive black holes residing in massive ellipticals are able to launch relatistic jets, and therefore a revision of the evolution and unification schemes of AGN is required. Also the nature of the diverse NLS1 population has remained unclear.

In this work large samples of NLS1 galaxies are examined, complemented by targeted studies of smaller samples. Extensive statistical studies, such as correlation and principal component analyses, and detailed investigation of selected individual sources were performed using novel radio, near-infrared, and large-scale environment data together with archival multifrequency data.

Aalto-DD 163/2018

ISBN 978-952-60-8153-3 (printed)
ISBN 978-952-60-8154-0 (pdf)
ISSN 1799-4934 (printed)
ISSN 1799-4942 (pdf)

Aalto University
School of Electrical Engineering
Metsähovi Radio Observatory
www.aalto.fi

BUSINESS + ECONOMY

ART + DESIGN + ARCHITECTURE

SCIENCE + TECHNOLOGY

CROSSOVER

DOCTORAL DISSERTATIONS